Dry powder inhaler:
Interaction between drug particles and the device

Dissertation

zur

Erlangung des Doktorgrades (Dr. rer. nat.)

der

Mathematisch-Naturwissenschaftlichen Fakultät

der

Rheinischen Friedrich-Wilhelms-Universität Bonn

vorgelegt von

Roman Groß

aus

Remscheid

Bonn 2023

Angefertigt mit Genehmigung der Mathematisch-Naturwissenschaftlichen Fakultät
der Rheinischen Friedrich-Wilhelms-Universität Bonn

Promotionskommission:

Erstgutachter: Prof. Dr. Alf Lamprecht

Zweitgutachter: Prof. Dr. Karl Wagner

Fachnahes Mitglied: Prof. Dr. Günther Weindl

Fachfremdes Mitglied: Prof. Dr. Andreas Schieber

Tag der Promotion: 09.08.2023

Erscheinungsjahr: 2023

Content

1. Introduction 7
   1.1 Overview of the subject of inhaled medicinal products 7
   1.2 Pharmaceutical aerosols and their requirements 8
   1.3 Delivery systems: From problems with pMDIs to solutions with DPIs 10
   1.4 Formulation aspects for the use of DPIs 12
   1.5 Dry powder inhaler: past-present 17
   1.6 In-vitro characterization of formulations for the pulmonary application 21
   1.7 Factor patient 25
2. Aim and scope 29
3. Fast onset of thrombolytic effect of efficiently inhalable spray-dried rivaroxaban powder formulations 32
   3.1 Introduction 32
   3.2 Materials & Methods 33
   3.3 Results 39
   3.4 Discussion 49
   3.5 Conclusion 52
4. Interim summary 54
5. State of the Art in Capsule-Based Dry Powder Inhalers: Deagglomeration Techniques and the Consequences for Formulation Aerosolization 55
   5.1 Overview of the work 56
6. Interim summary 59
7. Effect of texture and surface chemistry on deagglomeration and powder retention in capsule-based dry powder inhaler 60
   7.1 Overview of the work 61
8. Interim summary 64
9. Improving capsule-based dry powder inhalers: A new in-vitro method of assessing inhalation success conditions by tracking capsule rotation during actuation 65
   9.1 Introduction 65
   9.2 Materials and Methods 67
   9.3 Results 72
   9.4 Discussion 85
   9.5 Conclusion 87

10. Conclusions and future perspectives 89
11. References 96
12. Appendix 117
13. State of the Art in Capsule-Based Dry Powder Inhalers: Deagglomeration Techniques and the Consequences for Formulation Aerosolization 118
13.1 Graphical abstract 119
13.2 Abstract 119
13.3 Introduction 120
13.4 Materials and Methods 123
13.5 Results 127
13.6 Discussion 136
13.7 Conclusions 139
14. Effect of texture and surface chemistry on deagglomeration and powder retention in capsule-based dry powder inhaler 140
14.1 Graphical abstract 141
14.2 Abstract 141
14.3 Introduction 142
14.4 Materials & Methods 145
14.5 Results 150
14.6 Discussion 160
14.7 Conclusion 164
15. Supplements 165

1. Introduction

1.1 Overview of the subject of inhaled medicinal products

The pulmonary route of administration is an important area of research that has attracted growing interest in recent years. Treating a patient with an orally or intravenously administered drug that targets the lungs results in undefined therapy because, after the drug enters the bloodstream, it can travel to different organs and areas. This can lead to insufficient efficacy of the therapy, increased side effects, and thus lower patient adherence. Therefore, therapy with inhalers and formulations targeting the respiratory tract is of increasing interest because the site of action is targeted. This results in a rapid onset of action while reducing the dose of drug that must be administered to fulfill the therapeutic goal and thus reduces systemic side effects [1]. Currently, most delivery systems approved and commercially available for pulmonary therapy are directed toward the treatment of traditional respiratory diseases such as asthma or chronic obstructive pulmonary disease (COPD) and include active pharmaceutical ingredients (APIs) from the classes of inhaled corticosteroids (ICS), long-acting β-agonists (LABA), or long-acting muscarinic antagonists (LAMA) [2,3]. Regardless of the device and drug used for pulmonary therapy, the aerodynamic particle diameter is crucial for the deposition of the drug in the lungs and thus for the success of the therapy.

Particles larger than 10 µm are deposited in the mouth and throat, with a diameter of > 5 µm leading to impaction in the trachea and main bronchi. To achieve powder deposition in the lower airways, e.g. the alveoli, the particle size should be 1 - 5 µm, with the deposition mechanism based on sedimentation. In addition, to reach the alveoli in the broadest sense, a particle size of 1 - 3 µm should be delivered. In contrast, an aerodynamic diameter of less than 0.5 µm is characterized by Brownian motion, and the particles are exhaled more frequently by the patient's expiratory flow after inhalation, so this deposition mechanism can be neglected [4,5]. Apart from these requirements for aerosolized formulations, and in addition to the traditional treatment of lung disease, there is growing interest in the delivery of antibiotics and other agents to lung. Formulations of tobramycin, colistin, or aztreonam are marketed for cystic fibrosis (CF) and bronchiectasis without CF. Injectable gentamicin, tobramycin,

amikacin, ceftazidime, and amphotericin formulations, although not FDA-approved, are also currently nebulized for the treatment of noncystic fibrosis bronchiectasis, drug-resistant non tuberculous mycobacterial infections, ventilator-associated pneumonia, and post-transplant respiratory infections [6]. Although the mechanism is not known, it has been shown that administration of mannitol with a dry powder inhaler could help clear secretions from the airways of patients with cystic fibrosis [7].

In addition to the aforementioned local therapy at the site of action, there is also growing interest in the possibility of administering various agents for systemic therapies, since the respiratory tract of an adult has a surface area of 80 to 100 m^2, much larger than the skin (1.5 - 2 m^2) [5,8]. Despite setbacks in recent years, e.g., in insulin delivery via the lungs (Exubera, Afreza), this delivery method is proving to be advantageous compared to other delivery application routs. Due to the highly permeable membrane and numerous capillaries, a fast absorption rate is achieved and the absorbed drug can directly enter the bloodstream, avoiding elimination by first-pass metabolism in the liver. As a result, the necessary loading dose can be reduced, which is also associated with minimized side effects. The harsh conditions of the gastrointestinal tract and the influences of fasting and diet are also unimportant. Furthermore, when thinking of a diabetic patient, the pain which comes with the application by the needles falls away which could increase patient comfort and result in higher treatment adherent [8,9]. Innovative device and formulation technologies enable patients to treat their diseases with just one breath. Examples include the administration of iloprost for the treatment of pulmonary arterial hypertension using the Breelib® nebulizer (Vectura Group plc) or the Staccato® system from Alexza Pharmaceuticals, in which a thin film of the pure drug (loxapine) is vaporized on a metal substrate in a channel for inhalation air [10,11].

1.2 Pharmaceutical aerosols and their requirements

For a drug to be administered via the lungs, it must be in the form of an aerosol, i.e., liquid or solid particles dispersed in a gas phase, depending on the type of formulation and inhaler used. When an aerosol reaches the respiratory tract, it separates by several mechanisms that depend on the aerodynamic particle size at the various

deposition sites. In inhalation therapy, the aerosol should have a systemic or local effect at the target site, the lungs. As described in the previous section, it is generally assumed that particles with an aerodynamic diameter between 1 and 5 µm can be deposited in the lower airways. The aerodynamic diameter (d_{ae}) is defined as the diameter of a spherical particle with density 1 g/cm^3 that has the same sinking velocity as the particle under consideration. Equation 1 shows the relation between d_{ae} and the geometric diameter (d_{geo}):

$$d_{ae} = d_{geo}\sqrt{\frac{\rho_p C_p}{X\rho_{ae} C_{ae}}}$$

Equation 1 shows the most general case of the relationship between the aerodynamic diameter (d_{ae}) and the geometric diameter (d_{geo}), the particle density (ρ_p) and the reference particle density (ρae), the Cunningham slip correction factors for the particle diameters of the sample (C_p), the reference particles (C_{ae}), and a shape correction factor (X) [12]. Equation 1 states that d_{ae} of a particle can be effectively manipulated by changing its geometric diameter, density, or shape. The aerodynamic particle size reflects the behavior of a particle in the air stream and need not correspond to the actual particle size, since larger particles with a low density can behave comparably to small solid particles. In general, three deposition mechanisms can be distinguished (Fig. 1).

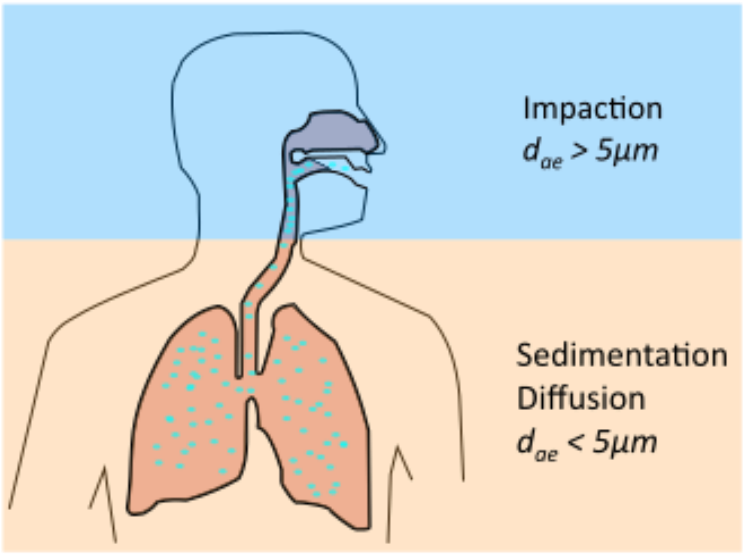

Figure 1: Schematic representation of the different deposition mechanism occurred during inhalation.

1. *Impaction* of particles occurs due to their mass inertia. When the direction of the airflow changes, they are unable to follow it and maintain at least part of their original direction of motion. They separate by impacting the obstacle. Large particles or those with a high kinetic energy in the aerosol often deposite as they pass through the throat. Particles that can follow the airflow into the lungs are classified as fine particles and are usually smaller than 5 µm.
2. *Sedimentation* describes the behavior of those particles in a size range of 0.5 - 5 µm which, after reaching the lower regions of the lungs, follow gravity and settle. This step is time-dependent, which explains the recommendation to patients to pause for breath after inhalation to achieve as complete deposition as possible.
3. Particles below a size of 0.5 µm are increasingly subject to *diffusion*. It is caused by Brownian molecular motion. Particle separation by diffusion is also dependent on time [13–15].

1.3 Delivery systems: From problems with pMDIs to solutions with DPIs

Inhaled administration is a form of therapy with a long tradition and is considered the best method of delivering medications to the lungs for the treatment of conditions such

as asthma, chronic obstructive pulmonary disease, and bacterial infections [16,17]. It began in the early 1900s with handheld nebulizers to administer epinephrine chloride as a bronchodilator, then electric and ultrasonic nebulizers were developed in the twentieth century [16,18].

It became interesting for industry after the development of the first pressured metered dose inhaler (pMDI) in 1956 by Riker Laboratories. This type of device quickly gained popularity because pMDIs are small, portable, inexpensive, silent compared to nebulizers, fast, and theoretically easy to use because the patient only has to inhale during actuation. In reality, pMDIs showed inadequate therapeutic outcomes because patients had difficulty coordinating actuation and respiratory maneuvers. In addition, since the drug is formulated as a solution or suspension, problems such as chemical instability of the active pharmaceutical ingredient (API) [19], instability of the suspension [20], low solubility of the API, or crystal growth phenomena [21] may occur. In addition, concerns were raised in the 1970s because chlorofluorocarbon (CFC) propellants were believed to lead to ozone depletion in the stratosphere [22]. The result was the Montreal Protocol on substances that deplete the Ozone Layer, signed in September 1987 [23,24].

Since then, major efforts have been made to overcome these limitations. CFCs have been replaced by less harmful hydrofluorocarbon (HFC) propellants [21]. The set-up of this class of devices has been increasingly optimized to produce aerosols with sufficient particle size for targeted deposition in the lungs. Ultimately, such a delivery system consists of 5 main components (container, propellant, formulation, metering valve, and actuator) that must be perfectly matched for therapeutic success. Aspects affecting the aerosol include type, mixture of propellants and resulting vapor pressure, the use of a drug solution or suspension, and the presence of other ingredients. The size and shape of the expansion chamber and the nozzle (actuator), which influence the spraying velocity, must also be chosen correctly [25]. This redesign of pMDIs and the use of the novel propellants resulted in a reduction in one of the reported inhalation problems, namely high oropharyngeal deposition, which in the case of glucocorticosteroids resulted in localized adverse effects. This high oropharyngeal deposition is largely due to the high velocity at which the aerosol leaves the device and

to the so-called cold Freon effect (Freon is DuPont's registered trademark for CFCs). Here, the patient has difficulty coordinating actuation and inhalation, so the formulation hits the back of the patient's throat, causing the cold, liquid propellant to deposit in this area as well, often startling the patient and forcing him or her to stop inhalation, as this is perceived as uncomfortable [25,26]. Although the modification of pMDIs led to better therapeutic success, the disadvantages of this class of devices could not be overcome. In addition, only a small amount of medication can be inhaled with such a device.

However, to counteract this and solve the problems of this class, a great deal of effort was required to overcome these limitations, which led to the development of some of the first dry powder inhalers (DPIs) in 1950-1980 [27]. The availability of capsule fill machines and the growing knowledge in dry powder formulations of potent drugs made a simple development with an inexpensive cost possible [28]. From the initial market entry to today, there has been steady progress, but the success of therapy with this type of delivery system then and now consists of three main areas, namely formulation development, powder deagglomeration concepts for DPIs, and patient safety. Only a coordinated interaction can lead to an ideal DPI, which is why such a device does not yet exist today, as the individual areas are known to varying degrees.

1.4 Formulation aspects for the use of DPIs

In the use of DPIs, the focus was always on the development and optimization of the respective formulation, with aspects such as solubility or suspension stability not playing a role. Since the production of dry powder formulations that aerosolize sufficiently without supporting propellants or further blowing agents is complex, this topic is of great interest and efforts in DPI development. Independent of the device used, it is known that the particles should have an aerodynamic parameter < 5 µm to achieve a suitable powder deposition in the lower airways [29]. In order to produce particles in the micrometer range, constructive (e.g., spray-drying) or destructive (e.g., milling) processes can be used. For destructive processes, as micrometer particles are created from larger crystals by pressure, friction, impact, shear or abrasion in this basic surgical technique, various mechanical treatments can be applied. In addition, this formulation method works economically and solvent-free. Despite this ease of

handling, the high energy input during grinding can lead to less controllable conditions in terms of particle size distribution, surface properties, morphology and electrostatic charging effects. This can lead to heterogeneity of the particles. However, in the pharmaceutical industry, the active ingredient is traditionally micronized using various technologies (e.g. ball mill, jet mill) [30–32]. Although this formulation method can produce particles in the inhalable size range that provide high storage stability of the crystalline drug, minimizing the particle size resulted in an increase in total surface area, leading to cohesive particles [33]. The problem with these particle formulations is their inadequate flowability and aerosolization during actuation, so the active ingredient is usually mixed with larger carrier particles. In these interactive blends the micronized active pharmaceutical ingredients are adsorbed on the carriers surface (e.g., lactose) [30,31]. These systems face the challenge that, on the one hand, the adhesive forces for the active ingredient-lactose must be high enough to allow homogeneous mixing and also dosing within the device, but on the other hand, they must also be weak enough to allow the active ingredient to detach from the carrier when actuated. Commercially available interactive mixtures are usually ternary mixtures consisting of the drug, larger carrier particles, and also a fine fraction of these carrier particles in a specific mixing ratio, since the addition of these fine particles results in increased fine particle fraction (FPF) [34–36]. Currently, there are two main hypotheses which try to explain this phenomenon. The first is the active site mechanism. The idea is that on the coarse carrier particles there is an active or also called high energy site, which is bounded by the fine particles, so that the active ingredient, which is mixed in a final step after the preparation of the coarse/fine mixture, can be adsorbed on the low surface energy side and detach during inhalation. For the development of the interactive blends, this means that the larger carrier lactose should be saturated with the fines so that sufficient aerosolization properties can be achieved. In contrast, the agglomerate hypothesis assumes that the active ingredient is distributed between large and fine carrier particles during mixing, resulting in agglomerates of low stability that are easily dispersed [37].

However, the addition of carrier particles seems to solve the problems of insufficient flowability and powder aerosolization compared to the deagglomeration behavior of the pure milled drug particles, also other disadvantages are added with this formulation

strategy. As mentioned earlier, destructive methods such as milling lead to uncontrollable conditions of drug properties such as overall particle size distribution, shape and also surface texture. It is precisely these properties that influence the overall deagglomeration behavior of the final formulation and lead to the fact that currently marketed formulations produced as interactive mixtures have a fine particle content of 20-30% with a high powder deposition in the oropharyngeal region, which is indicative of insufficient release of the active ingredient from the carrier [38]. Since the carrier particles are also produced by milling and sieving, more undefined and unknown variables come together in the development of the interactive blends, which ultimately led to this low powder deposition in the lungs.

It has been shown that the particle shape and the roughness have a great influence on the powder adhesion and also on the deagglomeration forces. When using spherical carrier particles, the number of contact points for the drug is lower compared to non-spherical particles. Surface texture also affects these adhesion forces, as this leads to an increase in the effective contact area for small drug particles, but also a decrease in the effective contact area for large drug particles, as they have only a few small contact points with the rough surface and cannot fit between the rough textures. Since milled drug and carrier particles with undefined surface shape and texture are present in the formulations on the market, a strong interaction between these two components would explain the insufficient release of the drug when the formulation is actuated. A spherical carrier shape would allow the drug particles to detach from the surface, while non-spherical carriers would allow the drug particles to hide in the voids and thus resist the detachment forces. In addition, the scale of roughness appears to be important, as a micron-scale texture could lead to the phenomena described, since the drug for pulmonary use also has a micron-scale size. However, increasing the surface roughness down to the nanometer range could lead to a reduction in the contact points and thus to lower adhesion strength [39,40]. Regardless of which case occurs, pulmonary delivery systems ultimately track three main components: a) delivery of a high emitted fraction (EF) and FPF, b) aerosolization efficiency independent of the flow profile, and c) high physical stability of the product.

A modern approach for the development of aerosolizable particle formulations is to design the particles by the method of spray-drying, which is now a well-established technology and is used in a wide range of applications. Spray-drying became popular during World War II as a way to reduce the weight of food in transit [41]. From then on, new and innovative applications for this method were found again and again. Besides the field of formulation of amorphous solid dispersions or spray-drying of biopharmaceuticals (e.g. proteins), this constructive method is also suitable for the development of dry powders for pulmonary applications [42]. Spray-drying is a single-stage continuous process that, with few exceptions, can produce spherical particles, where the particle size obtained can be described by the geometric diameter [43,44]. Since it allows manipulation and control of particle size distribution, particle density, shape, moisture content, flowability and crystallinity this formulation method was been approved as particle engineered approach [45]. In terms of particle design options, the appropriate formulation properties can be achieved by combining the right process parameters during spray-drying. Again, since small particles in a similar size range to milled drug particles can be achieved, these particles also tend to agglomerate due to the large surface area provided by the small particle size. However, because these particles are generally spherical, fewer contact points are available for particle-particle interactions, so that during inhalation, the inhalation force is sufficient to overcome these cohesive interactions. Therefore, this type of formulation can be more easily deagglomerated and impresses with easily accessible FPFs. Since the particle density is much lower compared to milled crystalline particles, this formulation strategy is convincing with particles that have better aerodynamic behavior, so these particles can follow the airflow even if the geometric particle size is above 5 µm. The advantages over the traditional formulation technique are clearly visible, so that instead of the mentioned fine particle fractions of 20-30% achieved with the interactive blends, FPFs of about 60% are possible [38,44].

During the process, the liquid feed, which can be a solution, suspension or even emulsion, is fed to the respective nozzle and sprayed into a hot medium to convert the liquid into a solid state. The principle of this process is the atomization of the liquid into small droplets and the subsequent evaporation of the solvent by the drying gas [46]. Overall, this process technology results from the following individual steps: a)

concentration of the liquid feedstock; b) atomization of the feedstock through the nozzle and contact of the droplets with the drying medium; c) droplet drying by evaporation of the solvent; d) separation of the dry powder from the gas stream by a cyclone (Fig. 2).

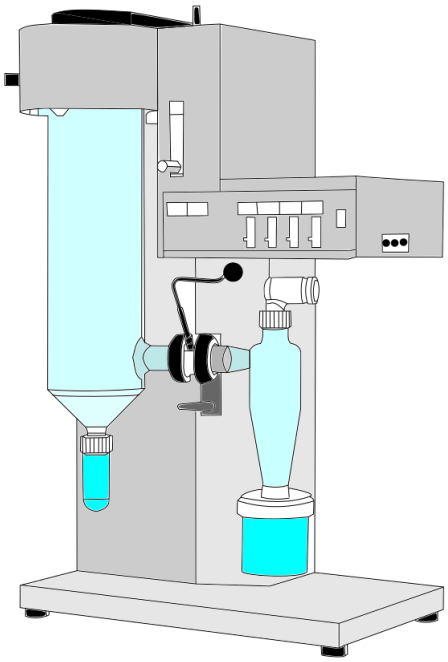

Figure 2: Schematic set-up of the spray-dryer used for the experiments.

In terms of desired product properties, there are some key elements for spray-drying those are critical for particle design.

1. The choice and installation of the *right atomizer* which is the core element of the entire process is crucial. Important functions of this element are the atomization of the feed material in droplets which are small enough to get dried without exhausting by the air flow. To enable a wide range of desired particle properties, different nozzle types are available (e.g., two-fluid, rotary, ultrasonic, pressure nozzles). In addition, the flow rate fed into the spray-dryer is also set and controlled at this point, so that the atomization acts like a metering system.
2. The *air flow* which is used to dry the spray which entering the drying chamber can be in a co-current flow (spray and air flow passed the chamber in the same direction), counter-current flow (spray and air flow enter the chamber on the

opposite side) and the *mixed flow* (combination of co-current and counter-current flow).

3. The *spray-drying chamber* influences the introduced air flow in such a way that a stable flow pattern is created which prevents the particles from being deposited in this component. Also in this area, the spray mist and the drying gas come into contact and the droplets are dried in a two-stage mechanism. In the first stage, this means that there is enough moisture inside the droplet so that the evaporated amount on the surface (liquid-air) can be constantly replaced. In the second phase, when moisture is insufficient to maintain saturated conditions on the surface, a dried shell forms on the surface. The final evaporation of the remaining solvent is a diffusion process through the shell. It follows that the inlet temperature of the air is important for the properties of the final product.
4. In the last step, the dry powder is *separated* from the air stream. Bag filters, electrostatic filters or cyclones are usually used for this purpose. It has been shown that when cyclones are used, the dimensions of their geometries are important for product recovery. Specifically with regard to particle formulations for lung therapy, improved cyclones have been developed in which the yield has been increased by tighter dimensioning of the airflow channel. During the process, centrifugal forces are exerted on the particles so that they can be collected in a final step [43,44] (Fig. 2).

1.5 Dry powder inhaler: past-present

A look at the past shows that the starting point was Abbott's Aerohaler, which was launched in 1948 and served as a prototype for several capsule-based DPIs developed during those years. Each DPI contained an interactive blend formulation of the respective drug. The Fisons Spinhaler®, the first device to be marketed during this period, in 1967, consisted of a drug dose of 20 mg of cromoglycate sodium, which was too high for the administration of pMDIs, so the advantages of this class of devices quickly became apparent [16,47,48]. Although many DPIs came on the market in the following years, they all had the same basic design, a gelatin capsule as the dosage storage and lactose as the carrier particle. Differences were only found in the piercing

and opening of the capsule and in the movement of the capsule during actuation. The use of hard gelatin capsules as filling containers was due to the fact that filling equipment for this dosage form was also available and did not need to be developed [49]. Some of the now well-known DPIs developed during this pioneering period were the Rotahaler® (Allen & Hanbury's) in 1969 or the Cycohaler® (Pharmachemie) introduced in the early 1990s [28]. In the following years, a major focus was on studying the adhesion effect of micronized particles to larger carrier particles occurring in interactive mixtures, as the required aerodynamic particle size fraction of the first capsule-based DPIs was quite low, with the carrier-free formulation of Turbohaler (AstraZeneca) resulting in much higher fine particle fractions [50]. These strong carrier-drug interactions, combined with the lack of effective deagglomeration concepts in the early DPIs, resulted in inadequate FPFs. Since the 1990s, when the importance of adhesive interactive mixtures and the goal of detaching the drug from the carriers came to the fore, multi-dose reservoir systems (DPI) with different dosing systems were introduced to the market. Representative examples were the Novolizer® (Meda Pharma), the Easyhaler (Orion Pharma) or the Twisthaler® (Merck,Sharp & Dohme Ltd) [28]. A trend has emerged: All DPI devices developed before 2010 were passive or breath-controlled. Despite the great advantage of being able to administer different agents and eliminating the coordination problem for patients, it should not be ignored that not every patient is able to generate a sufficient flow rate across the DPI to deagglomerate the powder [51,52]. One approach to overcoming this limitation has been the development of active DPIs that use the additional energy of a battery-powered rotating impeller (Spiros®, Dura Pharmaceuticals) or compressed ambient air from a pump handle (Exubera®, Pfizer) to aerosolize the powder [53,54]. The advantage of such delivery systems is that simultaneous actuation of the DPI and patient inhalation can be neglected, and the device also provides a fine particle fraction independent of the actuation flow profile [55]. Despite this breakthrough in powder delivery, the setup of these devices was so complicated that they were not user-friendly due to the various steps the patient must complete prior to inhalation and prone to error due to the partially installed technology. This resulted in both DPIs not being successfully marketed.

Ultimately, this led to many DPI designs being optimized today to increase the powder deagglomeration of the device for formulation. To ensure successful therapy and minimize the potential sources of error, the DPI and the corresponding formulation are developed and marketed in a fixed combination [56,57].

Currently, there are more than 20 different devices commercial available which are developed by different manufactures whereby several expected to be proofed in clinical trials [27,58]. Overall, it can be said that this type of delivery system consists of three major components, namely (a) the device, (b) the formulation, and (c) the metering system. Moreover, DPIs can be divided in three classes, namely

- the single-dose devices
- the multi-dose devices
- the multi-unit dose device

Since single-dose devices were the first representatives of DPIs, they are often referred to as first-generation DPIs because the patient must insert and pierce a capsule before inhalation, while the powder vehicle must be removed after the breathing maneuver is completed. The Handihaler® or the Aerolizer® are examples of this class of devices. The multi-dose and multi-unit dose DPI represent the second generation of DPIs, as the formulation in the device is premeasured and uniform. In the Turbohaler® (multi-dose) DPI, the dose is measured from a reservoir, while in the multi-unit dose (e.g., Diskus®) the individual doses are premeasured by the manufacturers in blisters, discs, dimples, tubes and strips. The third generation of DPIs is represented by Exubera® and Airmax®, for example, as they have supporting tools such as compressed gas or motor-driven impellers installed [59].

Except the third generation and as mentioned earlier, the passive or even breath-actuated DPIs are currently the main representatives of this class of devices, so the inhalation flow profile generated by the patient is the only source of energy and is very important to sufficiently deagglomerate the powder and deliver the active ingredient to the site of action [60]. Inhalation performed with insufficient respiratory force and duration results in an unintentionally low emitted dose with insufficient powder deagglomeration and thus insufficient therapeutic success [61,62]. It follows that the

DPI should be designed to achieve constant powder aerosolization regardless of the flow rate applied. Based on this criterion, different DPIs with different geometries and resistance to airflow (low - medium - high) have been developed and tested [63–65]. While the airflow paths are usually short, an additional grid or classifier is often installed to increase the deagglomeration efficiency of the DPI for the powder [66,67]. Since each component has characteristic dimensions, the flow profile within the entire device is complex and often not fully known. Therefore, computational fluid dynamic (CFD) analysis is often used to identify critical DPI parts for powder deagglomeration.

DPIs on the market are mostly made of plastic, while certain components must be made of metal, as special requirements are imposed here. The needles with their associated springs for piercing the capsule before inhalation are examples; the rest of the DPI is made of various plastics. The reasons for this include the favorable material costs and the possibility of producing the developed device geometry in large quantities using injection molding [68–72]. Injection molding is a primary molding process used mainly in plastics processing. In this process, the respective material is liquefied (plasticized) with the aid of an injection molding machine and injected under pressure into a mold. In the mold, the material returns to its solid state through cooling or a crosslinking reaction and is removed as a finished part. The cavity of the mold determines the shape and surface structure of the finished part. DPIs developed using this processing method are of consistent quality and have a smooth surface when the correct processing parameters are selected [73,74]. Although this process offers many advantages, developing the final molding process can be difficult and expensive. Since the plastic has a complex thermo viscoelastic property, it is a challenge to set the right molding conditions to achieve the desired product quality. In practice, therefore, the setting of process parameters relies mainly on the experience of the plastics engineer, or the process parameters are often selected from manuals and then adjusted by the trial-and-error method. It turns out that the trial-and-error method is costly and time-consuming [75,76].

In addition, a new strategy is gaining interest in recent years, as this method offers many advantages for simple prototyping. 3D printing is a processing tool that enables cost-effective production of the desired part regardless of the structural geometry. In

several studies, the rapid modification of DPI components or the production of add-on parts has been sufficiently carried out [77–79]. While this process has not yet been used to produce a complete DPI, possibly due to limited research and knowledge in this area, individual parts such as the mouth piece, mesh, or capsule chamber have been successfully printed to a high quality, although the surface texture of the resulting plastic part is not as smooth as after injection molding [80]. Since this method allows simple geometric modifications of the original DPI to evaluate such modifications on the emitted fraction and fine particle fraction, this research topic seems to be interesting in the future to challenge the issue of developing an ideal DPI.

1.6 In-vitro characterization of formulations for the pulmonary application

To classify the powder deagglomeration behavior of the device for formulation and to evaluate the aerodynamic properties of the fine particles, the European Pharmacopoeia currently describes four devices (Tab. 1). These apparatuses share the basic principle of separation from the air stream. Particles, but also droplets, are separated along curved paths due to their inertia (Fig. 3).

Table 1: Apparatus for characterization of the aerodynamic particle properties.

Apparatus	**Naming**	**Abbreviation**
Device A	Inhalation tester made of Glass	TSI
Device C	Multi-stage Liquid Impactor	MSLI
Device D	AndersenCascade Impactor	ACI
Device E	Next Generation Pharmaceutical Impactor	NGI

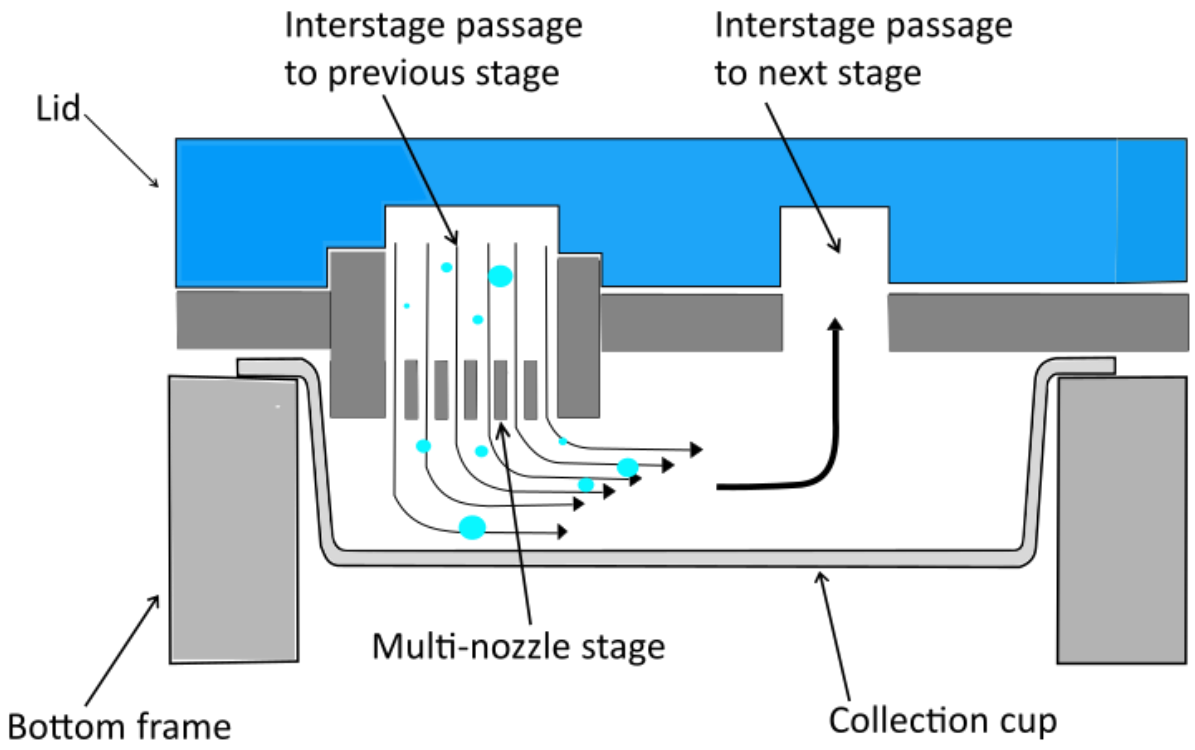

Figure 3: Schematic representation of the principle of operation of cascade impactors.

Currently, the Next Generation Impactor (NGI) is the state of the art for aerosol classification. Therefore, the NGI was used for all experiments on the aerosolization behavior of powders (Fig. 4).

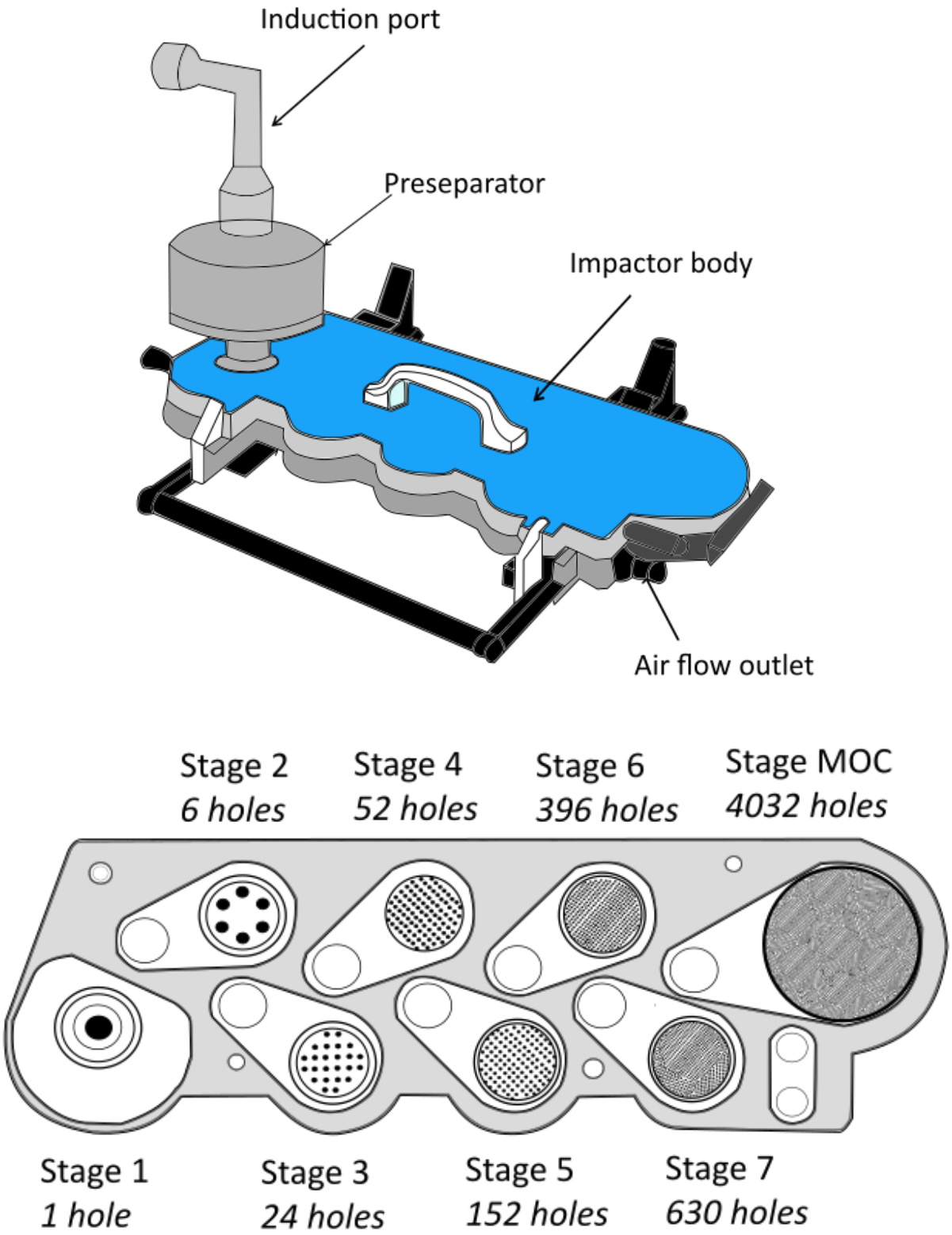

Figure 4: Schematic representation of the NGI and the Nozzle openings [81].

When analyzing devices with the NGI, the dry powder inhaler to be tested is connected airtight to the throat (induction port (IP)) via an adapter. The defined number of actuations then takes place at an applied air volume flow (L/min) (± 5%) into the NGI. The delivered aerosol must first pass through the 90° angle of the induction port followed by the preseparator. In the body of the NGI, the aerosol is then deposited in seven stages and the final micro-opening collector (MOC). In order to achieve a size distribution according to the principle of mass separation, the diameter of the nozzle openings becomes smaller and smaller as the number increases, which locally increases the flow velocity. In addition, the distance between the nozzle and the surface of the collection cup decreases, so that finer and finer particles are separated from stage to stage. The NGI also makes it possible to work with different flow rates as required, which shifts the diameter of the separator on the separation stages. The cutoff diameters of each stage for the tested flow rate($D_{50,Q}$) can be calculated as shown in equation 2:

$$D_{50,Q} = D_{50,Q_n}(Q_n/Q)^x$$

Q is the air flow used during the test, n refers to the nominal values determined when Q_n equals 60 L/min. For that, D_{50,Q_n} and x can be found in the table 2 [81].

Table 2: Cutoff Aerodynamic Diameter for the stages of the NGI.

Parameter to calculate $D_{50,Q}$ in the calibrated area of the NGI from 30 – 100 L/min with Q_n = 60 L/min		
Stage	D_{50,Q_n}	x
1	8.06	0.54
2	4.46	0.52
3	2.82	0.50
4	1.66	0.47
5	0.94	0.53
6	0.55	0.60
7	0.34	0.67

For the analysis of aerosol properties and deagglomeration behavior of DPIs for pulmonary formulations, several parameters can be calculated after release. In total, the mass of the powder separated in the different fractions (capsule, DPI, inlet, pre-separator, stage 1 - MOC) is determined. From this, the emitted fraction (EF) can be calculated. The emitted fraction represents the amount of particles of the loaded doses which leaved during actuation the capsule and the device. This mass is available for lung treatment. The median mass aerodynamic diameter (MMAD) represents the average size of a particle in the aerosol, 50% of the particle mass has a diameter smaller than the MMAD. The MMAD is calculated from the particle size distribution. The class lower limits of the individual separation stages are plotted logarithmically against the cumulative frequency converted to probit. From this plot, the MMAD is calculated as 50% by interpolation. The fine particle fraction (FPF) described the percentage amount of particles which have an aerodynamic diameter < 5 µm and are so able to potentially reach the lungs. The FPF can be related to the emitted fraction or the total dose (TD) loaded inside the device. The FPF and MMAD represent the degree of powder deagglomeration where a higher FPF in combination with a low MMAD represents a good formulation aerosolization [82–84].

1.7 Factor patient

While the aerosolization efficiency of the respective formulation and the deagglomeration concept of the device can be determined and controlled by the manufacturing process, so that the pharmaceutical industry has a significant influence on these two factors, the last parameter, the influence of the patient on the inhalation result, is a more or less unknown quantity. Unfortunately, the development of a beneficial DPI with an easy-to-inhale formulation does not guarantee successful therapy, because of all three factors mentioned, the patient has the greatest influence on the outcome of therapy. In general, DPIs are delivery systems that on the one hand offer many options for drug delivery, but on the other hand are highly prone to errors due to the patient and their influence on the inhalation process, which repeatedly leads to innovative delivery systems not being approved for the market. Although the point of coordinating actuation and inhalation maneuvers for inhalation is eliminated for

DPIs, since this class of device is mostly breath-controlled, many different potential sources of error can occur. In various studies, it has been shown that up to 89% of patients are unable to operate their device properly, regardless of whether it is a pMDI or a DPI [85–87]. In general, pMDIs are the class with the highest potential for error, with reported error rates high enough to cause ineffective therapy, lower patient adherence, wasted medications, and unnecessary costs. There are numerous publications that point out the most common mistakes patients make and list the hidden requirements for an ideal device. In general, inhalation errors can be divided into patient-independent and patient-dependent errors. While factors such as gender, age, or type and severity of disease can be assigned in the first class, patient-dependent factors can be more or less minimized and overcome by sufficient training and education. Since the influence of factors that are independent of the patient cannot really be changed, the pharmaceutical industry has focused on the formulation and device side aspect. Since the success of inhalation, as described, depends on many factors, the delivery systems on the market are designed as combination products consisting of the formulation and the DPI to minimize the number of possible sources of error. The formulation and the device are designed to work together to achieve a satisfactory therapeutic effect [56,57]. This is due to the fact that different inhalers result in different deagglomeration of the same powder, making the development and marketing of a generic product ultimately challenging. This means that a patient has to relearn how to use another device when changing medication, which in the worst case can lead to inadequate therapeutic effect and reduced adherence. In addition, the physiological conditions of the patients responsible for the inhalation profile produced during actuation may influence powder aerosolization. A COPD patient cannot achieve the same inhalation profile as a healthy person, which can result in minimal powder deagglomeration and therefore inadequate therapeutic effect. To focus on and overcome this problem, high intrinsic resistance devices are currently being developed that are designed to deliver the same amount of aerosol regardless of airway resistance and applied inhalation flow rate [65,88,89]. While this class of devices can increase the amount of drugs reaching the target region of the lung, it also cannot avoid the characteristic sources of error. Various studies have pointed out these critical errors. It has been shown that many patients do not exhale before inhalation or exhale

through the mouth piece. Unfortunately, there are a large number of users who do not properly prepare the DPI before inhalation (remove cap, insert and pierce the capsule or hold the device in the correct position for inhalation). One critical factor is also an inhalation performed with insufficient force and duration followed by no breath hold. It becomes particularly critical when not only one mistake, but a series of mistakes are made during the inhalation maneuver, which can thus influence the effect of the therapy [85,86]. It has also been shown that as the number of inhalers used for pulmonary therapy increases, the error rate increases [87]. Ultimately, this leads to the question of whether every patient is able to use different devices equally well. Currently, patients are unable to assess their own inhalation due to a lack of appropriate feedback mechanisms. When it comes to asking a patient with lung disease what is really needed for administration, device aspects such as ease of use, knowing that the dose has been taken, a dose counter or a small device are the most important values [90]. On the other hand, from the developers' point of view, accurate and consistent effective drug delivery, ease and convenience of use, ease of learning correct use, ability to deliver a range of drugs, accurate dose counter, patient feedback on the dose taken, ease and robustness of use are important requirements [51,91]. Even if the claims sound simple and trivial, the ideal device has not been developed to date. Since the outcome of inhalation is influenced by many factors and too many aspects are not well understood, the goal of developing the ideal device is not currently possible. Attempting to combine and meet all requirements in one device could result in the production of a complex and geometrically restrictive device that leads to a lack of ease of use and thus lower patient compliance. To assist the patient in this complex administration process, small windows can be used to verify the correct position of the capsule in the device, or transparent capsules can be used to provide feedback that the powder has been ejected during actuation. The most commonly used approach for multi-dose devices is a dose counter integrated into the device, which on the one hand provides the information that the loaded dose has been delivered and on the other hand displays the remaining doses. This system is designed to help patients better control their disease. Another approach aims to improve treatment adherence. To this end, the entire inhalation process was recorded for each actuation during the treatment interval to determine whether inhalation was performed with sufficient energy and

regularly. Analysis of audio fills allows to identify the duration of inhalation and the error of exhalation into the device immediately after inhalation. This could be used for supportive control of traditional training and for error detection by the physician, as this system reanalyzes each inhalation [92]. In addition, a 3D-printed device with acoustic recording was developed and a correlation between the airflow over the device and the frequency of the acoustic signals was calculated to evaluate the inhalation process [93]. Taking an outlook, the era of digitalism seems interesting for future device development and optimization. Currently, there is a great interest in equipping the devices with customized sensors to feedback the inhalation process and thus increase the therapeutic effect. These can be add-on sensors or sensors integrated directly into the device. A connection to the cell phone with the corresponding app is used to remind the patient of the next inhalation, to record the date and time of use or to record the airflow or the inhalation acoustics [94].

2. Aim and scope

Based on the situations described and the state of the art in the areas of formulation development, DPI concepts for powder deagglomeration, and patient safety, the goal of this work was to identify options for the above issues to overcome current drawbacks and improve pulmonary therapy. Since formulation development has always played an important role, the first study compared the traditional formulation process, in which the drug is milled and further mixed to form interactive mixtures, with a modern and common approach, namely spray-drying. Here, the active ingredient rivaroxaban was selected and both formulation techniques were compared with respect to the aerodynamic behavior of the developed formulations. Since, as previously reported, many drugs are available for asthma and COPD, this antithrombotic agent was used as an example to demonstrate new possibilities for pulmonary application and to use the lung area as an absorption pathway. This chapter explores the question of whether pulmonary embolism can be targeted through the use of a dry powder inhaler and a developed anticoagulant drug formulation. First, different batches were prepared and tested in-vitro to analyze the amount of particles that can potential enter the lungs. In the second step, a dry powder inhaler for the application of the formulations in rats was developed and 3D printed. Different formulations were tested in in-vivo experiments, and plasma concentrations over time were determined after application. It should be investigated whether rivaroxaban can be administered by this route so that a rapid onset and effect can be observed.

Besides the formulation side, where it was shown that formulation development by spray-drying is a promising way to develop easily aerosolizable formulations in the future, the second focus was on the comparison of DPIs with respect to their respective deagglomeration concept. Unfortunately, since many DPIs are available and marketed in a fixed combination with their respective formulations, little is known about which DPI works with which type of formulation, and developing a generic DPI is challenging. To this end, a prototype of a novel capsule-based DPI was developed for the application of various drug formulations. This DPI should have advantages over commercial capsule-based DPIs such that high FPF can be achieved regardless of the flow rate applied or the formulation used. The DPI should be able to deagglomerate interactive mixtures or formulations developed using particle-based methods such as

spray-drying. This chapter will also provide an overview of the state of the art in capsule-based dry powder inhalers. The novel DPI will be presented and compared with two marketed and commercially available DPIs that have been described in detail in the literature. Since they exhibit suitable deagglomeration behavior for their respective formulations, they are ideal candidates for comparing the novel DPI to the standard. Beside a commercial interactive blend formulation of albuterol sulfate – lactose two antibiotic formulations of amoxicillin and rifampicin were developed using the technology of spray-drying and tested. In this way, the deagglomeration behavior of a formulation on the market can be compared with the other two formulations, and statements can also be made about the powder aerosolization of formulations developed with particle-based approaches. Since each device tested in the study has a different geometry, intrinsic resistance to airflow and capsule motion, different deagglomeration concepts can be found. This study was intended to show which deagglomeration concept works with which type of formulation.

As mentioned before, most parts of the DPI are injection molded, and each part that is developed and integrated into the overall device has an impact on powder deagglomeration. Much research has been done, for example, on the dimensions of the air ducts, vortex breakers or classifiers, which together can be considered as a deagglomeration concept. Nevertheless, the critical factor of powder retention within the DPI is not yet known, so that when the device is actuated, a quantifiable amount of drug is not available for pulmonary treatment because it hangs within the DPI. While device geometries and the influence on powder deagglomeration are comparably better understood, the influence of surface properties (chemistry, texture) on powder ejection and deagglomeration is neglected. Since injection molding results in a smooth surface texture, this surface property was critically examined to determine whether the standard conditions for DPI development are contemporary or outdated, such that in addition to formulation development and device geometry, the device surface could be a critical adjusting screw to improve inhalation therapy. Therefore, the focus was on surface modification of the inside of this novel DPI to influence the interaction between the device surface and the formulation. To analyze the influence of chemical and also structural surface properties on powder deposition and deagglomeration, the devices were modified by cold plasma treatment. In this study, the activated/hydrophilic and

inert/hydrophobic surface properties produced by oxygen or octafluorocyaclobutane plasma represent the chemical change of the surface. To analyze the influence of surface texture, rough or smooth surfaces were generated by plasma etching or coating with different monomers. Since the novel DPI used for this study can be decomposed into four main parts, the influence of individual plasma-modified surfaces on powder retention at the respective surface can be analyzed.

Finally, the most critical factor, the patient's influence on the inhalation maneuver, was focused on. Since currently there is a lack in providing feedback to the patient after the inhalation process a prototype of a novel feedback mechanism for capsule-based DPIs is presented. Since the movement of the capsule is also decisive for powder deagglomeration in this class of device, and the speed of the respective capsule movement depends on the force and duration of the inhalation maneuver performed by the patient, this component seems to be ideal for feedback to evaluate inhalation. To evaluate the feedback mechanism, a Lupihaler device was chosen as a DPI device in which the capsule undergoes a rotational movement during inhalation due to the device geometry.

3. Fast onset of thrombolytic effect of efficiently inhalable spray-dried rivaroxaban powder formulations

3.1 Introduction

Rivaroxaban, marketed as Xarelto® and a class II BCS drug, is a direct Factor Xa inhibitor that limits thromboembolism by selectively inhibiting Factor Xa without the need for cofactors such as antithrombin [95,96]. With a high oral bioavailability of 80 - 100%, the product is approved in the EU and North America for the treatment and prevention of deep vein thrombosis and pulmonary embolism in adults [97,98]. Since currently only tablets of rivaroxaban are marketed, systemic drug availability subsequently leads to the elimination of emboli in the lungs, however also involving the known adverse effects such as acute renal failure [99]. In addition, the standard dose at the first treatment interval is two tablets of 15 mg per day, which may affect patient compliance and minimize the therapeutic effect. Since the clinical profile of pulmonary embolism requires emergency treatment, otherwise it can lead to cardiovascular arrest and death, oral medications in tablet form are not the appropriate option where a rapid onset of action is required.

A desirable alternative could be the drug administration via inhalation with the goal of reaching the lungs for a local and systemic effect [1,4]. The large surface area of the lungs and numerous capillaries result in a rapid absorption rate, and the absorbed drug can enter the bloodstream directly and avoid elimination by first-pass metabolism in the liver. Since the drug is delivered directly to the conducting zone of the lung, the required drug dose can be adjusted allowing for a reduction of adverse effects, too [8]. Due to the poor water solubility of rivaroxaban, formulating it as a dry powder for inhalation would be among the most suitable options [100,101]. To achieve adequate deposition in the lungs, drug particles usually micronized by a milling step, in order to reach an aerodynamic diameter < 5 µm [29]. However, this method has numerous shortcomings, including the production of cohesive particles that result in poor flowability and aerosolization efficiency due to the increase in total surface area and insufficient control of particle size, shape and morphology. In addition, grinding has been shown to affect the crystallinity of the material. Amorphous regions can form on

the surface of the crystals. Since such amorphous regions are thermodynamically unstable, recrystallization occurs, leading to crystal growth on the surface of the milled particles and the formation of solid bridges between the particles [31,102]. Another option for producing aerosolizable formulations is the method of spray-drying, which is used with the aim of optimizing particle properties for inhalation. While this method of formulation development has the disadvantage of low product yield as particles are exhausted by airflow during manufacture, the main advantages are products with a narrow particle size distribution, high purity, and easy scale up for commercial production [102–104]. However, also spray-dried particles tend to form agglomerates [105]. To partially overcome these problems and to produce flowable and deagglomerable formulations, the micronized active ingredient is usually mixed with larger carrier particles (e.g., lactose alpha-monohydrate) so that the active ingredient is adsorbed to the surface of these carriers and detaches from them during inhalation [34,106].

A first objective of this study was to design rivaroxaban particles by spray-drying and characterize for their physicochemical and inhalation properties. Such spray-dried particles were then investigated for their bioavailability after intrapulmonary administration in rats with a dry powder insufflator (DP Insufflator). Blood samples were collected over a 24-hour period after administration in order to obtain pharmacokinetic key parameter after pulmonary administration. In a final step, spray-dried particles were formulated as a binary mixture, using lactose particles with different particle size distribution (Inhalac® 70/251/400) to overcome the disadvantage of high powder retention in the capsule and/or inhaler using exemplarily the Breezhaler® DPI.

3.2 Materials & Methods

3.2.1 Materials

Rivaroxaban (riva) was purchased from Swapnroop Drugs & Pharmaceuticals (Maharashtra, India). To develop the coal suspension, Kohle-Compretten® (Klinge Pharma GmbH, Holzkirchen, Germany) were crushed before use. With the exception of water, which was purified in-house (Merck-Millipore Biocel A10, Burlington, MA,

USA), all solvents were HPLC grade. The Breezhaler® DPIs were a gift from Novartis Pharma GmbH (Nürnberg, Germany). The Inhalac® samples (70/251/400) were a kind gift from MEGGLE GmbH & Co. KG (Wasserburg am Inn, Germany) (Tab. S1).

3.2.2 Determination of the saturation solubility of the API in the different solvents

Saturation solubility of rivaroxaban was determined in various solvents. For this purpose the active ingredient was added in excess to the solvent. The samples were stirred at a constant temperature of 25°C for 24 h. Before analysis, the samples were filtered through 0.22 µm polytetrafluoroethylene syringe filter (VWR International GmbH, Darmstadt, Germany). 10 µL of the filtrate was analyzed and the API was quantified by HPLC analysis (section High-performance liquid chromatography analysis).

3.2.3 Spray-drying process for the different rivaroxaban formulations

Saturated solutions for the respective solvent were used for spray-drying different formulations of rivaroxaban. A B-290 spray-dryer equipped with a high-performance cyclone, a B-295 inert loop, a B-296 dehumidification unit (all Büchi, Flawil, Switzerland), and an anemometer (AF89-AD1AA13C0AA, Fluid components Intl. San Marcos, CA, USA) were used for spray-drying under inert atmosphere (N_2). For atomization each solution a modified three-fluid nozzle with a blocked internal channel (Büchi) was used. To develop spray-dried particles in different size ranges, either the feed rate or the atomization pressure of the gas were changed (Tab. 3).

Table 3: Parameters for the different spray-drying processes used (rivaroxaban = riva).

	Riva001	**Riva002**	**Riva003**	**Riva004**
Solvent [V/V (%)]	DCM:MeOH [50:50]	DCM:MeOH [50:50]	DCM:MeOH [80:20]	DCM:MeOH [80:20]
Feed rate API solution [mL/min]	7.4	2	7.4	7.4
Spray gas flow [L/h]	601	601	601	246
Outlet temperature [°]	40	40	40	40

3.2.4 Developing the interactive blends

To manufacture the binary blends, the API (raw (milled) or spray-dried) was mixed with the carrier lactose alpha monohydrate (Inhalac® 70/251/400) in a ratio of 1:99. For this, both materials were mixed in a sequential mixing process using a Turbula Mixer (Willy A. Bachofen, Muttenz, Schweiz) at 46 rpm for 5 min per mixing step until the mentioned mixing ratio was achieved.

3.2.5 3D printing settings for the development and printing of the dry powder insufflator

The device was drawn with Autodesk Inventor 2023 (Autodesk, Inc., California, USA). For printing a transparent model of the dry powder insufflator a masked stereolithography printer (SL1, Prusa, Partyzánská, Czech Republic) was used. A layer height of 50 µm was set for the printed geometry. After printing, post-processing steps were performed, which included cleaning the printed surface of excess resin with isopropanol and water, and then drying and curing the surface at 25 °C under UV conditions (CW1S, Prusa, Partyzánská, Czech Republic). The dry powder insufflator can be divided into three main components, the bottom part (loading chamber), the top part (connector) and the delivery pipe. A commercial syringe can be attached to the end of the loading chamber to inflate the powder with a defined volume of air during

dispensing. The delivery pipe is made of rigid stainless steel hollow tube with rounded tip and 120 degree bend. The pipe is hollow throughout with an inner diameter of 1 mm.

3.2.6 Test procedure for the aerosol classification with the Next Generation Impactor (NGI)

While 5 mg of the spray-dried rivaroxaban formulation was actuated, 30 mg of the binary blends were used. For the actuation with the Breezhaler, the formulations were filled in gelatin capsules size 3. To characterize the aerosol properties of the different formulations a Next Generation Impactor connected with two vacuum pumps (HCP 5) (all Copley Scientific Limited, Nottingham, United Kingdom) was used. Prior to the experiments, 15 mL of the dissolution medium was added to the preseparator, and each cup was coated with 1% glycerol-methanol solution (m/v). For quantification of the drug at different stages (cps - MOC), rivaroxaban particles were dissolved in acetone, except in DPI, which was rinsed with methanol. For each experiment, an actuation volume of 4 liters was used in combination with a flow rate of 100 L/min for the Breezhaler DPI, corresponding as closely as possible to USP conditions at a pressure drop of 4 kPa [81].

3.2.7 High-performance liquid chromatography analysis (HPLC)

The quantification of rivaroxaban deposited in the different NGI stages was performed by high-performance liquid chromatography analysis (Shimadzu, LC-2030C 3D Plus, Kyoto, Japan) using an RP18 column (Lichrospher 100 RP 18-5µ EC, 250 x 4.6 mm). For this, the photodiode array detector was set to 247 nm. The mobile phase of acetonitrile – water (45:55 v/v (%)) was set to a flow rate of 1.4 mL/min and the API was quantified by a column temperature of 40°C. To calculate the limit of detection (LOD) and the limit of quantification (LOQ) the values of the intercepts and the slope of the calibration curve were used. The LOD and LOQ were determined to be 1.21 µg/mL and 3.67 µg/mL [107].

3.2.8 Analysis of residual solvents using gas chromatography

Solvent residue analysis was performed using a Focus GC with TriPlus headspace autosampler (Thermo Scientific, Waltham, MA, USA). Chromatography was performed on a FS-CS-624 (CS Chromatographie service GmbH, Langerwehe, Germany) quartz capillary column (inner diameter = 0.32 mm, length = 30 m) coated with 6% poly(cyanopropyl)phenylsiloxane and 94% poly(dimethyl)siloxane. The parameters of the gradient program were set as follows: 1) 1 min isothermal elution at 50 °C, 2) ramp to 140 °C at 10 °C/min, and 3) 4 min at 140 °C. The temperature of the headspace incubator was set at 220 °C, and the incubation time before sampling was 14 min. The sampling volume was 1 mL and the split ratio was 1:5.

To investigate whether the amount of residual solvent in the prepared particles could be reduced below the required limits of 3000 ppm (MeOH) and 600 ppm (DCM) by drying, the formulations were post-treated in a vacuum-heated drying chamber (Binder VDL series, Tuttlingen, Germany) at 40 °C for 48 hours.

3.2.9 X-ray powder diffractometry

XRD was performed in transmission mode using the X'Pert MRD Pro from PANalytical (Almelo, The Netherlands) equipped with an X'Celerator detector. Nickel-filtered CuKα1 radiation was generated at 45 kV and 40 mA. Scanning was performed in a range from 10° to 30° 2Θ containing the most prominent reflection peaks, with a step size of 0.017°.

3.2.10 Scanning electron microscopy (SEM)

The samples were fixed with carbonaceous conductive paste on an aluminum sample holder and then coated with gold for two cycles of two minutes each. Subsequent imaging was performed in high vacuum using a Hitachi SU-3500 SEM (Hitachi Ltd., Tokyo, Japan). While the accelerating voltage for imaging the spray-dried particle batches was 5 kV, the binary blends were imaged at 10 kV. The magnification and working distance were adjusted as needed and are indicated on the SEM images.

3.2.11 Laser diffractometry (LD)

The geometric particle size distribution of the samples was determined with a LA-940 laser scattering particle size distribution analyzer (Horiba ltd., Kyoto, Japan) using following procedure: Rivaroxaban was suspended in a solution of 0.1 w/w (%) Span 80 in n-hexane in an amount that resulted in suitable attenuation of the laser beams. The suspension was stirred in a quartz cuvette during analysis (n = 5).

3.2.12 In-vivo experiment procedure

All animal experiments were performed in accordance with the EU Directive 2010/63/EU on the protection of animals used for scientific purposes. In-vivo experiments were performed at the animal facility of the University of Burgundy/Franche-Comté (Besançon, France) in compliance with French legislation on animal experimentation within the framework of the Exp An N2 EA4267 2015-2020 project, previously approved by the CEBEA 58 ethics committee. 450 g male Sprague-Dawley albino rats were acclimated to laboratory conditions in a ventilated room at 22 °C and 45% relative humidity with a 12:12 hour light-dark cycle for one week prior to the start of the experiment. Rats were given free access to food and water.

Rivaroxaban blood concentrations after administration of the selected formulations were determined as follows: The rats were kept fasting for one hour before the start of the experiment. Each formulation was loaded at 2 mg/kg body weight into the insufflator and delivered (n = 4).

After loading and preparing the pulmonary insufflator, a charcoal suspension was applied to the anesthetized rat. The cannula of the insufflator was inserted into the trachea just proximal to the carina until the cannula arch rested against the incisors. After removing the speculum, the loaded dose was delivered by pressing on the syringe plunger so that the powder was delivered from the insufflator. The delivered dose was determined by differential weighing of the insufflator.

Blood samples were taken from the tail vein at specific time intervals (0, 5, 20, 40, 60, 120, 240, 480, 1440 minutes after administration), mixed with citrate and centrifuged

at 1500g immediately. Plasma samples were frozen and stored at -20°C until further analyses. The respective rivaroxaban concentrations were determined using Coamatic Heparin kit Factor Xa inhibitor assay (Haemochrom Diagnostica, Essen, Germany).

The analytical procedure was performed according to the kit - manufacturer's instructions. The calibration curve was constructed using 5 calibration standard concentrations in plasma (0, 28.4, 77.3, 113.1, 157.4 ng/mL), also obtained from Haemochrome Diagnostica. Plasma samples were pipetted into 96-well plates, and after application of the heamochrome reagent media, absorbance was measured at 405 nm using an EnSpire® multimode plate reader (Perkin Elmer, Massachusetts, United States). Plasma concentrations were calculated from the calibration curve.

3.2.13 Data processing

The NGI plots show the relative powder deposition of rivaroxaban on the different stages (capsule – MOC). Error bars indicate one standard deviation. Cumulative undersize plots from S1 to MOC were created and linearized by log transformation of the stage boundaries and probit transformation of the relative abundances. For calculating the fine particle fraction ($FPF_{TD/EF}$ (fraction of particles with an aerodynamic diameter < 5 µm of the total dose/emitted fraction)), a linear regression model was used, as described in USP <601> [81]. All experiments were performed in triplicate, unless otherwise reported. To determine statistically significant differences in the relative powder deposition for the different formulations in the different stages of the NGI (capsule - MOC) after actuation with the Breezhaler DPI, results were compared using Kruskal-Wallis test followed by Dunn`s test ($p < 0.05$) [108,109]. A two-tailed, unpaired t-test was performed to analyze the in-vivo data for statistically significant differences ($p < 0.05$), (Prism 8.0.2, GraphPad software).

3.3 Results

3.3.1 Determination of the solubility

The results of the saturation solubility study show that rivaroxaban is poorly soluble in mostly all common solvents. While it is known that rivaroxaban is soluble in dimethyl sulfoxide the high boiling points limits a potential use for spray-drying [110]. While the

solubility of this drug was poor in the pure solvents methanol (MeOH) or dichloromethane (DCM), a mixture of both at a mixing ratio of 50:50 v/v (%) or 20:80 v/v (%) resulted in improved solubility of rivaroxaban, so these two mixed solvents were used to develop the spray-dried batches (Tab. 4).

Table 4: Determination of the saturated solubility of rivaroxaban in various solvents.

Solvent	**Solubility [mg/mL]**
H_2O (pH 7)	0.01 ± 0.00
Methanol (MeOH)	0.40 ± 0.00
Acetonitrile (ACN)	1.17 ± 0.01
Acetone	1.10 ± 0.03
Dichloromethane (DCM)	2.90 ± 0.09
MeOH:DCM (75:25 v/v (%))	2.07 ± 0.04
MeOH:DCM (50:50 v/v (%))	9.62 ± 0.23
MeOH:DCM (20:80 v/v (%))	23.34 ± 0.78
Acetone:MeOH (90:10 v/v (%))	1.50 ± 0.01

3.3.2 Characterization of the different spray-dried particle formulations

Four formulations of pure rivaroxaban were prepared by spray-drying using different process parameters. The milled material had an undefined and irregular particle shape and all cases spray-drying enabled to transform into spherical particles (Fig. 5).

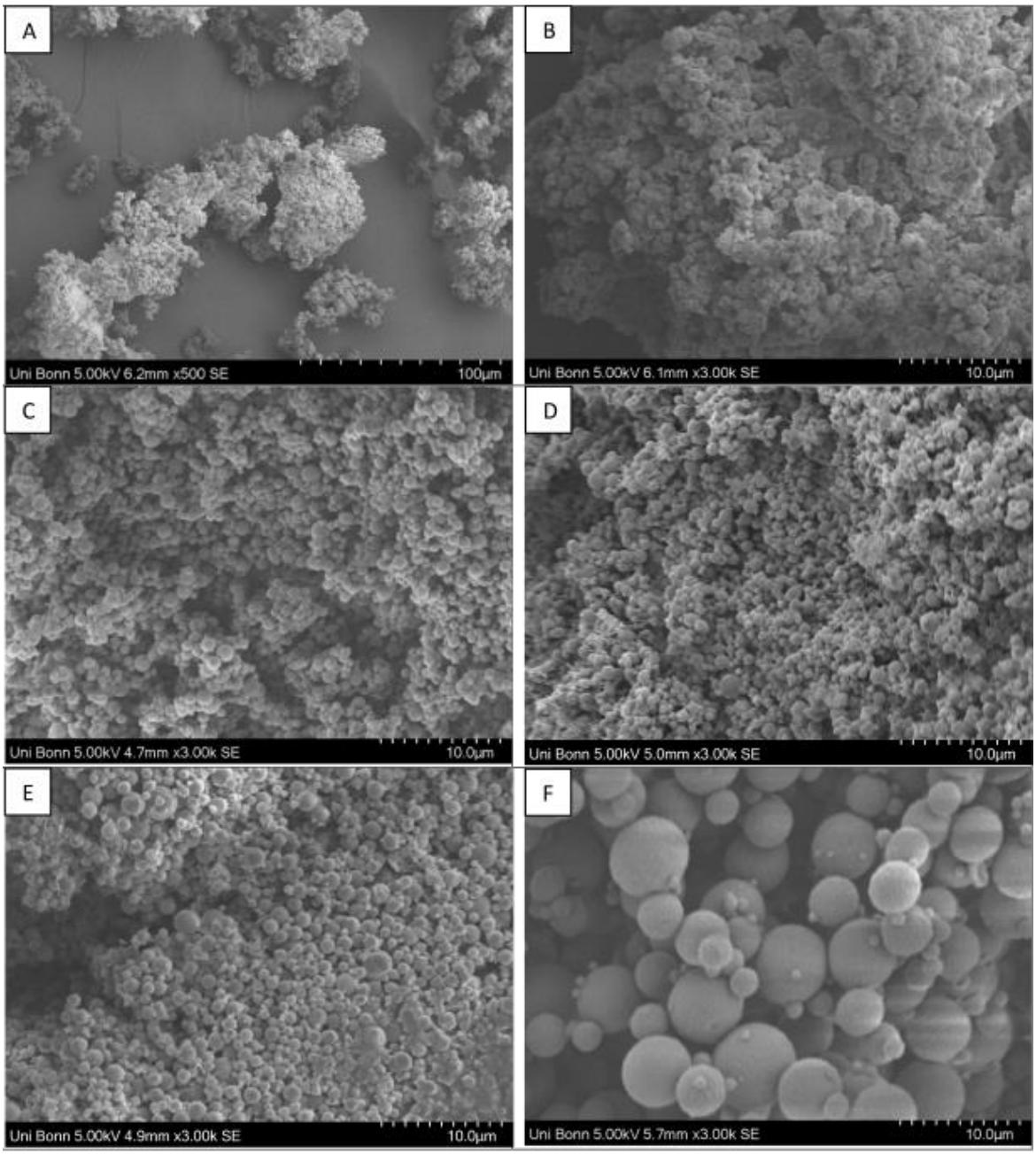

Figure 5: SEM images of the milled rivaroxaban material (A, B) and the different batches of rivaroxaban manufactured by spray-drying (riva001 = C; riva002 = D; riva003 = E; riva004 = F).

While riva004 was composed of larger particles, particles of one micron in diameter and even below were found in the other batches (Tab. 5). Accordingly, laser diffraction data indicated that all formulations had a D_{50} in the lower micrometer range. Primary particles in the upper nanometer range were also observed for the milled material

rivaroxaban. While the narrowest particle size distribution was found for the riva002 formulation, the distribution of riva004 was wider. Since the particle size distribution was similar for the two batches riva001 and riva002, the influence of the feed rate on the obtained particle size was not as crucial as the spray gas flow parameter, since a decrease in atomization pressure resulted in the formulation with the largest particle size.

Table 5: Particle size distribution of the milled material and the manufactured formulations.

	Milled material	**Riva001**	**Riva002**	**Riva003**	**Riva004**
D_{10} [µm]	0.08 ± 0.00	0.55 ± 0.20	0.16 ± 0.00	0.95 ± 0.26	1.96 ± 0.43
D_{50} [µm]	0.72 ± 0.03	1.10 ± 0.08	0.47 ± 0.02	1.46 ± 0.03	5.90 ± 0.47
D_{90} [µm]	2.11 ± 0.17	1.93 ± 0.15	1.09 ± 0.03	3.56 ± 0.23	10.62 ±1.49

Spray-drying of the various batches yielded either particles with a quantifiable residual amount of methanol that did not exceed 850 ppm or particles that contained no quantifiable residual amount. Vacuum drying allowed the remaining solvent to be completely removed. While the batches with smaller particle diameters had a maximum DCM content of 1% immediately after the spraying process, the formulation riva004 had a residual DCM solvent content of about 3%. After drying, the residual DCM content of formulation riva001-003 had fallen below the limit of 600 ppm. For formulation riva004, 48 hours was not sufficient to reduce the DCM content below the limit and 2700 ppm was detected (Tab. S2). The X-ray diffractograms of the different formulations show that the spray-dried batches with the small and similar particle size distribution (riva001 - 003) were amorphous, while the milled material and batch riva004 with the largest particle size were at least partially crystalline (Fig. S1).

3.3.3 Characterization of the in-vitro aerosolization behavior of the different formulations manufactured

Aerosolization of the milled material or the binary blends of rivaroxaban milled material with the various lactose carrier particles (Inhalac® 70/251/400) resulted in high powder deposition in the induction port (IP) or in the preseparator (Fig. S2). Although the use of carrier particles increased the emitted fraction, the FPF was not affected and was similar to that of the milled material (Tab. 6).

Actuating of the different batches of the pure spray-dried rivaroxaban resulted in a high powder deposition within the DPI of approximately 20% in each case. While a low amount of powder was quantified in the IP for the formulations riva001 - 003, 60% of the active ingredient was deposited in this fraction for formulation riva004 (Fig. 6). While riva003 showed the lowest powder deposition in the preseparator, this formulation resulted in the highest amount of particles that could potentially reach the lungs and leads to the highest $FPF_{TD/EF}$ (Tab. 6). While for the milled material the amount of deposited particles decreased from stage 1 to 4, an opposite effect was observed for the pure spray-dried batches riva001-003, which have a similar particle size distribution as the milled material, resulting in an increased deposition rate from stage 1 to 4).

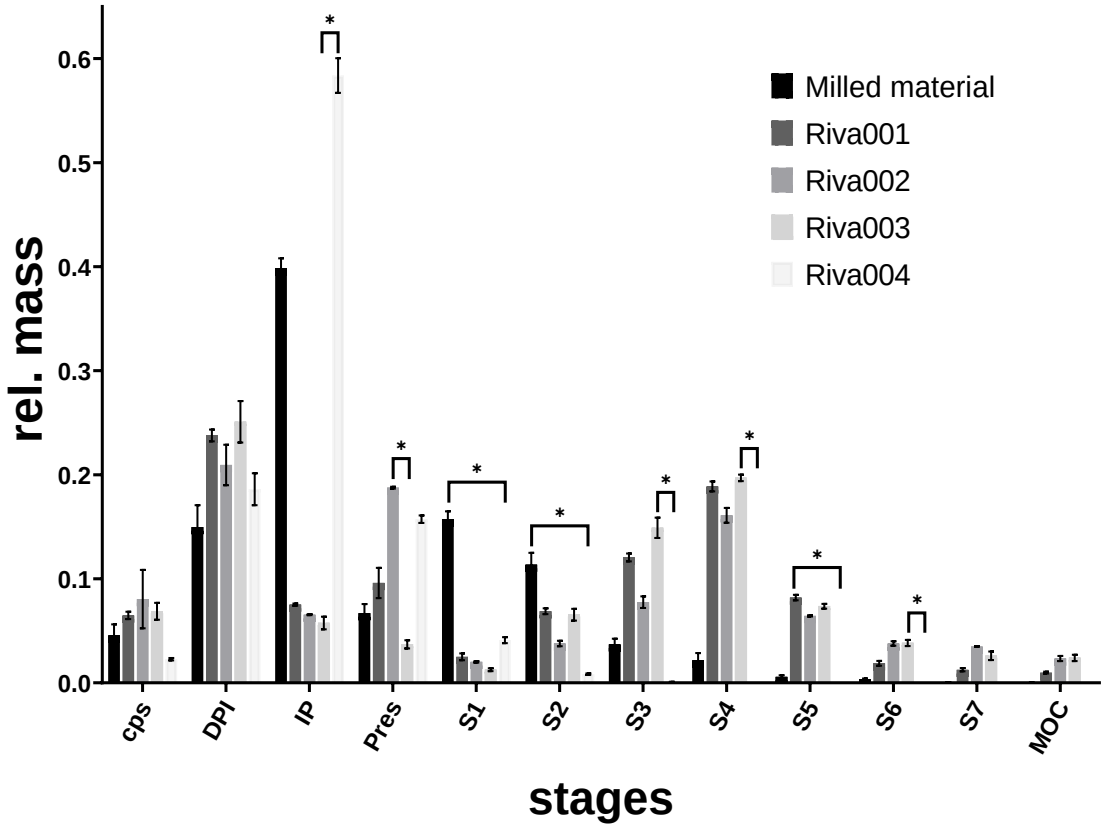

*Figure 6: NGI results obtained with the Breezhaler when actuating the milled material and the different spray-dried formulations (riva001 – 004), (capsule = cps; dry powder inhaler = DPI; induction port = IP; preseparator = Pres), (*p < 0.05).*

3.3.4 In-vivo testing of selected formulations

After intratracheal administration in-vivo in rats the spray-dried particle formulations (rive003 and riva004) exhibited a very rapid onset within 5 minutes followed by a plateau phase over about 4 hours (Fig. 7). After this sampling point, a decrease in plasma concentration is observed up to the 24-hour time point. The riva003 formulation, which had amorphous particle properties and a smaller particle size, resulted in a slightly higher blood concentration, which however was statistically not significant. In addition, in both cases the highest concentration was detected within the first hour after application (Fig. 7, Tab. 7).

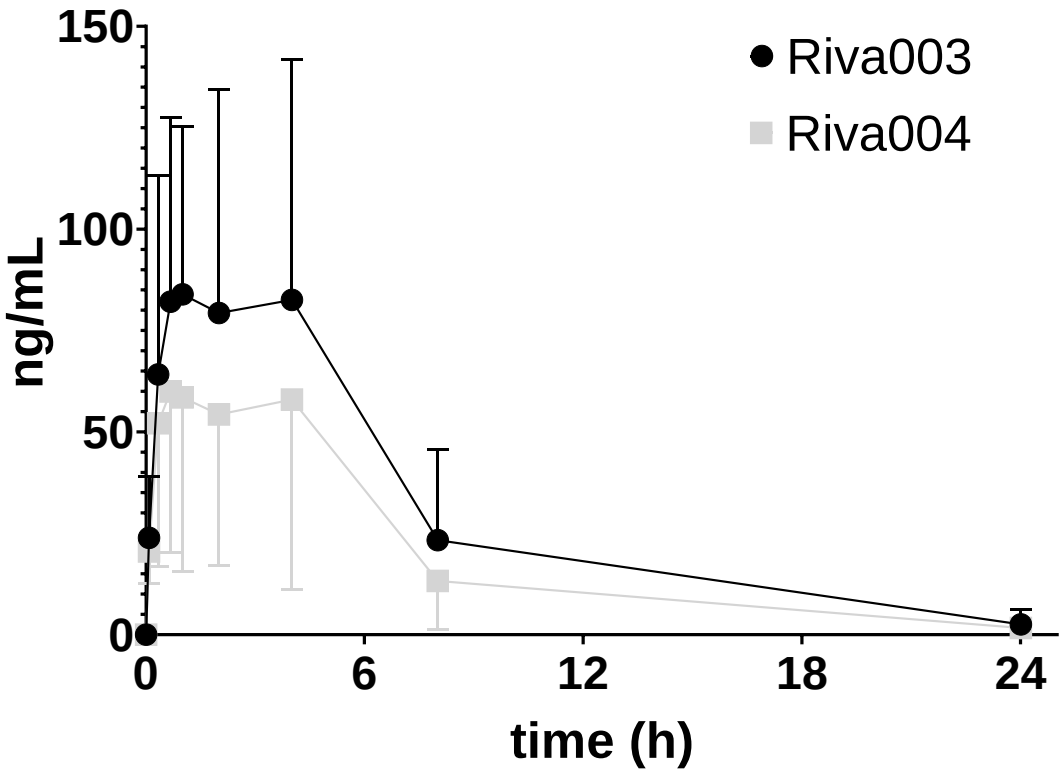

*Figure 7: Rivaroxaban plasma concentration versus time profile over a 24-hour period for the formulations riva003 and riva004, (*p < 0.05).*

*Table 7: Pharmacokinetic parameters determined for both formulations used, (*p < 0.05).*

Formulation	**Dose (mg/kg)**	**C_{Max} (ng/mL)**	**T_{Max} (min)**	**AUC_{0-t} (µg*h/mL)**	**AUC_{0-inf} (µg*h/mL)**	**$t_{1/2}$ (h)**
Riva003	2	83.9 ± 41.4	60	0.726 ± 0.537	0.745 ± 0.566	4.992 ± 2.823
Riva004	2	60.0 ± 39.8	40	0.479 ± 0.347	0.492 ± 0.342	5.368 ± 4.709

3.3.5 Riva003 binary mixtures using different carrier particles

Riva003 was subsequently formulated as binary mixtures using different lactose carriers (Inhalac® 70/251/400) to increase the emitted fraction and also the FPF_{TD}. SEM analyses revealed in all blends the spherical active ingredient being adsorbed on the carrier surface (Fig. 8).

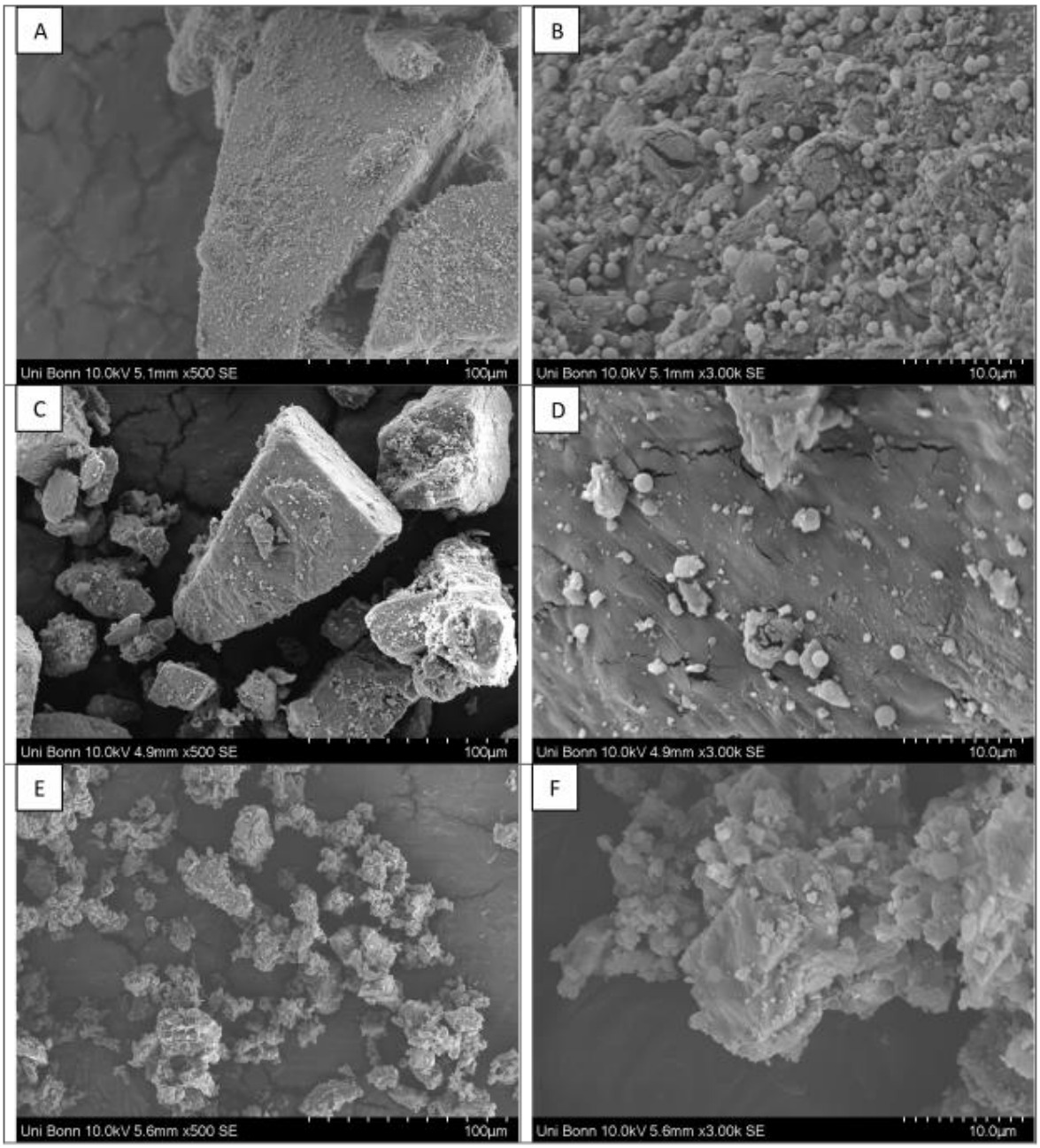

Figure 8: SEM images of the different binary blends consisting of riva003 and the different lactose batches in two different magnifications: (A, B) riva003 – Inhalac® 70; (C, D) riva003 – Inhalac® 251; (E, F) riva003 – Inhalac® 400.

A trend of decreasing deposition of the active ingredient in the preseparator with decreasing size of the carrier particles was observed for the different binary blends prepared. While the binary mixture formulated with Inhalac® 70 resulted in a powder deposition of about 70% in this fraction, only 20% of rivaroxaban was found in the

formulation with Inhalac® 400. While riva003 exhibited high powder deposition within the DPI, a higher emitted fraction was observed for all binary blends (Fig. 9). The mixture riva003 - Inhalac® 400 reduced the deposition in the IP and also in the preseparator and led in turn to the highest FPF_{TD} (Tab. 6).

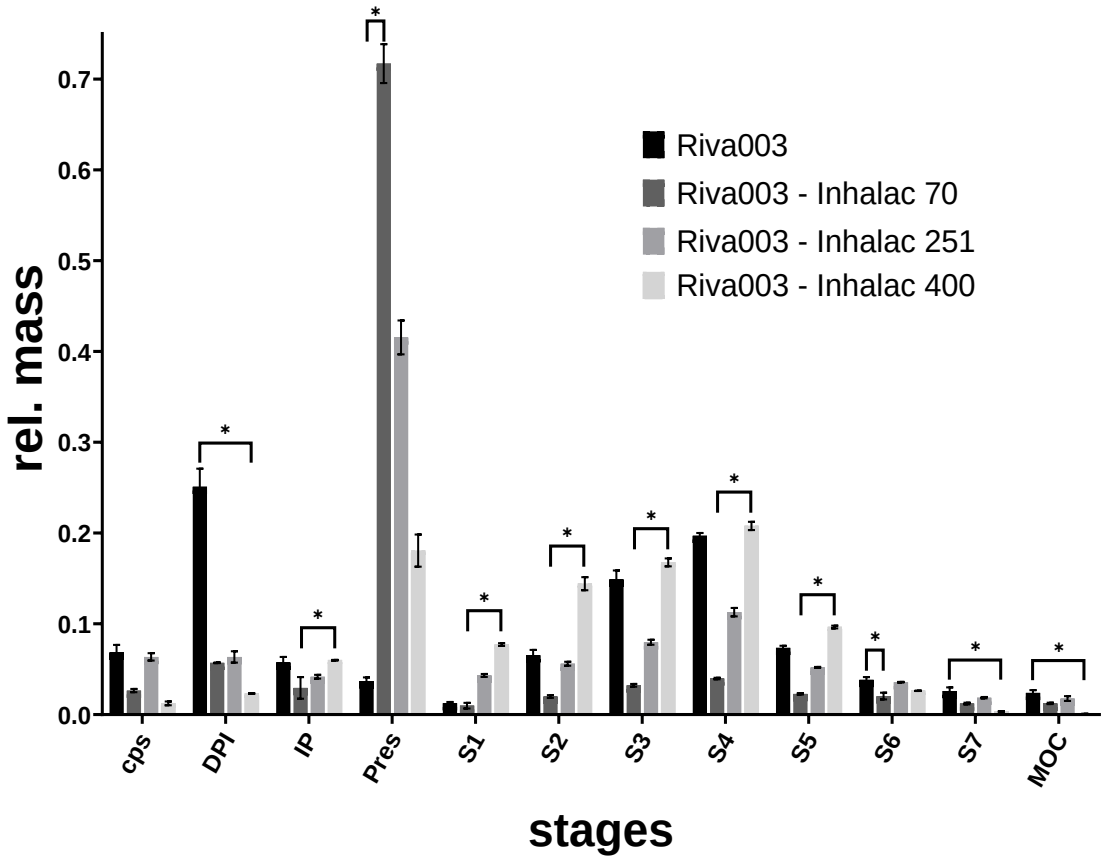

*Figure 9: NGI results obtained with the Breezhaler when actuating the binary blends consisting of the spray-dried batch riva003 ± Inhalac® 70/251/400, (capsule = cps; dry powder inhaler = DPI; induction port = IP; preseparator = Pres), (*p < 0.05).*

Table 6: Fine particle fraction of the total dose and emitted fraction for each formulation tested using the Breezhaler DPI (rivaroxaban = riva).

Batch	FPF_{EF}	FPF_{TD}
Milled material	15.8 ± 3.5	12.7 ± 1.9
Raw material + Inhalac 70	11.1 ± 4.1	10.2 ± 3.8
Raw material + Inhalac 251	16.6 ± 0.6	14.9 ± 2.0
Raw material + Inhalac 400	16.6± 0.6	16.0 ± 0.6
Riva001	67.4 ± 3.1	47.0 ± 2.2
Riva002	59.1 ± 1.7	42.0 ± 1.2
Riva003	79.7 ± 3.1	54.2 ± 2.1
Riva004	0	0
Riva003 + Inhalac 70	16.5 ± 1.5	15.1 ± 0.4
Riva003 + Inhalac 251	39.8 ± 1.5	34.7 ± 1.3
Riva003 + Inhalac 400	62.7 ± 1.3	60.5 ± 1.3

3.4 Discussion

The combination of rivaroxaban being a BCS class 2 drug with the fact that the solubility in diverse common organic solvents is also rather limited, leads typically to micronization via milling being the first choice for a dry powder formulation. Despite this ease of handling, this method of formulation development has several drawbacks, usually resulting in cohesive particles with poor flow properties, uncontrollable particle size, shape and morphology, and unsuitable aerosolization behavior. For this reason the particles were also prepared by spray-drying. Since this process allows manipulation and control of particle size distribution, particle density, shape, moisture content, flowability and crystallinity, this type of formulation can be more easily deagglomerate and convince by easily accessible FPF's [44]. The advantages over the traditional formulation technique are clearly visible, so that instead of fine particle fractions of 20-30% achieved with the binary blends, FPF's of about 60% are possible [38]. Here, sufficiently high solubilities of 9 and 23 mg/mL were achieved by the respective solvent mixtures, allowing for stable spray-drying processes with an acceptable feed concentration.

Impactor results when comparing the milled material with and without the different lactose carriers showed that this formulation technique is seemingly not suitable, since the high powder deposition in the IP or preseparator indicates insufficient powder

deagglomeration. In the experiments performed, this could be due to the fact that the cohesive or adhesive (drug-lactose) particle interactions are too large to be overcome by a conventional DPI.

Considering the mentioned advantages of spray-drying, actuation of the spray-dried particle formulations with the Breezhaler resulted in high $FPF_{EF/TD}$ in the case of the formulations riva001 - 003, with the best aerosolization characteristics found for batch riva003. Nevertheless, the classical problems of this type of formulation occurred, namely the retention of the powder in the capsule and in the DPI. Similar to the milled material, these enhanced interactions could be due to the fact that a small particle size associated with a larger particle surface area was also achieved after spray-drying, so more particle-particle/ -capsule or -DPI interactions may occur [105]. This is underscored by the fact that formulation riva004, which has the largest particle size among the formulations prepared for this study, has the lowest powder retention in the capsule and DPI, while batches riva001 - 003, which all have similar particle size, result in similar retention in both compartments.

Since both formulation techniques have advantages, either the high emitted fraction (traditional approach) or a suitable aerosolization behavior (spray-drying) achieved during inhalation, a combination of both approaches was used to combine the different advantages in a final formulation. Pure riva003 was the most efficient in terms of FPF, as only a small amount of the powder deposited in the oropharyngeal area in-vitro, this formulation was subject to further formulation steps aiming for increasing the fraction delivered and also the FPF_{TD}. For this purpose, this batch was also formulated as binary blends using the aforementioned lactose carriers. Impactor results of the rivaroxaban Inhalac® formulations showed a similar trend in terms of deposition rate as the milled material using the different batches of Inhalac®. The use of large carrier particles for the drug in the nanometer range resulted in insufficient detachment of the drug from the carriers, causing a large amount of the mixture to settle in the preseparator. Matching the size of the carrier particles to that of the drug resulted in improved aerosolization behavior, with Inhalac® 400 achieving the highest FPF with a d_{10} of about 1 µm, which can be attributed to improved drug detachment and powder

aerosolization. The effect of the improved deagglomeration behavior of the spray-dried drug compared to that of the milled material is clearly seen in the increased amount of particles having suitable aerodynamic properties to achieve the lung in-vitro.

While it has been shown that the formulation of binary blends of spray-dried particles formulated as an interactive mixture can result in a higher FPF_{TD}, at the same time, a quantitatively smaller amount of drug can enter the lungs since the amount of carrier limits the dose that can be used for a given capsule. Therefore, the influence of the mixing ratio between the drug and the carrier should also be investigated in future studies. In the experiments performed, the mixing ratio of 1:99 (drug:carrier) should mask the properties of the manufactured drug particles in a higher amount than those of the carrier, which is shown in the trend of powder deposition in the preseparator.

A rapid absorption rate of the drug in-vivo was also observed, reflected by high plasma concentrations and a low T_{Max}, indicating a significant deposition in the deep lung followed by dissolution of the particles in the lungs. Although no significant differences in plasma concentrations were observed between the two formulations, there is a tendency for a smaller particle size and/or amorphous drug particles to result in a comparatively higher C_{Max} concentration. It should also kept in mind that the DP Insufflator is only a simple delivery device that does not have a real deagglomeration concept like the Breezhaler, so the drug was still rapidly bioavailable even when the formulation was not deagglomerated as efficiently as with the commercial DPI. This aspect of using an insufflator, combined with the potentially more difficult handling to deposit the particles in the lungs of rats, may explain the plasma concentrations measured in this study resulting in a comparatively lower inhibition of endogenous factor Xa, as the IC50 in rat plasma of 126 ng/ml calculated in a previous study after i.v. application was not reached [111]. Nevertheless, this route of administration can be shown to result in plasma concentrations similar to those obtained in a previous study in rats following oral administration by gavage. Since a similar plasma profile was obtained, it can be concluded that the particles dissipate rapidly after deposition in the lungs, otherwise a higher T_{Max} would be expected without a plateau concentration over 4 hours [112].

Comparison of the pharmacokinetic parameter T_{Max} from the experiments performed in this study with values obtained after oral administration of a tablet containing various concentrations of rivaroxaban in humans and found in the literature suggests that a rapid onset of action could be achieved by this route of administration. Since the T_{Max} after pulmonary administration is lower at 40-60 min compared with tablet administration (120-240 min), and blood concentrations were measurable as early as 5 min, the rivaroxaban dry powder formulation could be used as emergency therapy for the treatment of pulmonary embolism [100,113–115]. This becomes important, for example, in COVID-19 patients who are at increased risk of developing pulmonary embolism, so this type of formulation could be an option for acute treatment or thromboprophylaxis in COVID-19 patients [116,117].

The question of whether the dissolution behavior and initial absorption rate of rivaroxaban are comparatively more likely to be high or low because rivaroxaban is a BCS II agent could be answered by comparing the plasma profile achieved with that of another BCS II agent also administered by inhalation. In previous studies reported in the literature, budesonide was inhaled by adults suffering from asthma. Since a C_{Max} of about 1.7 ng/ml was measured here after inhalation of a dose of 800-1000 µg of the active ingredient, it can be assumed that the plasma concentrations of 84 ng/ml of rivaroxaban achieved in this study after pulmonary administration are to be regarded as high [118,119].

Ultimately, this study suggests a novel therapeutic approach for the treatment of pulmonary embolism, in terms of the application of the formulation. The development of a potential formulation and the associated in-vivo results open up new possibilities for the treatment of the aforementioned disease. Further studies need to confirm whether pulmonary administration of rivaroxaban actually allows for higher local doses with lower systemic doses that also limit subsequent side effects such as renal failure.

3.5 Conclusion

This study suggests that administration of rivaroxaban by inhalation may be a potential future option to increase drug levels in the therapeutic range of interest for pulmonary embolism. Despite the poor solubility of this active ingredient, the preparation of

aerosolizable powder formulations by spray-drying could be an option. This study demonstrated that high FPF and measurable blood concentrations after deposition in the lung were achieved with different formulations. A rapid onset of action could lead to therapy in which only a minimal dose of the drug is inhaled, resulting in minimal side effects such as renal failure because only the lungs are affected. Future studies need to provide a differential picture of the local and systemic drug concentration available after inhalation of rivaroxaban and then analyze the potential pharmacological effects on inhibition of Factor Xa to limit thromboembolism, particularly in the lung.

4. Interim summary

The study conducted was able to show that the selected method for formulation development has a significant influence on the aerodynamic behavior of the respective particle formulations and thus on the lung targeting. The spay-drying method as a modern manufacturing process allows the production of formulations that deagglomerate more easily than conventional interactive mixtures, so that instead of a high powder deposition in the oropharynx, this amount can reach the lungs. Although milling is currently the method of choice, spray-dried particles have also been shown to be suitable for mixing with carrier particles to overcome cohesive particle interactions. Since this type of formulation resulted in increased FPF compared to the interactive mixtures of milled particles with lactose, it can be said that the adhesion forces between the drug and lactose might have been reduced due to the minimized contact points of spray-dried spherical particles.

Apart from this, inhalation of a formulation with suitable aerodynamic properties, but with a DPI that does not have a true deagglomeration concept, also results in inadequate powder aerosolization. Although many DPIs are currently available, there is still a lack of knowledge about which type of device achieves adequate results with which type of formulation because delivery systems are marketed in a fixed combination. Therefore, the studies performed only analyze the lung deposition of a formulation with the respective DPI and no comparative studies are performed to show how the deagglomeration concepts work for different formulations developed with different manufacturing processes. The aim of the following study was to highlight the state of the art on this topic in general and to show advantages and disadvantages of selected DPIs.

5. State of the Art in Capsule-Based Dry Powder Inhalers: Deagglomeration Techniques and the Consequences for Formulation Aerosolization

This work was published as:

Groß, R.; Berkenfeld, K.; Schulte, C.; Ebert, A.; Sule, S.; Sule, A.; Lamprecht, A. State of the Art in Capsule-Based Dry Powder Inhalers: Deagglomeration Techniques and the Consequences for Formulation Aerosolization. Pharmaceutics 2022, 14, 1185, doi:10.3390/pharmaceutics14061185.

5.1 Overview of the work

The aim of this work was to analyze the market situation of capsule-based dry powder inhalers and the formulations actuated, and to compare the influence of the development technique used on the overall aerosolization behavior of the individual formulations. Since the therapeutic success depends on many factors and the patient has a major influence on the output of the inhalation maneuver, pulmonary delivery systems are marketed in a fixed combination of device and the particular formulation. In addition, changing the DPI when actuating the same formulation would result in altered powder deagglomeration and thus altered FPF. Since many DPIs with different device geometries, air channels, capsule motions, and intrinsic resistances to air flow are available today, the question arose as to which deagglomeration concept would provide suitable aerosolization for which type of powder formulation.

To this, the study aimed to compare three capsule-based DPIs in terms of their in-vitro deagglomeration behavior for different formulations. Since the devices have different geometry and structure, different capsule movements occurred during actuation, which ultimately led to different deagglomeration concepts. While the Lupihaler (rotating capsule movement) and the Handihaler (axial capsule movement) are already on the market, a novel DPI with an oscillating capsule movement during actuation was tested. To evaluate the different deagglomeration concepts, a commercial interactive mixture of albuterol sulfate, an in-house developed spray-dried particle formulation of rifampicin, and also amoxicillin were tested, the latter being further formulated as a binary mixture in a second step. To analyze the influence of inspiratory air flow on powder deagglomeration, a low (50 L/min) and a high (100 L/min) flow rate were tested and the relative powder deposition in each stage and the FPF were determined.

Measurement of the airflow across the devices at a pressure drop of 0 - 8 kPa shows that the Handihaler and the novel DPI, with 0.046 and 0.044 $kPa^{0.5}$ L/min, respectively, can be classified as high intrinsic resistance DPIs, while the Lupihaler, with an intrinsic resistance of 0.018 $kPa^{0.5}$ L/min, represents the low intrinsic resistance class of devices.

Testing the albuterol sulfate formulation with the different DPIs resulted in high powder deposition in the preseparator in each case. While at 50 L/min this powder deposition was similar for the three devices, at 100 L/min the lowest amount of powder was found in the aforementioned stage for the novel DPI, resulting in the highest FPF_{EF} of 41.3 ± 2.4 here. When the binary mixture of amoxicillin - lactose was actuated with the different DPIs, it was found that the oscillatory motion of the capsule resulted in the highest powder ejection, so regardless of the flow rate tested, this DPI achieved the highest FPF. While 40% or more of the drug settled in the preseparator with the interactive albuterol sulfate mixture, the self-developed amoxicillin formulation appears to deagglomerate more readily, as a lower mass was quantified in this section. This is also underlined by the fact that a decrease in powder deposition was observed at the higher flow rate, regardless of the equipment used.

The last formulation (rifampicin) tested in this study resulted in comparatively high powder retention in the capsule, possibly due to the fact that the particle size of the spray-dried drug without carrier particles is in the lower micron range, which allows more capsule-particle interactions due to the larger particle surface area available. Of all the DPIs tested, the highest powder retention in the capsule was observed for the novel DPI with approximately 10% quantified drug, which was independent of the airflow tested. Despite this hereby reduced amount of drug available for pulmonary treatment, the novel DPI achieved the highest FPF_{EF} when actuated at 50 or 100 L/min. Since a large amount of drug was found in the induction part after actuation with the Handihaler, this DPI resulted in the lowest amount of particles having suitable aerodynamic properties to reach the lungs.

From the device side, it can be concluded that the oscillating capsule motion in the novel DPI leads to low powder retention in this compartment in the case of interactive mixtures, since the powder can be easily shaken out. Moreover, under the conditions tested in the study, the deagglomeration concept of this DPI resulted in the best powder aerosolization described by the FPF, regardless of what type of formulation was used. It has been shown that the development of dry powder inhalers with a suitable deagglomeration concept may result in a greater amount of drug being delivered to the

lungs, which could improve therapy compared to DPIs, which are currently the state of the art.

Apart from the device side, it has been shown that the formulations developed for this study using the method of spray-drying with or without the use of lactose in a second step resulted in formulations with better aerosolization behavior compared to the standard formulations manufactured in the industry. While grinding the active ingredient and making interactive mixtures resulted in FPFs around 30%, designing the particles in a way that matches the particle properties to those required for inhalation seems to be more promising, as FPFs of at least 50% were achieved.

Author Contributions: Roman Groß (R.G.), Kai Berkenfeld (K.B.), Christoph Schulte (C.S.), Anselm Ebert (A.E.), Sunita Sule (S.S.), Ameet Sule (A.S.) and Alf Lamprecht (A.L.)

Conceptualization, R.G., K.B., A.E. and A.L.; methodology, R.G. and K.B.; formal analysis, R.G.; investigation, R.G. and K.B.; resources, A.E. and A.L.; data curation, R.G.; writing—original draft preparation, R.G.; writing—review and editing, R.G., K.B., C.S., A.S., S.S. and A.L.; supervision, A.S. and A.L.; project administration, A.E. and A.L.; funding acquisition, A.E. and A.L.

6. Interim summary

It was shown that in addition to formulation properties, a suitable deagglomeration concept is also crucial for successful lung targeting with the particular formulation. Thus, it was demonstrated that DPI manufacturing should focus more on this delivery tool in the future, as DPIs are not only a piece of plastic, but can also play a major role in increasing the amount of particles that have the right aerodynamic properties to reach the lungs. Although the complexity of the interaction between such devices and formulation has been demonstrated, these DPIs could improve therapy by not only increasing drug delivery but also allowing drug delivery independent of inspiratory flow rate through tools such as a classifier and a vortex breaker combined with a suitable capsular motion during actuation. However, it has also been shown that the critical factor of powder retention within the DPI could not be overcome with the aforementioned equipment modifications. Here, the problem might be more in the properties of the DPI surface and the resulting interactions with the formulation. Since there is currently no commercial surface coating for DPIs and these phenomena are not yet fully understood, the next step was to investigate the DPI surface properties and make various chemical and structural modifications, as well as analyzing the effects on powder retention on the modified surface and overall powder aerosolization.

7. Effect of texture and surface chemistry on deagglomeration and powder retention in capsule-based dry powder inhaler

This work was published as:

Groß, R.; Berkenfeld, K.; Schulte, C.; Ebert, A.; Sule, S.; Sule, A.; Lamprecht, A. Effect of Texture and Surface Chemistry on Deagglomeration and Powder Retention in Capsule-Based Dry Powder Inhaler. AAPS PharmSciTech 2022, 23, 281, doi:10.1208/s12249-022-02436-0.

7.1 Overview of the work

This study focused on the influence of texture and chemistry of DPI surfaces on powder retention in the device and deagglomeration behavior. Today, many devices are marketed in a fixed combination with the intended formulation to minimize potential sources of error. Despite the progress and optimization achieved, the development and realization of an ideal DPI is challenging, as many mechanisms are not yet fully understood and require further investigation. While one focus has always been on increasing powder deagglomeration and thus FPF, which can be influenced by DPI geometry and additionally installed classifiers or vortex breakers, the important point of minimizing powder retention within DPI has gained in importance over the last decade. Retention of powder in inhalation devices can significantly compromise therapeutic outcomes due to mechanical anchoring of the powder to the device surface and/or electrostatic charge generated during dispersion of the powder. To overcome these problems, various methods such as “dry powder” or “polytetrafluoroethylene (PTFE)” coating have been developed and tested. Despite promising and interesting results, the critical factor of powder adhesion to the inhaler wall is still not fully understood, so there is no commercially approved surface modification for DPIs to reduce powder retention.

Based on this, the surface of the novel DPI presented in the previous study was modified with a low-pressure plasma system. Since this DPI can be divided into four main parts, it is easier to see which surface modifications affect the powder deposition, as the DPI components can be plasma treated separately.

The species generated during the plasma process, such as ions, radicals, etc., which have a temperature close to room temperature, can interact with the surface of the starting material, resulting in altered surface properties, which can be chemical or structural. On this basis, oxygen plasma was used to generate hydrophilic surfaces, while an octafluorocyclobutane (OFCB) process was intended to generate hydrophobic surfaces. Both processes also cause the surface topography to become irregular and the roughness to increase. To estimate not only the effects of a plasma-induced rough surface, but also the extent of a smooth and non-adherent surface produced by plasma coating, the monomer hexamethyldisiloxane (HMDSO) was used for in situ

polymerization. To analyze the changes in aerosolization and retention of the powder, a spray-dried particle formulation of rifampicin was tested. For this in-vitro characterization, the DPI was connected to an NGI and a flow rate of 50 L/min was set until a volume of 4 liters was reached.

Visual comparison with a scanning electron microscope of the mesh of the DPI showed that similar and smooth surfaces were found for the untreated surface and after plasma treatment with HMDSO, while oxygen and OFCB resulted in roughened surface textures, with nanotexturing being more dominant after oxygen plasma treatment.

Measurement of the contact angle with deionized water on the untreated surfaces and after plasma treatment with oxygen or OFCB resulted in different values for the wettability. While oxygen increased the wettability compared to the untreated material (from 60° to 30°), the OFCB plasma treatment resulted in a higher contact angle of about 120°. This hydrophobic coating remained constant over time, in contrast to the hydrophilic surface modification.

Treatment of the upper unit (mesh, classifier, mouth piece) of the novel DPI with the different plasma processes partially resulted in altered deagglomeration behavior of the device for the tested formulation compared to the untreated DPI. While similar powder deposition was observed when using the untreated DPI and the DPI treated with HMDSO plasma, oxygen and OFCB plasma resulted in increased powder deposition in the IP and preseparator. In addition to this increased powder deposition in the above stages, lower powder deposition was also observed in the treated mouth piece. While under the conditions tested in this study, the plasma treatment of the upper unit has a significant effect on powder aerosolization, the treatment of the capsule chamber with the different plasma processes showed no differences in powder deagglomeration.

To determine whether the lower powder deposition in the mouth piece or the increased amount of powder in the IP and preseparator was a combination effect of all the parts treated in the upper unit of the DPI, or depended only on the influence of one part modified with plasma, the following experiment was conducted to determine the

component that could have a decisive influence on powder deagglomeration after surface treatment. Therefore, the focus was on the oxygen process, and for each experiment only one treated part was installed and tested, while the rest of the DPI remained untreated. The results show that an oxygen plasma treated mouth piece resulted in lower powder deposition on the treated surface without changing the deagglomeration behavior for the powder, so that no differences in powder deposition were observed in the IP and preseparator compared to the untreated device. In contrast, a modified classifier or even a mesh resulted in more drugs being detected at the above stages, but not as much as when the entire upper unit was treated with plasma.

In summary, this study has shown that the DPI surface properties influence the powder retention in the device and also the deagglomeration behavior. Since similar aerosolization behavior was obtained for the powder when the surface was plasma treated with oxygen (hydrophilic surface) or OFCB (hydrophobic surface), the chemical properties seem to have less influence than the texture. This is also underlined by the fact that both experiments with smooth surfaces resulted in similar deagglomeration of the powder, which was different from the two processes with rough surface texture.

Author Contributions: Roman Groß (R.G.), Kai Berkenfeld (K.B.), Christoph Schulte (C.S.), Anselm Ebert (A.E.), Sunita Sule (S.S.), Ameet Sule (A.S.) and Alf Lamprecht (A.L.)

Conceptualization: R.G., K.B., A.E., and A.L.; methodology: R.G. and K.B.; formal analysis: R.G.; investigation: R.G. and K.B.; resources: A.E. and A.L.; data curation: R.G.; writing original draft preparation: R.G.; writing—review and editing: R.G., K.B., C.S, A.S., S.S., and A.L.; supervision: A.S. and A.L.; project administration: A.E. and A.L.; funding acquisition: A.L.

8. Interim summary

In summary, these three chapters have shown that not only aspects of formulation and equipment design affect powder aerosolization, but also surface properties have a major impact on powder deagglomeration and retention in the DPI. It can be concluded that this issue has been underestimated so far and should be further investigated, as the change in surface texture has a significant impact on micron-scale particles and can both improve and worsen powder deagglomeration, so that the selection of the right surface texture seems to be essential for the generation of an ideal DPI. As mentioned earlier, a delivery system consisting of a slightly deagglomerated formulation and a DPI with an excellent deagglomeration concept has no therapeutic benefit if the patient does not use the device as described by the manufacturer.

Given the current lack of applications and capabilities related to patient safety and inhalation maneuver assessment, a prototype feedback mechanism for capsule-based DPI is presented in the next chapter. Since the movement of the capsule during actuation is directly related to the inhalation maneuver, this component was focused on and recorded to evaluate inhalation.

9. Improving capsule-based dry powder inhalers: A new in-vitro method of assessing inhalation success conditions by tracking capsule rotation during actuation

9.1 Introduction

According to the World Health Organization, approximately 235 million patients suffer from asthma and 65 million patients suffer from COPD [120]. Due to the low systemic effects, the inhalation therapy is mainly used to treat these diseases [121]. Although there are many different DPIs with different functions for powder deagglomeration on the market, a successful inhalation process depends on more factors than the formulation and device attributes [27]. One critical issue is adherence to treatment, which depends primarily on the patient's physiological conditions and ability to use the device [122,123]. Therefore, a reason for inadequately controlled asthma is poor inhalation technique. This may include several factors, such as improper preparation technique or performing an inhalation with inadequate force and length, resulting not only in poor clinical outcomes but also in higher healthcare costs and wasted medications [124–126]. A previous study indicated a fundamental problem with inhalation using this class of device. Although they used a different device (Turbohaler®) for their study compared to ours, they indicated that actuation of a formulation with a DPI and a low flow rate of 30 L/min or less resulted in a reduced therapeutical success. They postulated that optimal medication with this class of device is achieved with an airflow greater than 30 L/min or, in the best case, greater than 60 L/min, which resulted in an increased amount of respirable powder particles [127]. Because of these potential causes of error leading to uncontrolled fluctuations in therapeutic success, a meaningful feedback mechanism is needed to assess whether the inhalation maneuver was successful. In recent years, several different approaches to feed back the inhalation have been developed to improve the therapeutical success. The most commonly used approach for multidose devices is a dose counter integrated into the device, which on the one hand provides information that the loaded dose has been delivered and on the other hand shows the remaining doses. This system is designed to help the patient to achieve better disease control [128]. In the last years another approach has been established with the aim of

recording the biological noise of the chest and the trachea during bronchoconstriction to recognized pathophysiological changes [129,130]. Since the patient would always have to carry a microphone with analyzer for this purpose and the system can thus only be used to detect emergency and acute medication, this is not feasible for a patient in real life. Therefore, other strategies such as feedback the inhalation with acoustic recordings were developed. In a recent study, the Discus® device was used to develop an acoustic method that includes the determination of changes in acoustic features during inhalation as markers of bronchoconstriction and exacerbation of disease progression [131]. Another approach aims to improve treatment adherence. For this purpose, the entire inhalation process was recorded for each actuation during the treatment interval to determine whether inhalation was performed with sufficient energy and on a regular basis. Analysis of audio fills allows to identify the duration of inhalation as well as the error of exhalation into the device immediately after inhalation. This could be used for supportive control of traditional training and for error detection by the physician, as this system reanalyzes each inhalation [92]. In addition, an acoustic capsule-based 3D printed device was developed and a correlation between the air flow over the device and the frequency of acoustic signals was calculated to assess the inhalation process [93]. Despite the feedback of force and duration of actuation, there is one drawback that could be critical for this approach. Since only the frequency of the sound generated by the airflow through the modified inhaler geometry during inhalation is controlled and the movement of the capsule is neglected, spontaneous sticking of the capsule in the inhaler during actuation would not be assessed.

Hence, to overcome this disadvantage and to verify the actuation conditions and detect inadequate inhalation profiles in-vitro, the central aim of this study was to demonstrate an approach to develop a feedback mechanism for a capsule-based DPI (Lupihaler®) to determine the flow rate and duration of the inhalation performed. Therefore, the possibility of follow-up should facilitate the evaluation of inhalation and could be used in future attempts to increase the success of therapy. Since the deagglomeration of the powder in this class of device depends mainly on the strength and duration of inhalation and the resulting capsule movement, as well as the collisions of capsule and

powder with the inhaler wall, the number of capsule rotations during inhalation was recorded and the capsule rotation frequency was calculated. Since a longer inhalation time leads to more such collisions, this measurement was hypothesized to be a surrogate parameter for these interactions, since only capsule movement was defined as a response parameter for inhalation assessment [57,72]. For this purpose, a small neodymium magnet was inserted into a 3D printed holder and the entire assembly was placed into a capsule. The voltage generated during rotation was induced in a coil placed on the DPI and could be readout via a connected oscilloscope. To verify the new readout system, three different formulations were tested and in-vitro correlations were made between the actuation volume and the number of capsule rotations, as well as the rotation frequency and the applied flow rate. In addition to two marketed binary salbutamol sulfate mixtures (Cyclocaps®, Ventilastin®), a self-developed spray-dried rifampicin formulation for inhaled therapy was also tested and classified. To determine the limits of the feedback system for different inhalation conditions, different actuation volumes (0 - 4 liters) and flow rates (50/80/100 L/min) were tested in-vitro with the NGI. In addition, to evaluate the inhalation process in terms of the amount of respirable particles, the above interactions were correlated with the FPF_{EF} (fraction of the emitted mass with an aerodynamic diameter < 5 µm) obtained from the NGI experiments.

9.2 Materials and Methods

9.2.1 Materials

The Cyclocaps® (PB Pharma GmbH, Meerbusch, Germany) and Ventilastin® (MEDA Pharma GmbH & Co. KG, Bad Homburg, Germany) formulations were purchased from a pharmacy, for spray-drying, the rifampicin was ordered from TCI (Tokyo, Japan). Sodium dihydrogen phosphate monohydrate (Carl Roth GmbH, Karlsruhe, Germany), di-sodium hydrogen phosphate dihydrate, orthophosphoric acid 85% and triethylamine 99% (TH. Geyer GmbH & Co.KG, Chemsolute, Renningen, Germany) were obtained from VWR. The ascorbic acid was obtained from Sigma Aldrich (St. Louis, MO, USA). The water used was purified internally with a purification system (Merck-Millipore

Biocel A10, Burlington, MA, USA), and all other solvents were HPLC grade. The Lupihaler® device was purchased from Lupin Limited (Mumbai, India).

9.2.2 Spay-drying of the rifampicin particles

Rifampicin was spray dried as reported [132]. Briefly summarized, 10 g of the drug was suspended in a given volume of 798 mL isopropanol and sonicated in an ultrasonic bath (Typ DT 106, Bandelin electronic, Berlin, Germany) under controlled temperature conditions (25°C) for 10 min. To obtain a constant temperature a thermostat (DC 10, Haake Technik GmbH, Vreden, Germany) was used for the water exchange. The suspension was spray-dried under inert atmosphere (N_2) using a Buchi B-290 (Flawil, Switzerland) equipped with a high-performance cyclone, a dehumidifier unit B-296 (Buchi), an inert loop B-295 (Buchi) and an anemometer (AF89-AD1AA13C0AA, Fluid components Intl. San Marcos, CA, USA). For atomizing the suspension, a three-fluid nozzle (Buchi) was used where the inner channel was blocked. During the whole manufacturing process the suspension was stirred constantly.

9.2.3 3D printing settings for the development and printing of the magnet holder prototypes and the Lupihaler DPI

To obtain the geometry for printing the Lupihaler DPI, a computed tomography scan of the injection molded device was performed. For printing both, a transparent Lupihaler device and the magnet holders, a masked stereolithography printer (SL1, Prusa, Partyzánská, Czech Republic) was used. A layer height of 50 µm was set for each printed geometry. After printing, post-processing steps were performed, which included cleaning the printed surface of excess resin with isopropanol and water, and then drying and curing the surface at 25 °C under UV conditions. Three different magnet holder prototypes were designed and printed to investigate the influence of geometry on the deagglomeration behavior of a spray-dried rifampicin formulation (Fig. 10). To guarantee a fix position of these set up in the middle of the capsule during inhalation the holder has small feet, which keep the distance to the bottom of the capsule.

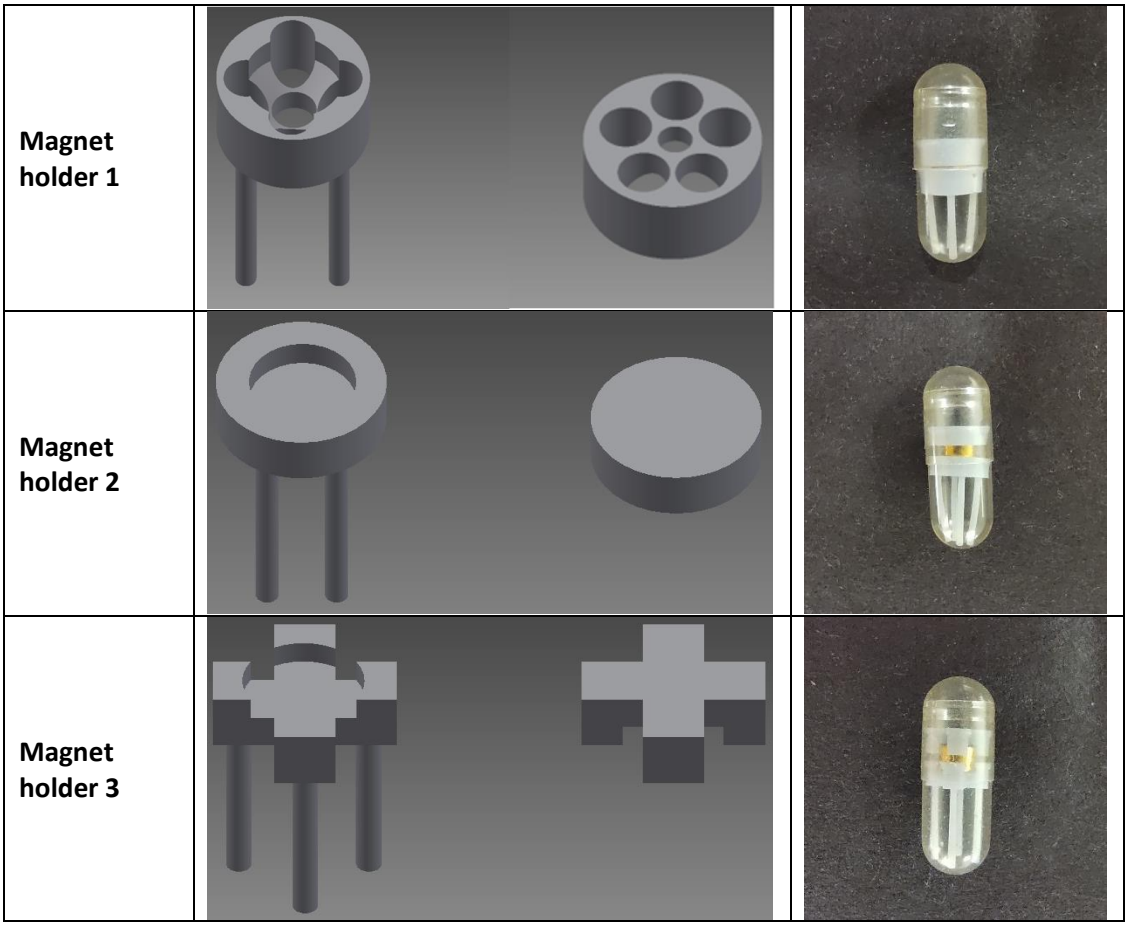

Figure 10: Geometry of the different magnet holders.

9.2.4 Test procedure

10 mg of the rifampicin formulation (5 mg per capsule half), 60 mg of a Ventilastin® or Cyclocaps® formulation (30 mg per capsule half) were filled into size 3 gelatine capsules and actuated with a RS01 equivalent DPI (Lupihaler). For recording the number of rotations, a neodymium magnet (Magnet experts, England, Tuxford, 3mm dia x 2mm thick) was inserted into a 3D printed magnet holder and this set up was placed in the middle of the capsule (Figs. 10, 11). To characterize the aerosol properties of the formulations, a Next Generation Pharmaceutical Impactor (NGI) (Copley Scientific Limited, United Kingdom, Nottingham) was used. Each cup was coated with a 1% glycerol-methanol (m/v) solution to minimize rebound effects of the impacted powder particles. Prior to the experiment, 15 mL of the recovery medium was

placed in the preseparator (pres). To characterize the deagglomeration behavior of the inhaler for the powder with and without the magnet system, we dissolved the powder particles from each compartment (capsule - MOC) obtained from the full NGI experiments in the case of rifampicin with a methanol-ascorbic acid (0.5 % m/v) solution and for the salbutamol formulations with a methanol-miliQ water mixture (1:1 % v/v). To evaluate the feedback system with counting the capsule rotations and calculating the frequency during actuation, flow rates of 100, 80 and 50 L/min and actuation volumes of 0 - 4 L were applied. The FPF_{EF} was set as the response parameter to compare the powder deagglomeration of the respective formulation at different inhalation conditions.

On the outside of the inhaler, a coil (470 µH and 0.28 A, Conrad electronic stores GmbH & Co.KG, Bonn, Germany) connected to the oscilloscope (PicoScope 2000, 2204 A, 2 chanel, Pico technology, Cambridgeshire, England, PC connected, 10 MHz) was placed directly in the center of the extended side of the capsule compartment to record capsule rotations during inhalation (Fig.11). All experiments were performed as triplicates, unless reported otherwise.

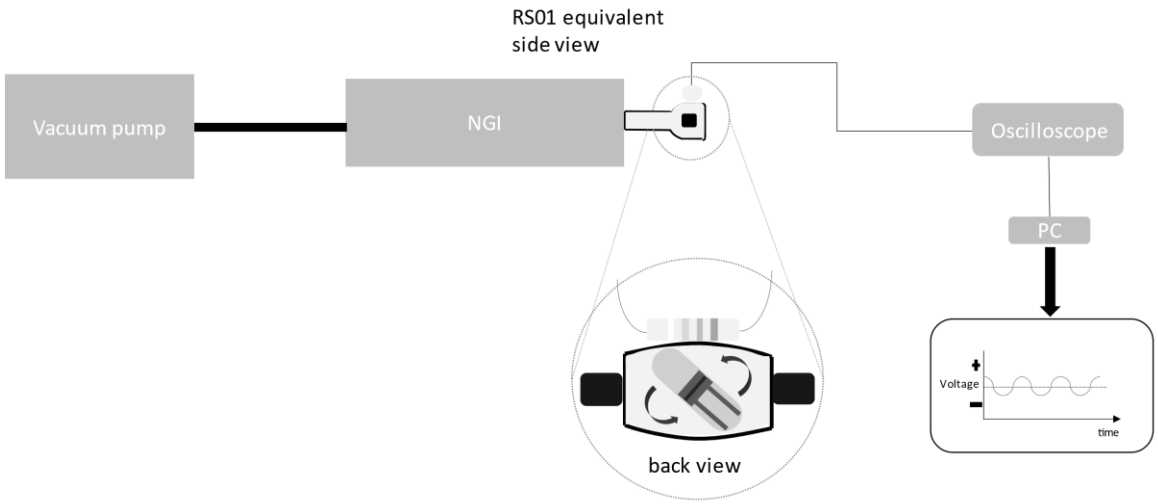

Figure 11: Schematic representation of the experimental setup.

9.2.5 Frequency measurement and evaluation of the feedback mechanism

The feedback system consisted of a neodymium magnet, the 3D printed magnet holder, a coil and an oscilloscope connected with a PC. For counting and evaluating the signals obtained, a self-made program (Microsoft Visual Studio 2019, 16.8; programming language: C#) was established, which counted each peak and calculated also the rotations per minute (rpm) and the resulting frequency. To set the experimental conditions, a fixed threshold was defined for each flow rate, above which the signal was counted as a peak.

To verify the hypothesis that this set up can record the rotations of the spinning magnet, and to validate the analysis program so that the maxima and minima of voltage peaks from the set threshold are counted, the magnet was placed on a stirring rod and set to a fixed number of rotations and compared with the counted results of the analysis program.

To analyze the voltage peaks received from the oscilloscope and to cross-validate our programed counting system, a transparent and modified 3D printed Lupihaler (the bottom part has a flat surface, the recess in which the capsule is pierced has been omitted) was used to record the capsule rotations with a camera of a mobile phone (Samsung Galaxy s20, 960 fps). A frame-by-frame analysis was performed to count the rotations of the capsule and compare them with the number of respective induction voltage peaks recorded by our feedback system.

9.2.6 Scanning electron microscopy

Samples were prepared by fixing with carbonaceous conductive paste on an aluminum sample holder and coated with gold by sputtering for two cycles of two minutes each. Subsequent imaging of the different formulations was performed in high vacuum using a Hitachi SU - 3500 SEM (Hitachi Ltd., Tokyo, Japan). While the accelerating voltage was set at 10 kV, the magnification and working distance for each sample were adjusted as needed and can be found on the SEM images.

9.2.7 HPLC analysis

For all formulations the quantification of the active ingredient was carried out with high-performance liquid chromatography (HPLC) (Waters 2695 Separations Module) using a RP18 column (Lichrospher 100 RP 18-5µ EC, 250 x 4.6 mm). To detect the APIs, a Waters 996 photodiode array detector was used and set to 337 nm in the case of rifampicin, whereas salbutamol was detected at a wavelength of 275 nm. While the column temperature for rifampicin was hold by 25 °C, the salbutamol sulphate was analyzed at 40°C.

Although for rifampicin the mobile phase was a mixture of phosphate buffer pH 5.2/methanol/acetonitrile (33/50/17 % v/v/v) and set to a flow rate of 1 mL/min [132], the mobile phase for salbutamol consisted of a phosphate buffer pH 3.0/methanol (80:20 v/v (%)) and was set to an isocratic flow rate of 1.4 mL/min. For salbutamol, the limit of detection (LOD) and limit of quantification (LOQ) were calculated using the values of the intercepts and the slope of the calibration curve. The LOD was calculated to be 0.10 µg/mL, while the LOQ was found to be 0.32 µg/mL.

9.2.8 Statistics

To show statistically significant differences in relative powder deposition between the magnet holder system and normal use of the instrument without the holder setup, the results were compared using a one-way ANOVA ($p < 0.05$) (Prism 8.0.2, GraphPad Software).

9.3 Results

9.3.1 SEM imaging of the tested formulations

While the Cyclocaps® and Ventilastin® formulations are formulated as binary mixture, a spray-dried, carrier free rifampicin formulation was also tested with the new feedback system. SEM pictures (Fig. 12a – c) show the shape and particle size of the three formulations. For the rifampicin, micro particles are recognizable.

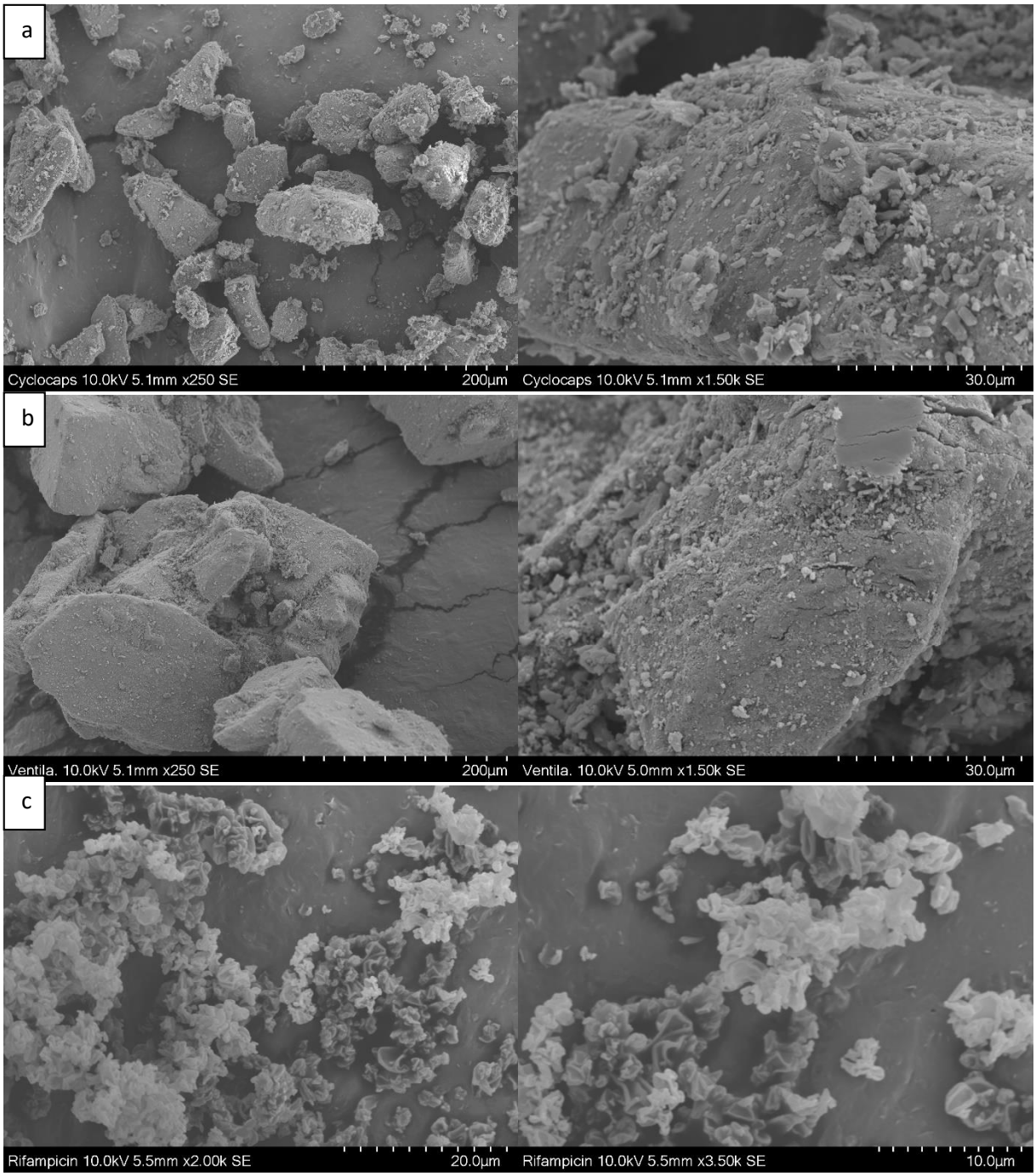

Figure 12: Scanning electron microscope images of the tested formulations: a = Cyclocaps®, b = Ventilastin®, c = spray-dried rifampicin for two different magnifications.

9.3.2 Establishing the new feedback mechanism

Figure S3 shows the alternating voltage induced in a coil by a neodymium magnet rotating nearby, either on a stirring rod (a: 8 Hz) or after placement inside a capsule (b:

40 Hz). The results confirm the idea that, first, the modified capsule rotates during actuation despite the weight increase from 47.5 ± 0.3 mg for an empty capsule to 206.8 ± 1.3 mg for the modified capsule and, second, with the experimental setup it is possible to detect the voltage induced in a coil by the rotation of the magnet. The transition from the maximum to the minimum voltage indicates the spin of the magnet from the north to the south pole and reverse, where the magnitude of the amplitude resulted from the speed of the rotating system. In comparison, the results show that there were no differences in the considered waveform of the signals from these setups. The time span between two maximum or minimum represents a full revolution of the magnet, which would be equivalent to one full capsule turn in our following experiments.

To verify the measuring principle that we detect the capsule rotation, a 3D printed transparent Lupihaler equivalent was actuated and the capsule rotation during the inhalation time was recorded for 6 experiments using the camera of a mobile phone. Visual evaluation by counting the capsule rotations using single image analysis and comparison with the number of peaks recorded by the oscilloscope in the same experiments showed no differences (data not shown). Also, it could be seen that the rotational velocity of the capsule slowed down somewhat after hitting the inhaler wall and increased again due to the sustained flow rate, indicated in our recordings by a randomly decreasing amplitude intensity combined with an increasing peak width.

9.3.3 Determination of the influence of the magnet holder geometry on the deagglomeration of the rifampicin formulation using the Lupihaler device

The tested flow rate for this device of 100 L/min in figure 13 was chosen because it is closest to actual European Pharmacopeia conditions at a pressure drop of 4 kPa (> 100 L/min) and is within the calibrated range of the NGI (30 - 100 L/min) [133]. The NGI results indicate that a higher powder retention in the capsule is observed in the case where the magnet holder was inserted. The FPF_{EF} for the different experiments performed show that when the magnet holder was inserted, no differences are observed compared to the experiment without the set up. Despite these similarities in

the FPF_{EF}, differences in the powder deposition in the individual stages (cps – moc) can be observed. Due to the greater similarities in the individual fractions compared to the setup without the use of the magnet, magnet holder 1 was used for all of the following tests.

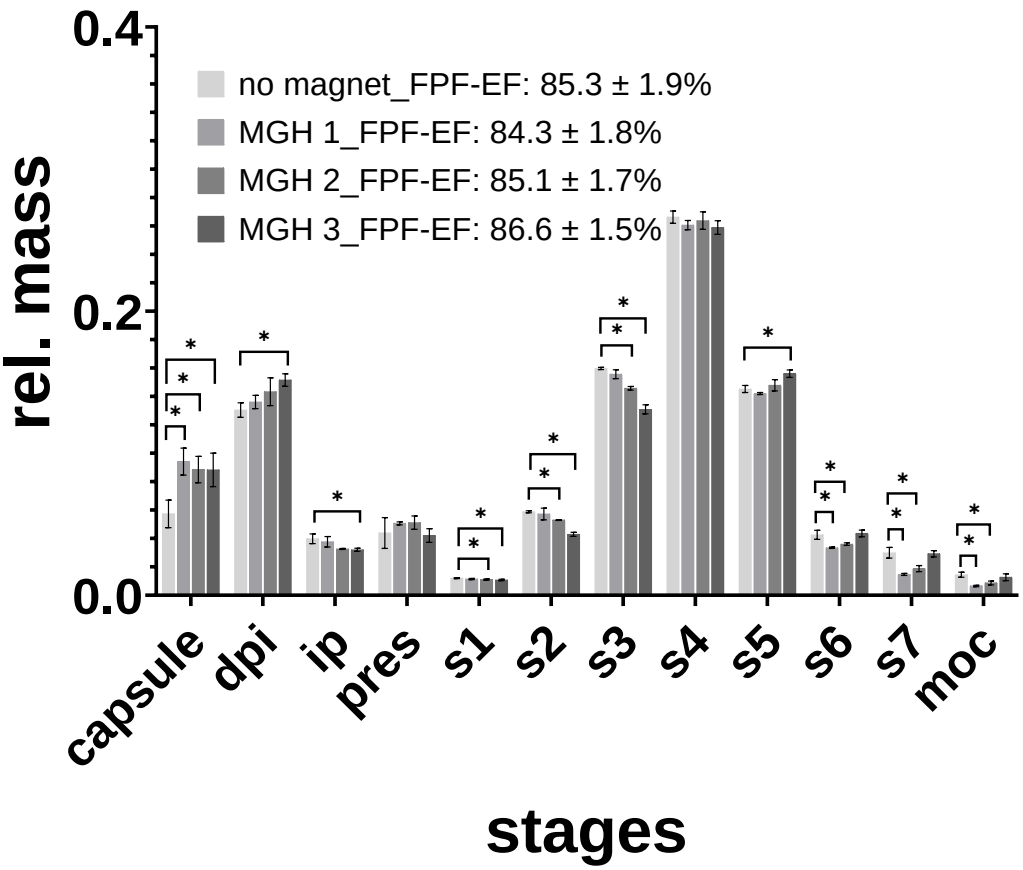

*Figure 13: NGI results with the Lupihaler device and the spray-dried rifampicin using this setup normally (without magnet system) and with different magnet holders for an air flow of 100 L/min and an actuation volume of 4 liter, (*p < 0.05,* one-way ANOVA*).*

9.3.4 Correlation between capsule rotation/the rotating frequency, the actuation volume and the FPF_{EF}

The results in figure 14a, b show that the feedback system works independently of the formulation placed inside the capsule. The correlation coefficients indicate that it is possible to detect any changes in airflow during inhalation, whether it is the duration or

the applied flow rate of the actuation. Comparing the number of capsule rotations and the calculated rotation frequency for the different formulations tested, it is noticeable that despite a powder filling weight of 60 mg for the two binary mixtures and only 10 mg for the rifampicin, the same values are obtained for the given actuation volume.

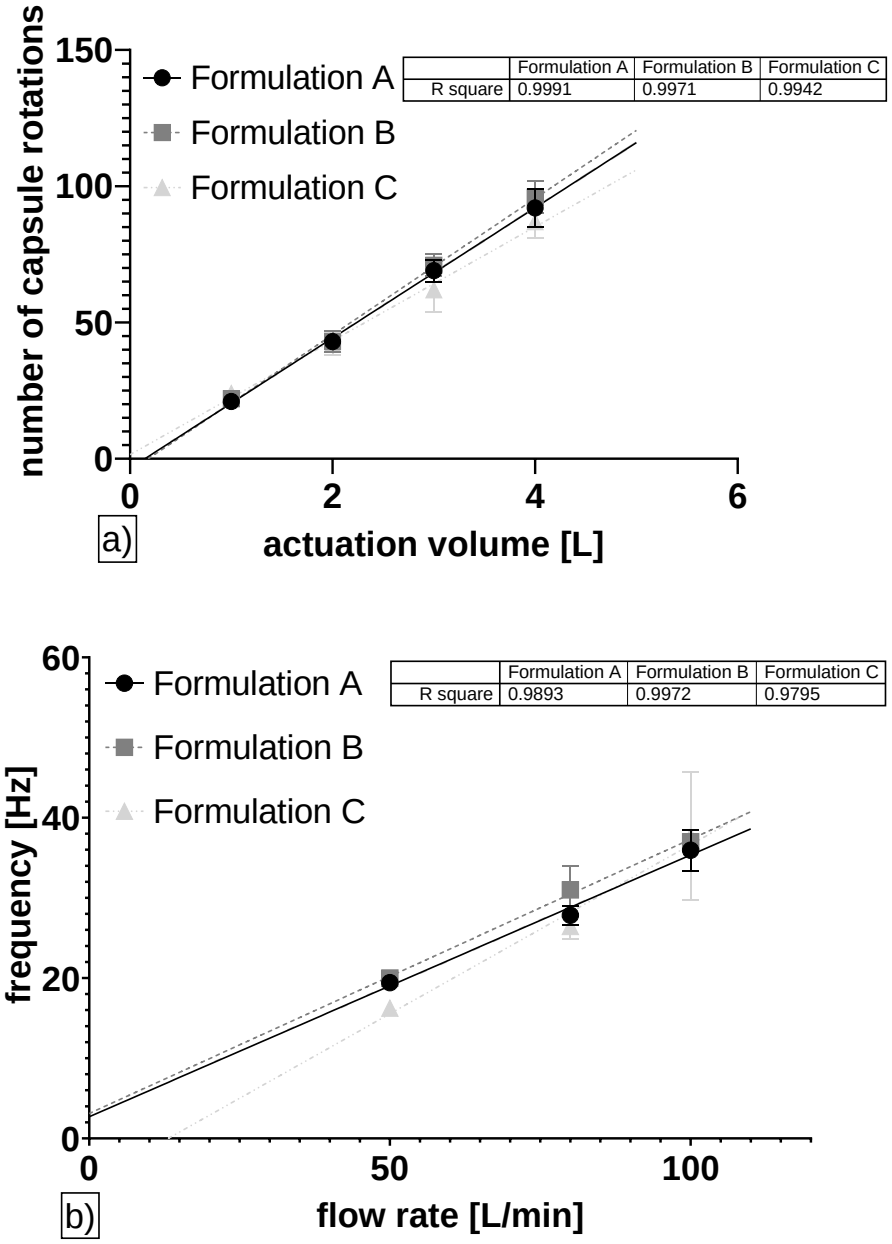

Figure 14: a: Correlation of the average of the capsule rotations and the actuation volumes independent of the applied flow rate and b: Correlation of the average of the calculated rotation frequency and the applied flow rate independent of the actuation volume for the different formulations (A = Cyclocaps®; B = Ventilastin®; C = Rifampicin).

Figure 15a shows, in addition to the tested air volume of 1 - 4 liters, a correlation between the number of capsule rotations and the actuation volume over a range of 0 - 4 liters for the tested flow rates to verify the number of rotations at the beginning of an inhalation. The results also show a linear relationship when smaller volumes than 1 liter are considered.

To analyze the change in the rotation frequency for each flow rate from the start of an inhalation to the end of actuation, the frequency was calculated every 0.05 liters from the starting point to a volume of 0.35 liters and then every 0.33 liters until the end of inhalation after reaching 4 liters. The results show that the rotational speed of the capsule increased in the first 0.35 liters, regardless of the applied flow rate, until the maximum rotational speed for that flow rate was reached. Once the specified inhalation volume was reached, the capsule rotated at a constant speed for the respective air flow over the entire inhalation period (Fig. 15b).

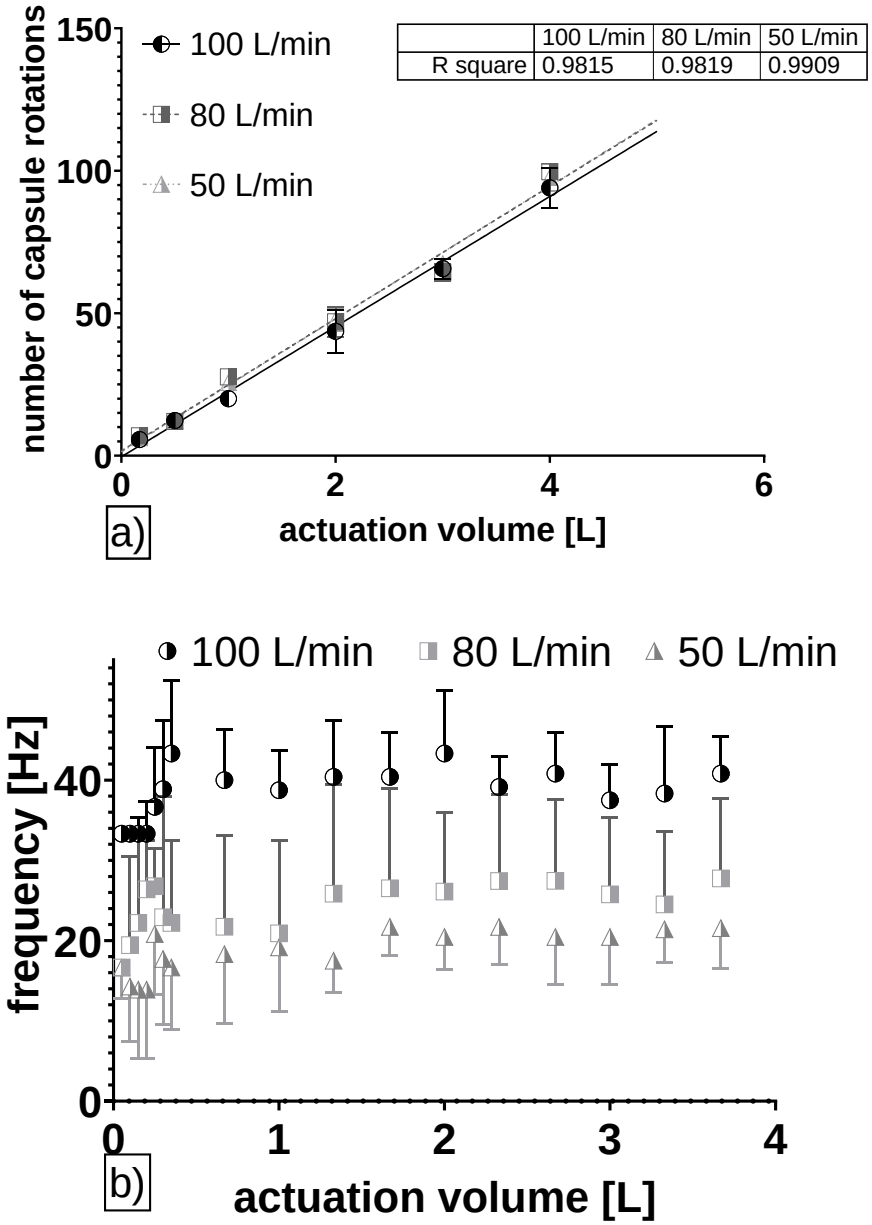

Figure 15: a: Correlation between the capsule rotations and the actuation volumes over the area from 0 - 4 liter; b: Determination of the rotation frequency for a defined duration interval for an inhalation volume of 4 liter and applied flow rates of 50, 80 and 100 L/min (n = 10).

The results in figure 16a for the Cyclocaps® formulation indicate that at an actuation volume of 2 liter, the powder deagglomeration behavior was disturbed and resulted in a higher powder deposition in the pres. Comparing this with the results obtained after actuating the device at 80 L/min, similar powder aerosolization characteristics are

observed at an actuation volume of 4 liters (Fig. S4). At the lowest flow rate of 50 L/min, a high deposition of the powder in the pres of 50 - 60 % is observed depending on the applied actuation volume (Fig. S5).

In the case of Ventilastin®, it should be noted that the deagglomeration of the powder at a flow rate of 100 L/min was independent of the air volume actuated (Fig. 16b). Comparing this with the results for 80 and 50 L/min, an increased powder deposition in the pres from 60 to 80% is observed with decreasing flow rate (Figs. S6, S7).

For the rifampicin (Fig. 16c), higher powder deposition in the DPI is observed when the actuation volume was reduced, which is reflected in a lower FPF (Fig. 16f). Comparing this to the results for the other two flow rates, a higher deposition in the DPI and also in the pres at 80 and 50 L/min can be seen, regardless of actuation volume (Figs. S8, S9). In addition, higher powder retention in the capsule is shown when the magnet holder assembly was placed in the capsule.

The results in figure 16d - f indicate that the device deagglomerated the powder similarly at an air flow of 100 and 80 L/min in the case of the rifampicin or Cyclocaps® formulation, respectively. Linear correlations are observed between the number of capsule rotations and the FPF_{EF} for the respective flow rates, with larger correlation coefficients calculated for formulations with good aerosolization properties reflected in a high FPF.

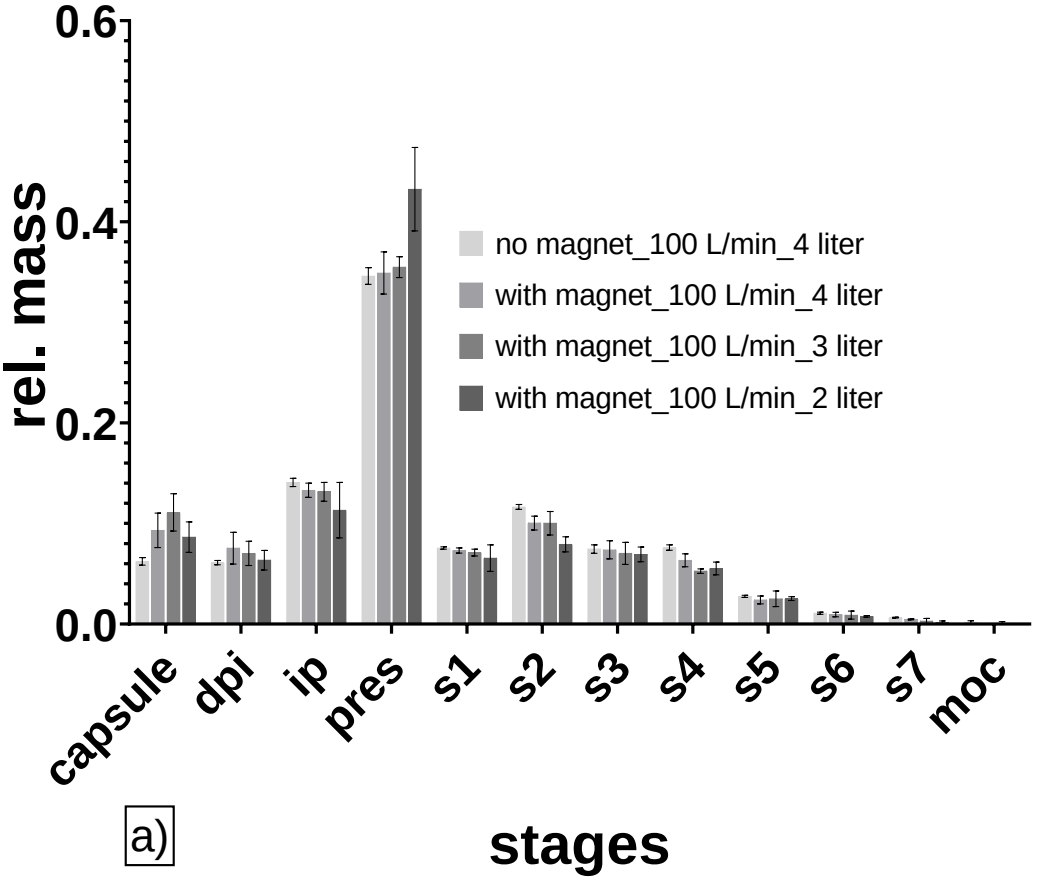
0.6
0.4
0.2
0.0
rel. mass
no magnet_100 L/min_4 liter
with magnet_100 L/min_4 liter
with magnet_100 L/min_3 liter
with magnet_100 L/min_2 liter
capsule
dpi
ip
pres
s1
s2
s3
s4
s5
s6
s7
moc
stages

a)

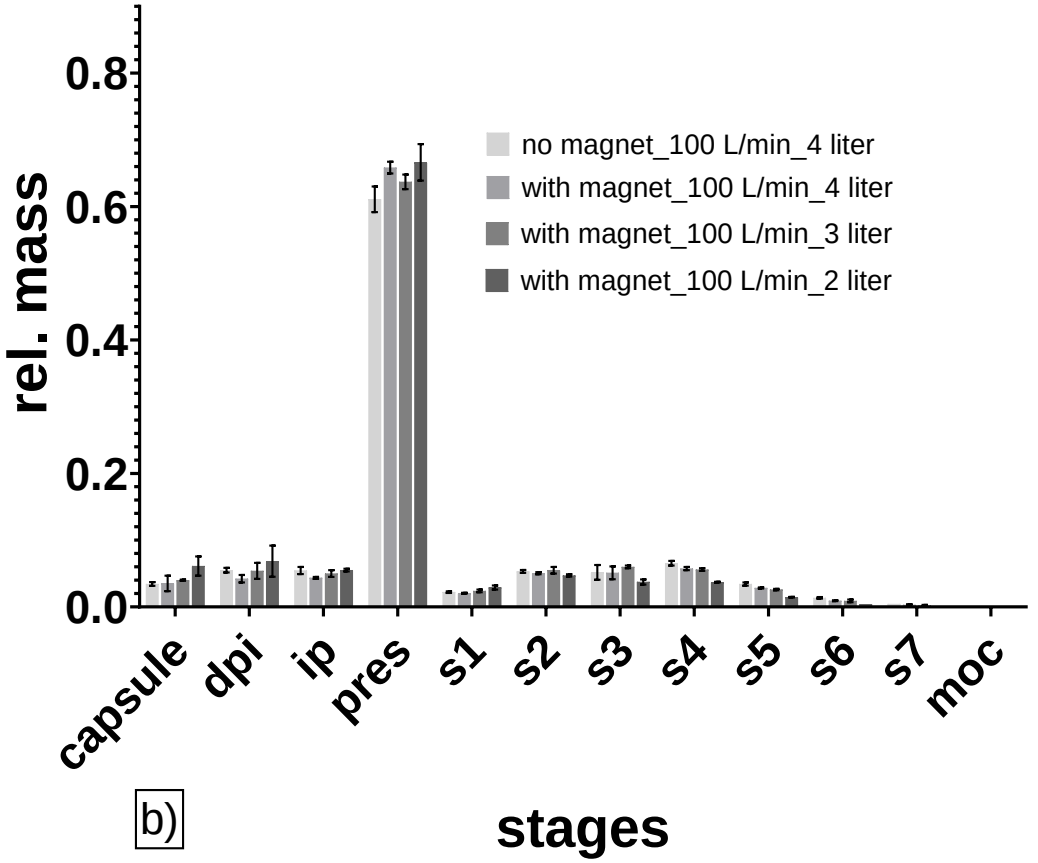
0.8
0.6
0.4
0.2
0.0
rel. mass
no magnet_100 L/min_4 liter
with magnet_100 L/min_4 liter
with magnet_100 L/min_3 liter
with magnet_100 L/min_2 liter
capsule
dpi
ip
pres
s1
s2
s3
s4
s5
s6
s7
moc
stages

b)

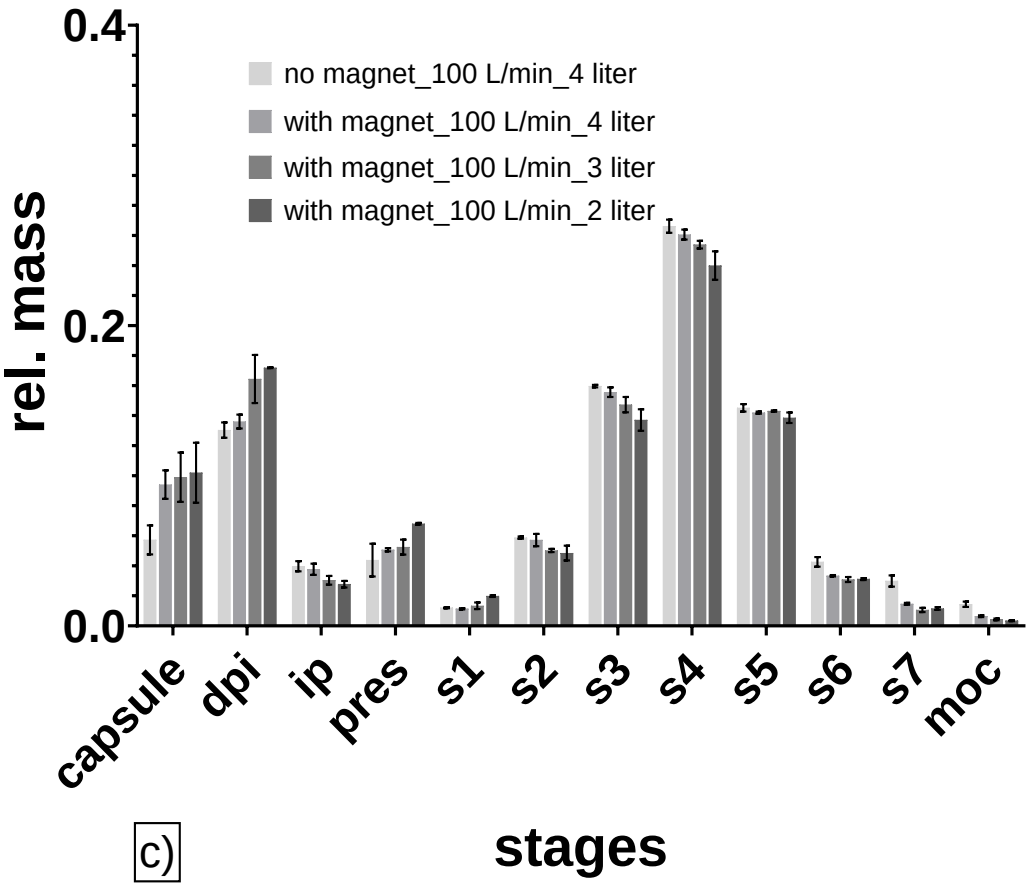
0.4
0.2
0.0
rel. mass
no magnet_100 L/min_4 liter
with magnet_100 L/min_4 liter
with magnet_100 L/min_3 liter
with magnet_100 L/min_2 liter
capsule
dpi
ip
pres
s1
s2
s3
s4
s5
s6
s7
moc
stages

c)

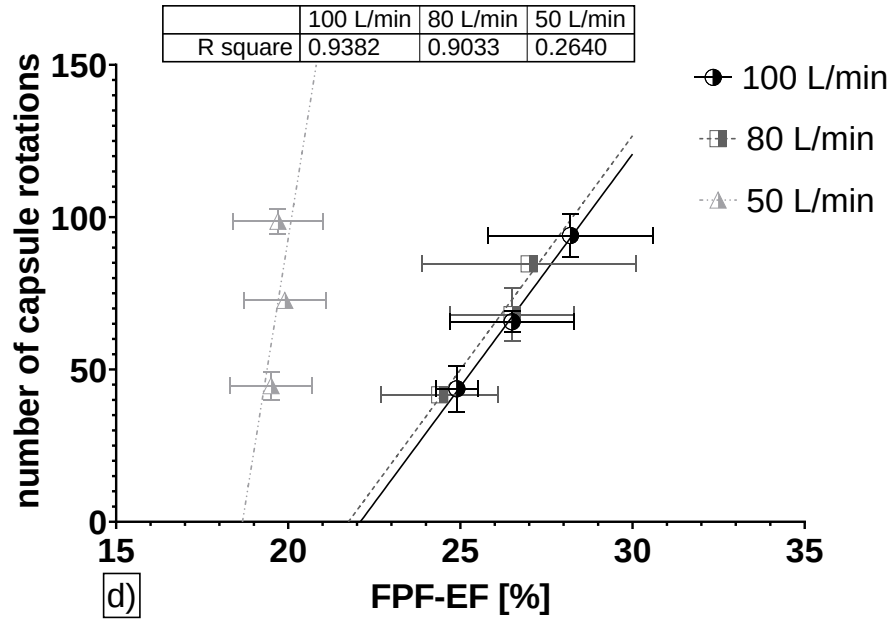
100 L/min
80 L/min
50 L/min
R square
0.9382
0.9033
0.2640
150
100
50
0
number of capsule rotations
15
20
25
30
35
FPF-EF [%]

d)

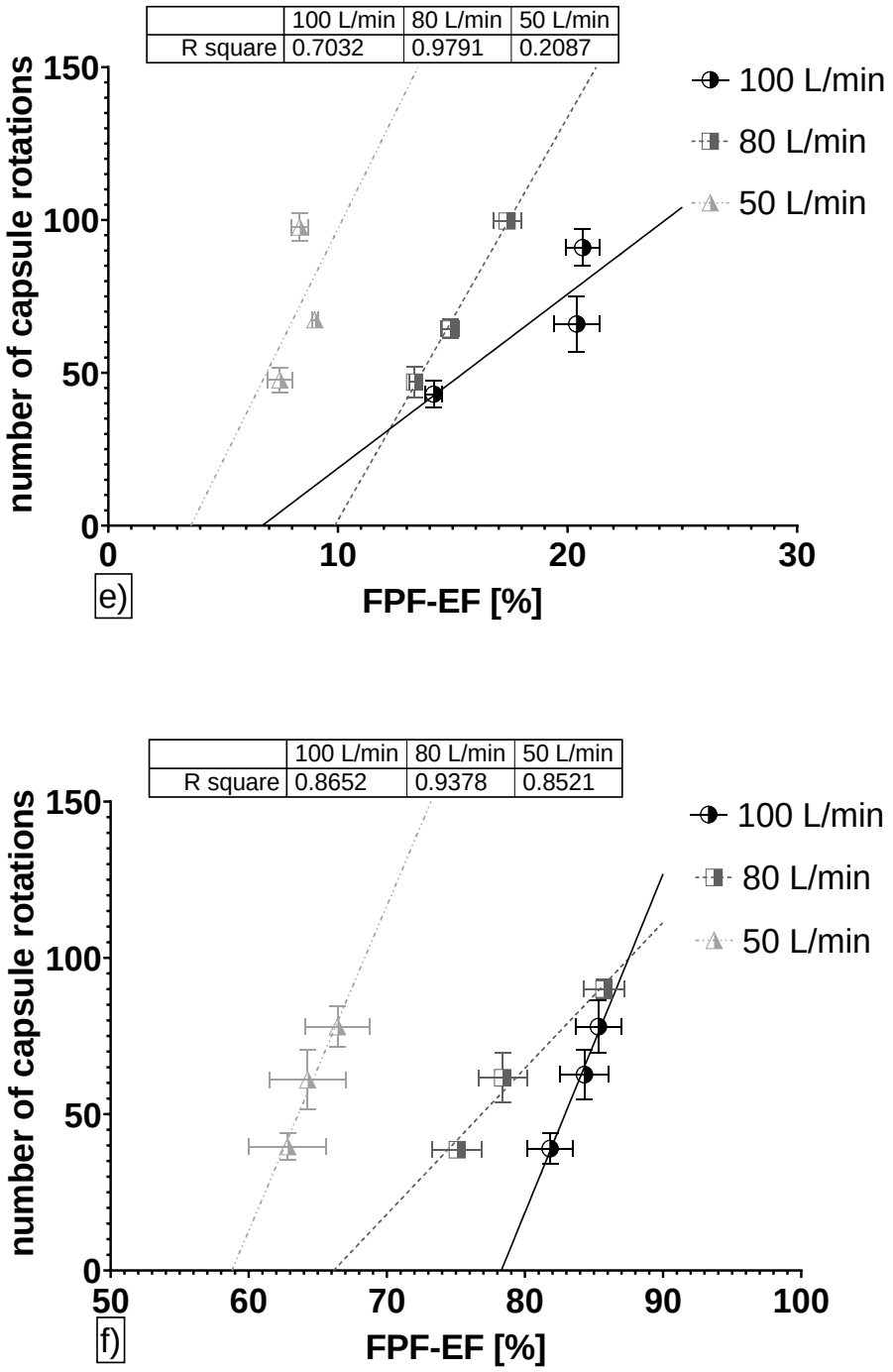

Figure 16: NGI results of the different formulations (a = Cyclocaps®; b = Ventilastin®; c = rifampicin) by using the Lupihaler device for different actuation volumes (2 - 4 liter) and a tested flow rate of 100 L/min; Correlation between the FPF_{EF} and the number of capsule rotations obtained from the NGI experiments (d = Cyclocaps®; e = Ventilastin®; f = rifampicin) for the actuation volumes tested at different flow rates.

The results in figure 17 show that the FPF_{EF} depends on the flow profile generated. It was found that inhalation with a higher number of capsule rotations combined with a high rotation frequency resulted in increased FPF_{EF} and is represented by colored arrows. Using the Cyclocaps® formulation as an example to compare the influence of the number of capsule rotations or frequency on the FPF_{EF} obtained, the rotation frequency had a greater influence, as the FPF_{EF} increases from 14% at the lowest frequency tested to 26% at the highest frequency. When considering one frequency and observing the influence of the number of capsule rotations on the FPF_{EF}, no significant differences were found (Figs. 16d, 17a). Also, two different aerosolization profiles are recognizable. The first one is represented by the higher flow rates of 80 and 100 L/min, resulting in a FPF_{EF} around 24%. The second shows the trend of the low flow rate leading to a FPF_{EF} of 16% as the maximum.

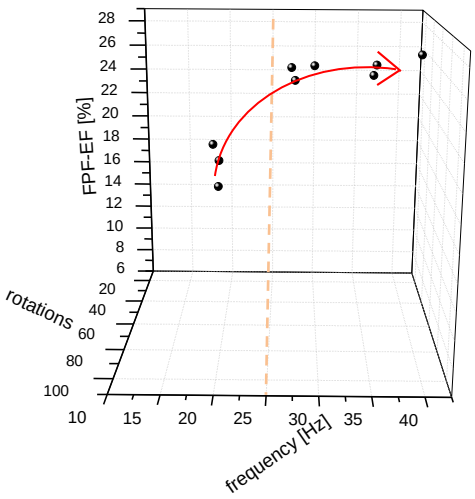

a)

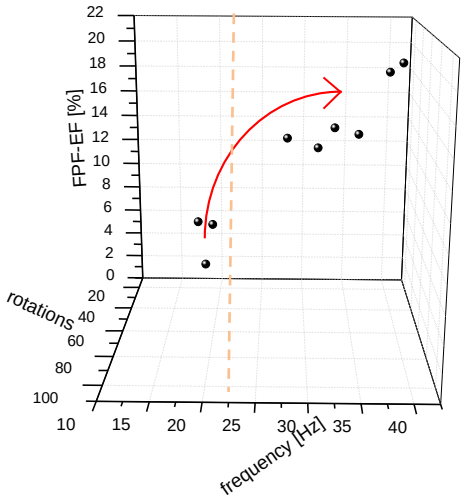

b)

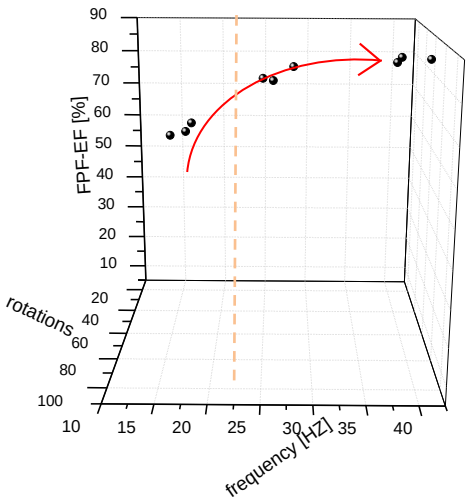

c)

Figure 17: 3D correlation between the FPF_{EF} [%], number of capsule rotations and the resulting frequency [Hz] for the different formulations (a = Cyclocaps®; b= Ventilastin®; c = rifampicin) obtained from the experimental set.

9.4 Discussion

To increase the therapeutical success for inhaled therapy, a new feedback mechanism for capsule-based DPI was developed due to insufficient possibilities for patients to monitor the inhalation performed with marketed devices [134,135]. Considering that the deagglomeration of the powder in this class of devices depends mainly on the inhalation profile and the associated movement of the capsule, the aim of this study was to determine the number of capsule rotations and the rotation frequency as surrogate parameters for the flow profile applied.

Since both, the number of capsule rotations and the frequency were similar for all tested formulations, the rotation was not influenced by the powder filling weight in the capsule. Since the modified capsule had a higher weight compared to an empty capsule, this resulted in a reduced rotation speed and frequency of the capsule during actuation, but this had no influence on the deagglomeration behavior of the device for the powder. It follows that a rotational frequency of 70 Hz, measured with an unmodified capsule when actuated with an RS01-equivalent device at 100 L/min, is not required to achieve a high FPF for the formulation in question [136]. On the contrary, it can be argued that satisfactory in vitro results can be obtained with inhalation resulting in a capsule rotation frequency of 40 Hz, which was measured with the setup shown. Although no differences were observed for the FPF_{EF} obtained from the NGI experiments performed with and without the modified capsules, all holders used have in common that a higher powder retention in the capsule in the case of rifampicin was detectable. This could be explained by the additional surface of the 3D printed geometries. Nevertheless, the NGI results for the different flow rates in combination with the actuation volumes performed with all formulations underlines that the geometry of the inserts can be designed in a way that does not influence the emptying behavior significantly. Since the holder system was placed in the center of the capsule and the powder was filled into the recesses of the two halves of the capsule, it can be concluded from the unaffected powder deagglomeration and the low retention inside the capsule, that the powder leaves the capsule at the respective insertion points and does not have to cross the capsule during powder ejection.

The results of the experiments are consistent with the observations of a previous study, which postulated that when using a DPI, the powder retention in a capsule during actuation decreases with increasing flow rate, and furthermore, that no significant differences in powder deagglomeration are observed at flow rates of 75 L/min or higher [137].

It was shown that the capsule does not rotate at maximum speed for the entire duration, but an increase in speed was observed in the first milliseconds, which is due to the dead volume of the NGI of about 2 liters [138]. Because NGI results for actuation volumes less than 1 liter would not be meaningful due to dead volume and would confound the observed correlations between FPF and capsule rotations, these data were not presented.

Based on the determined linear relationships between the number of capsule rotations and the actuation volume, as well as the frequency and the applied flow rate, the sticking of the capsule in the inhaler during inhalation would be detected and could be taken into account during the evaluation, so that an assessment of the actuation conditions and furthermore a statement about the quality of the inhalation process in vitro performed could be made.

For a formulation that has been characterized for different actuation volumes and flow rates, and for which the variables (number of capsule rotations, frequency and FPF_{EF}) have been correlated for the in-vitro tests, this system offers the possibility to show at what point a therapeutic success can be expected. For this purpose, a threshold value can be set for the respective parameters based on the determined correlations, as indicated by the colored dashed line for the frequency in figure 16. For all formulations tested under the mentioned conditions a minimum frequency for the capsule rotation of approximately 25 Hz is needed to achieve therapeutical success, since the FPF does not change dramatically above this threshold value. The threshold was set so that the actuated volume is not critical to achieving the target FPF values. Although this system is suitable for in-vitro studies, the therapeutic effect would need to be re-evaluated under in-vivo conditions, as linear correlations between critical parameters cannot be established in patients based on their respiratory profile, as the patient does

not inhale constantly with the same airflow over a defined time interval, but reaches a maximum inhalation followed by a flattening of the airflow. The interactions of the above parameters would need to be determined for the particular respiratory profile in order to define thresholds at which inhalation should be considered successful. Instead of FPF, which was chosen as the response parameter in this experimental setup, the extent of bronchoconstriction or disease exacerbation would be a more realistic parameter under in-vivo conditions to analyze the relevance for pulmonary treatment.

Nevertheless, this feedback system should be more optimized as it is a cost-effective tool and for a marketed system, a formulation dependent threshold for the flow rate and the capsule rotations could be set from which an inhalation can be assess as successful. Such an electronic device, in combination with a suitable cell phone app, could provide feedback to the patient immediately after actuation as to whether the inhalation was successful or whether a further dose needs to be administered. In the longer term, this would increase patient adherence and promote patient health by allowing better control of lung disease therapy. By recording the capsule rotations and automatically evaluating the inhalation, the physician's personal training to detect patient errors can be reduced. By connecting to the cell phone, all inhalation applications for a treatment interval can be stored, making it easy for the clinician to check the patient's compliance with the treatment and track the patient's inhalation progress, whether the patient is inhaling with increasing and sufficient duration and force. Whether the patient is properly medicated could be assessed by the frequency of capsule rotations and the inhalation time per inhalation for an interval. Deterioration in disease progression would be reflected in a lower number of capsule rotations or a lower frequency of rotations during an inhalation because the patient would not be able to produce the same flow rate over the inhaler as at a time in better health.

9.5 Conclusion

A new feedback mechanism for a capsule-based DPI has been introduced. Based on the correlations determined in the experiments for the critical parameters, it was shown that the velocity and duration of capsule rotation can be favorable surrogate

parameters for evaluating the success and quality of an inhalation performed. Since the experimental setup evaluates the feedback measurement principle, industrial approaches could use this feedback method. A modified capsule, in which one half of the capsule has a magnetic dipole moment, would not only replace the installation of the magnet holder system in the capsule, but also lead to a lower capsule weight and thus to higher rotational frequencies. This would eliminate the additional interactions between the powder and the magnet holder system that occurs with the prototype used, and would not affect powder retention in the capsule. It would also be conceivable to have an inhaler on a two-capsule basis, in which the magnet unit is installed in one capsule and the revolutions are counted here during inhalation, while a second capsule contains only the powder formulation for treatment. This could also avoid the additional powder retention in the capsule.

10. Conclusions and future perspectives

In general, this work has shown that there are several innovative methods to improve the pulmonary delivery system that could improve pulmonary therapy. Starting from the topic of DPI formulations, it has become apparent that novel options are available for the development of powder formulations that could result in particles with suitable aerodynamic properties and, when commercialized, result in higher pulmonary targeting compared to the state of the art. It is well known, and has also been shown in this work, that while interactive mixtures of milled drug and carrier particles result in high emitted fractions, a large portion of the formulation also settles in the preseparator and is thus not available for therapy and may also increase the potential for side effects. This shows that despite the advantages of easy preparation or high storage stability, this type of formulation technique is not ideal from the patient's point of view to achieve high powder deposition in the lungs. On the basis of this, novel formulation strategies should be used in industry.

First, it was shown that the spray-drying method seems to be suitable to produce a particle formulation with excellent aerosolization behavior when different DPIs are used, and that it is advantageous over milled particles. Since particle properties such as size, shape, density, and moisture can be controlled, the particles can be designed to meet the requirements for suitable aerodynamic behavior. Since these formulations result in low powder deposition in the IP or preseparator in-vitro, they should theoretically minimize the potential risk of side effects that could occur due to powder deposition in the oropharyngeal region. Despite the higher powder retention in the capsule or device compared to commercially available mixtures, this type of formulation should be used in future delivery systems brought to market. Although more powder sticks in the mentioned compartments, it also has the advantage that the powder hangs there and not in the IP and preseparator area, which would lead to less side effects in-vivo, too. The high powder retention in the device and in the capsule can be explained by the similar geometric particle size as after milling, so that cohesive interactions also occur here. Since the particle size can be controlled, resulting in a narrow size distribution, and the particles produced by spray-drying mostly have a spherical particle shape, these cohesive interactions between these particles could be weaker, since the number of possible contact points between round particles should

be as small as possible. Thus, these formulations appear to deagglomerate more readily because these weaker cohesive interactions can be overcome by the DPI upon release, allowing large quantities of particles with the correct aerodynamic particle size to enter the lungs and more drug to be available at the site of action. Ultimately, this leads to a reduction in the dose of drug that must be administered to achieve therapeutic effects. For all active ingredients spray-dried in the various studies, it was found that, in contrast to standard and commercial formulations, a higher fine particle fraction of well over 30% was achieved.

Comparison of the two formulation development methods indicates that the formulation using spray-dried particles reaches the lungs in-vitro better than the formulations developed using the traditional approach. Since there is the disadvantage of high powder retention in the device and capsule, the idea arose to combine both methods. Testing of the formulation of amoxicillin mixed with the lactose carriers showed improved powder ejection when actuated with different DPIs. Tests of interactive mixtures consisting of either milled or spray-dried rivaroxaban with lactose showed that the spray-dried drug carrier formulation resulted in a higher FPF when both formulations were actuated with the mentioned DPI. Accordingly, an important parameter could be the spherical particle shape of the spray-dried particles, making them easier to detach from the carrier particles due to the lower number of contact points associated with a spherical shape. Since the milled particles have a more undefined and heterogeneous surface, there may also be more mechanical anchoring with the carrier particles, which also increases adhesive particle interactions. The deagglomeration behavior of the device is therefore only sufficient to separate the spray-dried active ingredient in large quantities from the lactose, which can thus enter the stages. Further studies should therefore investigate the properties of the spray-dried particles that influence the aerosolization behavior of such interactive blends. The mixing ratio between the active ingredient and the carrier should also be investigated in the future, since only a fixed mixing ratio without modification was selected in the experiments carried out. This should influence the overall aerosolization behavior of the formulation. While at a mixing ratio of 1:99 (drug:carrier) the properties of the carrier should predominate, so that, for example, a large amount of powder would settle in the preseparator, since this is the area where the large carriers normally

deposit, a quantitatively increased amount of drug should also affect the aerosolization behavior of the final formulation.

However, the flowability of this type of formulation is worse when small particles are used, so a suitable method for powder filling into the capsule needs to be developed, which may be a challenge for the future. Another aspect is the storage stability of the drug, as spray-drying often results in amorphous particle properties instead of crystalline active ingredients. Depending on the mechanism of action in the lung, altered modification of the active ingredient could result in an adverse therapeutic effect or no therapeutic effect at all.

When considering the drugs used in the various chapters of this thesis, it is apparent that instead of the classic agents used for classic lung diseases, emphasis was placed on novel strategies. Since most formulations currently on the market contain drugs for asthma or COPD therapy, there is growing interest in delivering antibiotics or using the lung as an absorption route due to its large surface area for delivery of various drugs not directly intended for these types of diseases.

For this purpose, rifampicin and amoxicillin were integrated as antibiotics, whereas rivaroxaban was chosen as an antithrombotic for pulmonary embolism, as oral therapy is currently the state of the art.

As discussed in chapter three, the administration of anticoagulant drugs via the lungs appears to be of interest for the future. Since a rapid onset of action can be expected within 5 minutes after application, it seems logical to use this type of therapy in pulmonary embolism rescue. An example of this is the scenario of Covid-19 patients who are at increased risk for developing pulmonary embolism; inhaled rivaroxaban may be a future option to directly address efficacy and minimize adverse side effects. Another advantage of this administration routine is that it is painless for patients compared to commercially available anticoagulants, where the formulation is often administered with a pen and needle, leaving many patients unable to self-administer the necessary medication due to anxiety about the actual application. Therefore, it seems logical that taking the drug by deep inhalation might be a more patient-friendly method that could lead to better treatment adherence.

Also of interest is the manner in which the pulmonary formulation can be tested in-vivo and was demonstrated in this work. Since a rat does not inhale the formulation as humans do in a clinical trial, the development of the DP insufflator is a step in the right direction to test such formulations in preclinical studies in the future to estimate the in-vivo dissolution and bioavailability of the drug after deposition in the lung. In this way, initial data could be obtained to show whether the particular formulation could lead to therapeutic success or failure. With such a tool, in addition to the classical formulation tests in-vitro with an NGI, which evaluate the aerodynamic behavior in a first step, more realistic statements can be made about the possible extent of therapy.

Apart from the development aspect of the formulations, there are currently many drugs for the treatment of classical lung diseases, but all formulations have more or less the same problem, namely insufficient powder deagglomeration by the device. In reviewing DPIs from the past to the present, this work has shown that while there has long been a plateau in novel DPI technologies and developments, progress has generally been made in recent years in delivering comparable higher amounts of drugs to the lungs or in improving patient safety. With respect to DPI and deagglomeration concepts, it has been shown in the various chapters that there are several ways to overcome this problem and produce fine particle fractions above 30%, which are normally obtained with these insufficiently aerosolizable interactive blends. Although many aspects influence the process of powder aerosolization, it seems clear that simple DPIs with no suitable deagglomeration concept are not sufficient to achieve suitable therapeutic success. This is reflected, on the one hand, in the idea of adding external sources for powder deagglomeration and, on the other hand, in the concept and structure of the novel DPI presented in the various chapters, which can be decomposed into four main parts showing the complexity of future DPI designs for generating forces for powder aerosolization. Rather, the thinking should move away from the stand that the DPI is just a piece of plastic for delivering the powder and the focus is thus only on formulation optimization. The development of high performance equipment could be a challenge for the future, which also offers opportunities for better powder delivery.

It has been shown that novel deagglomeration concepts that deviate from the known and previously described concepts can lead to increased deposition of particles in the

lungs. While in the past DPIs had more or less the same basic design and the focus was on developing the formulation, today one focus is on optimizing the device, which inevitably leads to a better understanding of how the device works and how it interacts with the formulation. This led to the fact that each component used throughout the DPI makes a specific contribution to improving the inhalation process. The movement of the capsule, the airflow within the unit, the dimensions of the mesh and the air ducts are now of growing interest. Sometimes an additional classifier is also installed to increase the interactions between the particles or the particles and the device. During equipment development, flow simulations are carried out to evaluate the device aspects in relation to powder delivery. Since it has been shown that devices with a high intrinsic resistance to the air flow result in powder deagglomeration and delivering that is more independent of the flow rate applied, compared to devices with a low resistance, the future development of this type of device seems logical. Delivering a constant and consistent amount of the drug could minimize the influence of the patients and their diseases on the therapeutic outcome, so that a person suffering from COPD, who is not able to generate the same inspiratory force as a healthy person, receives the needed drug in an appropriate amount. Increasing the intrinsic resistance of the DPI could also be a way to increase turbulent flow and deagglomeration forces within the device, as intrinsic resistance results from device geometry, air channel thickness, and the use of different tools that could further interact with the particular formulation. This could be one reason why high intrinsic resistance devices result in fine particle fractions that are independent of the flow rate applied.

On the other hand, it has been shown that, in addition to the tools installed in the novel DPI to improve powder deagglomeration, the surface properties of the DPI have a significant influence on powder retention in the device and powder deagglomeration. While various mechanisms are described in the literature that could lead to retention of the powder in the device, there is as yet no way to overcome this problem and thus no commercially available coating for DPI surfaces. In the last decade, different approaches have been taken to increase the emitted fraction. In light of the results described in chapter 7, the overall manufacturing process should be reconsidered for future device development. Since surface texture has been shown to have a major influence on powder retention, future studies should focus on this topic to answer the

question of which dimensions of surface roughness affect powder deposition and which method is suitable to meet the set goals. Although nanometer-scale surface roughness affects powder aerosolization, micrometer-scale surface roughness could have a greater impact on powder deposition, considering that commercial formulations have micrometer-scale particle size. Since it has been demonstrated that proper surface texture can minimize powder retention, a higher emitted fraction could be achieved, making a greater amount of drug available for pulmonary therapy. For an industrial approach, a process should be used and evaluated where only the surface texture is changed, not the chemical properties, so that different size ranges of the texture can be tested. An interesting approach is also whether the particle size has an influence when working with a DPI with rough surface properties. Whether there is an ideal scale of the surface texture or whether it has to be adapted to the particle size of the respective formulation should be clarified in the future. A device that results in comparatively lower powder retention due to the surface structure could make the use of carrier particles unnecessary, since adhesion of the powder inside the device and a simultaneous poor flowability due to cohesive powder properties can be overcome. Thus, the drug particles do not have to detach from the carriers during actuation, and a poor deagglomeration concept of the device would not lead to a high drug deposition in the oropharyngeal region.

While the described benefits for formulation and device development only address the options and opportunities for the pharmaceutical industry to improve pulmonary treatment, marketing a device with a suitable deagglomeration concept in a fixed combination with an easily aerosolized formulation does not guarantee successful therapy. Therefore, DPIs currently marketed and in development are vulnerable and dependent on the inspiratory flow profile that the patient can achieve during inhalation. Until there is a solution to control the patient factor, the development of an ideal device will not be possible.

While in the early days of pulmonary powder delivery, the focus was on the formulation and the device as a simple delivery tool, it is now known that the patient has a major influence on the success of therapy. Therefore, delivery systems should be designed so that the patient knows that he or she has taken the required dose. Supportive

feedback mechanisms in the age of digitalization are of growing interest here. The prototype for feedback the capsule movement and also the inhalation maneuver could be a step to improve patient safety. The development of an intelligent DPI using this feedback system with the magnetic capsule system and the connected oscilloscope, presented in chapter 9, has shown that progress can also be made on the subject of patient safety. Since only the movement of the capsule is detected and this depends on the actuation process of the patient, this system is not disturbed and affected by ambient noise or the sticking of the capsule in the inhaler during inhalation, which would lead to deteriorated powder deagglomeration. It can be concluded that inhalation therapy can be influenced independently of the selected feedback mechanism, as the patient's influence on powder aerosolization can be controlled to a certain extent, since the inhalation maneuver can be evaluated as a whole. Ultimately, the use of smart devices involves the patient to a large extent in the actual inhalation process and also in the handling, as all information is directly available to the patient.

In summary, progress has generally been made on the three main factors affecting lung therapy. Different approaches have been demonstrated for each topic, indicating that a new era of powder delivery to the lung has been initiated. Since this topic is of increasing interest today, several innovative delivery systems may be approved in the future, whether the device, formulation, or specific additives are critical. While in the past the goal was to deliver the drug to the lungs, which initially resulted in low powder deposition, the requirements to treat more disease areas via the lungs and the aspect of patient safety are forcing the pharmaceutical industry to bring highly efficient delivery systems to the market.

11. References

1. Kaialy, W.; Ticehurst, M.; Nokhodchi, A. Dry Powder Inhalers: Mechanistic Evaluation of Lactose Formulations Containing Salbutamol Sulphate. *Int. J. Pharm.* **2012**, *423*, 184–194, doi:10.1016/j.ijpharm.2011.12.018.

2. Singh, D.; Agusti, A.; Anzueto, A.; Barnes, P.J.; Bourbeau, J.; Celli, B.R.; Criner, G.J.; Frith, P.; Halpin, D.M.G.; Han, M.; et al. Global Strategy for the Diagnosis, Management, and Prevention of Chronic Obstructive Lung Disease: The GOLD Science Committee Report 2019. *Eur. Respir. J.* **2019**, *53*, 1900164, doi:10.1183/13993003.00164-2019.

3. Scichilone, N.; Pedone, C.; Battaglia, S.; Sorino, C.; Bellia, V. Diagnosis and Management of Asthma in the Elderly. *Eur. J. Intern. Med.* **2014**, *25*, 336–342, doi:10.1016/j.ejim.2014.01.004.

4. Pilcer, G.; Wauthoz, N.; Amighi, K. Lactose Characteristics and the Generation of the Aerosol. *Adv. Drug Deliv. Rev.* **2012**, *64*, 233–256, doi:10.1016/j.addr.2011.05.003.

5. Sorino, C. Inhalation Therapy Devices for the Treatment of Obstructive Lung Diseases_ the History of Inhalers towards the Ideal Inhaler. 4.

6. Quon, B.S.; Goss, C.H.; Ramsey, B.W. Inhaled Antibiotics for Lower Airway Infections. *Ann. Am. Thorac. Soc.* **2014**, *11*, 425–434, doi:10.1513/AnnalsATS.201311-395FR.

7. Nevitt, S.J.; Thornton, J.; Murray, C.S.; Dwyer, T. Inhaled Mannitol for Cystic Fibrosis. *Cochrane Database Syst. Rev.* **2018**, doi:10.1002/14651858.CD008649.pub3.

8. Daniher, D.I.; Zhu, J. Dry Powder Platform for Pulmonary Drug Delivery. *Particuology* **2008**, *6*, 225–238, doi:10.1016/j.partic.2008.04.004.

9. Csóka, I.; Karimi, K.; Mukhtar, M.; Ambrus, R. Pulmonary Drug Delivery Systems of Antibiotics for the Treatment of Respiratory Tract Infections. *Acta Pharm. Hung.* **2019**, *89*, 43–62, doi:10.33892/aph.2019.89.43-62.

10. Dinh, K.; Myers, D.J.; Glazer, M.; Shmidt, T.; Devereaux, C.; Simis, K.; Noymer, P.D.; He, M.; Choosakul, C.; Chen, Q.; et al. In Vitro Aerosol Characterization of Staccato® Loxapine. *Int. J. Pharm.* **2011**, *403*, 101–108, doi:10.1016/j.ijpharm.2010.10.030.

11. Gessler, T.; Ghofrani, H.; Held, M.; Klose, H.; Leuchte, H.; Olschewski, H.; Rosenkranz, S.; Fels, L.; Li, N.; Ren, D.; et al. The Safety and Pharmacokinetics of Rapid Iloprost Aerosol Delivery via the BREELIB Nebulizer in Pulmonary Arterial Hypertension. *Pulm. Circ.* **2017**, *7*, 505–513, doi:10.1177/2045893217706691.

12. Marple, V.A.; Roberts, D.L.; Romay, F.J.; Miller, N.C.; Truman, K.G.; Van Oort, M.; Olsson, B.; Holroyd, M.J.; Mitchell, J.P.; Hochrainer, D. Next Generation Pharmaceutical Impactor (A New Impactor for Pharmaceutical Inhaler Testing). Part I: Design. *J. Aerosol Med.* **2003**, *16*, 283–299, doi:10.1089/089426803769017659.

13. Darquenne, C. Aerosol Deposition in the Human Lung in Reduced Gravity. *J. Aerosol Med. Pulm. Drug Deliv.* **2014**, *27*, 170–177, doi:10.1089/jamp.2013.1079.

14. Yu, C.P.; Diu, C.K. Total and Regional Deposition of Inhaled Aerosols in Humans. *J. Aerosol Sci.* **1983**, *14*, 599–609, doi:10.1016/0021-8502(83)90065-4.

15. Kaye, S.R.; Phillips, C.G. The Influence of the Branching Pattern of the Conducting Airways on Flow and Aerosol Deposition Parameters in the Human, Dog, Rat and Hamster. *J. Aerosol Sci.* **1997**, *28*, 1291–1300, doi:10.1016/S0021-8502(97)00024-4.

16. Anderson, P.J. History of Aerosol Therapy: Liquid Nebulization to MDIs to DPIs. *Respir. CARE* **2005**, *50*, 12.

17. Sanders, M. Inhalation Therapy: An Historical Review. *Prim. Care Respir. J.* **2007**, *16*, 71–81, doi:10.3132/pcrj.2007.00017.

18. Dessanges, J.-F. A History of Nebulization. *J. Aerosol Med.* **2001**, *14*, 65–71, doi:10.1089/08942680152007918.

19. Ooi, J.; Traini, D.; Boyd, B.J.; Gaisford, S.; Young, P.M. Determination of Physical and Chemical Stability in Pressurised Metered Dose Inhalers: Potential New

Techniques. *Expert Opin. Drug Deliv.* **2015**, *12*, 1661–1675, doi:10.1517/17425247.2015.1046834.

20. Chierici, V.; Cavalieri, L.; Piraino, A.; Paleari, D.; Quarta, E.; Sonvico, F.; Melani, A.S.; Buttini, F. Consequences of Not-Shaking and Shake-Fire Delays on the Emitted Dose of Some Commercial Solution and Suspension Pressurized Metered Dose Inhalers. *Expert Opin. Drug Deliv.* **2020**, *17*, 1025–1039, doi:10.1080/17425247.2020.1767066.

21. Smyth, H.D.C. The Influence of Formulation Variables on the Performance of Alternative Propellant-Driven Metered Dose Inhalers. *Adv. Drug Deliv. Rev.* **2003**, *55*, 807–828, doi:10.1016/S0169-409X(03)00079-6.

22. Lovelock, J.E. Halogenated Hydrocarbons in the Atmosphere'. 8.

23. Noakes, T.J. CFCs, Their Replacements, and the Ozone Layer. *J. Aerosol Med.* **1995**, *8*, S-3-S-7, doi:10.1089/jam.1995.8.Suppl_1.S-3.

24. D'Souza, S. The Montreal Protocol and Essential Use Exemptions. *J. Aerosol Med.* **1995**, *8*, S-13-S-17, doi:10.1089/jam.1995.8.Suppl_1.S-13.

25. Newman, S.P. Principles of Metered-Dose Inhaler Design. *Respir. CARE* **2005**, *50*.

26. Gabrio, B.J.; Stein, S.W.; Velasquez, D.J. A New Method to Evaluate Plume Characteristics of Hydrofluoroalkane and Chlorofluorocarbon Metered Dose Inhalers. *Int. J. Pharm.* **1999**, *186*, 3–12, doi:10.1016/S0378-5173(99)00133-7.

27. Berkenfeld, K.; Lamprecht, A.; McConville, J.T. Devices for Dry Powder Drug Delivery to the Lung. *AAPS PharmSciTech* **2015**, *16*, 479–490, doi:10.1208/s12249-015-0317-x.

28. de Boer, A.H.; Hagedoorn, P.; Hoppentocht, M.; Buttini, F.; Grasmeijer, F.; Frijlink, H.W. Dry Powder Inhalation: Past, Present and Future. *Expert Opin. Drug Deliv.* **2017**, *14*, 499–512, doi:10.1080/17425247.2016.1224846.

29. Labiris, N.R.; Dolovich, M.B. Pulmonary Drug Delivery. Part I: Physiological Factors Affecting Therapeutic Effectiveness of Aerosolized Medications: Physiological Factors Affecting the Effectiveness of Inhaled Drugs. *Br. J. Clin. Pharmacol.* **2003**, *56*, 588–599, doi:10.1046/j.1365-2125.2003.01892.x.

30. Mangal, S.; Park, H.; Nour, R.; Shetty, N.; Cavallaro, A.; Zemlyanov, D.; Thalberg, K.; Puri, V.; Nicholas, M.; Narang, A.S.; et al. Correlations between Surface Composition and Aerosolization of Jet-Milled Dry Powder Inhaler Formulations with Pharmaceutical Lubricants. *Int. J. Pharm.* **2019**, *568*, 118504, doi:10.1016/j.ijpharm.2019.118504.

31. Pilcer, G.; Amighi, K. Formulation Strategy and Use of Excipients in Pulmonary Drug Delivery. *Int. J. Pharm.* **2010**, *392*, 1–19, doi:10.1016/j.ijpharm.2010.03.017.

32. Weers, J.G.; Miller, D.P. Formulation Design of Dry Powders for Inhalation. *J. Pharm. Sci.* **2015**, *104*, 3259–3288, doi:10.1002/jps.24574.

33. Ling, J.; Mangal, S.; Park, H.; Wang, S.; Cavallaro, A.; Zhou, Q.T. Simultaneous Particle Size Reduction and Homogeneous Mixing to Produce Combinational Powder Formulations for Inhalation by the Single-Step Co-Jet Milling. *J. Pharm. Sci.* **2019**, *108*, 3146–3151, doi:10.1016/j.xphs.2019.05.011.

34. Chan, H.-K.; Chew, N.Y.K. Novel Alternative Methods for the Delivery of Drugs for the Treatment of Asthma. *Adv. Drug Deliv. Rev.* **2003**, *55*, 793–805, doi:10.1016/S0169-409X(03)00078-4.

35. Louey, M.D.; Stewart, P.J. Particle Interactions Involved in Aerosol Dispersion of Ternary Interactive Mixtures. 8.

36. Jones, M.D.; Santo, J.G.F.; Yakub, B.; Dennison, M.; Master, H.; Buckton, G. The Relationship between Drug Concentration, Mixing Time, Blending Order and Ternary Dry Powder Inhalation Performance. *Int. J. Pharm.* **2010**, *391*, 137–147, doi:10.1016/j.ijpharm.2010.02.031.

37. Grasmeijer, F.; Lexmond, A.J.; van den Noort, M.; Hagedoorn, P.; Hickey, A.J.; Frijlink, H.W.; de Boer, A.H. New Mechanisms to Explain the Effects of Added Lactose Fines on the Dispersion Performance of Adhesive Mixtures for Inhalation. *PLoS ONE* **2014**, *9*, e87825, doi:10.1371/journal.pone.0087825.

38. Ambrus, R.; Benke, E.; Farkas, Á.; Balásházy, I.; Szabó-Révész, P. Novel Dry Powder Inhaler Formulation Containing Antibiotic Using Combined Technology to Improve Aerodynamic Properties. *Eur. J. Pharm. Sci.* **2018**, *123*, 20–27, doi:10.1016/j.ejps.2018.07.030.

39. Scherließ, R.; Bock, S.; Bungert, N.; Neustock, A.; Valentin, L. Particle Engineering in Dry Powders for Inhalation. *Eur. J. Pharm. Sci.* **2022**, *172*, 106158, doi:10.1016/j.ejps.2022.106158.

40. Mönckedieck, M.; Kamplade, J.; Fakner, P.; Urbanetz, N.A.; Walzel, P.; Steckel, H.; Scherließ, R. Dry Powder Inhaler Performance of Spray Dried Mannitol with Tailored Surface Morphologies as Carrier and Salbutamol Sulphate. *Int. J. Pharm.* **2017**, *524*, 351–363, doi:10.1016/j.ijpharm.2017.03.055.

41. Cal, K.; Sollohub, K. Spray Drying Technique. I: Hardware and Process Parameters. *J. Pharm. Sci.* **2010**, *99*, 575–586, doi:10.1002/jps.21886.

42. Vehring, R. Pharmaceutical Particle Engineering via Spray Drying. *Pharm. Res.* **2008**, *25*, 999–1022, doi:10.1007/s11095-007-9475-1.

43. Dobry, D.E.; Settell, D.M.; Baumann, J.M.; Ray, R.J.; Graham, L.J.; Beyerinck, R.A. A Model-Based Methodology for Spray-Drying Process Development. *J. Pharm. Innov.* **2009**, *4*, 133–142, doi:10.1007/s12247-009-9064-4.

44. Malamatari, M.; Charisi, A.; Malamataris, S.; Kachrimanis, K.; Nikolakakis, I. Spray Drying for the Preparation of Nanoparticle-Based Drug Formulations as Dry Powders for Inhalation. *Processes* **2020**, *8*, 788, doi:10.3390/pr8070788.

45. Sakagami, M.; Byron, P.R. Respirable Microspheres for Inhalation: The Potential of Manipulating Pulmonary Disposition for Improved Therapeutic Efficacy. *Clin. Pharmacokinet.* **2005**, *44*, 263–277, doi:10.2165/00003088-200544030-00004.

46. Patel, R.P. Spray Drying Technology: An Overview. *Indian J. Sci. Technol.* **2009**, *2*, 44–47, doi:10.17485/ijst/2009/v2i10.3.

47. Bell, J.H.; Hartley, P.S.; Cox, J.S.G. Dry Powder Aerosols I: A New Powder Inhalation Device. *J. Pharm. Sci.* **1971**, *60*, 1559–1564, doi:10.1002/jps.2600601028.

48. Robson, R.; Taylor, B.; Taylor, B. Sodium Cromoglycate: Spincaps or Metered Dose Aerosol. *Br. J. Clin. Pharmacol.* **1981**, *11*, 383–384, doi:10.1111/j.1365-2125.1981.tb01136.x.

49. Clark, A.R. Medical Aerosol Inhalers: Past, Present, and Future. *Aerosol Sci. Technol.* **1995**, *22*, 374–391, doi:10.1080/02786829408959755.

50. Jones, T.M.; Pilpel, N. Some Physical Properties of Lactose and Magnesia. *J. Pharm. Pharmacol.* **2011**, *17*, 440–448, doi:10.1111/j.2042-7158.1965.tb07700.x.

51. O'Connor, B.J. The Ideal Inhaler: Design and Characteristics to Improve Outcomes. *Respir. Med.* **2004**, *98*, S10–S16, doi:10.1016/j.rmed.2004.02.006.

52. Stein, S.W.; Sheth, P.; Hodson, P.D.; Myrdal, P.B. Advances in Metered Dose Inhaler Technology: Hardware Development. *AAPS PharmSciTech* **2014**, *15*, 326–338, doi:10.1208/s12249-013-0062-y.

53. LiCalsi, C.; Christensen, T.; Bennett, J.V.; Phillips, E.; Witham, C. Dry Powder Inhalation as a Potential Delivery Method for Vaccines. *Vaccine* **1999**, *17*, 1796–1803, doi:10.1016/S0264-410X(98)00438-1.

54. White, S.; Bennett, D.B.; Cheu, S.; Conley, P.W.; Guzek, D.B.; Gray, S.; Howard, J.; Malcolmson, R.; Parker, J.M.; Roberts, P.; et al. EXUBERA®: Pharmaceutical Development of a Novel Product for Pulmonary Delivery of Insulin. *Diabetes Technol. Ther.* **2005**, *7*, 896–906, doi:10.1089/dia.2005.7.896.

55. Han, R.; Papadopoulos, G.; Greenspan, B.J. Flow Field Measurement inside the Mouthpiece of the Spiros Inhaler Using Particle Image Velocimetry. *Aerosol Sci. Technol.* **2002**, *36*, 329–341, doi:10.1080/027868202753504524.

56. Atkins, P.J. Dry Powder Inhalers: An Overview. *Respir. CARE* **2005**, *50*, 9.

57. Adams, W.P.; Lee, S.L.; Plourde, R.; Lionberger, R.A.; Bertha, C.M.; Doub, W.H.; Bovet, J.-M.; Hickey, A.J. Effects of Device and Formulation on In Vitro Performance of Dry Powder Inhalers. *AAPS J.* **2012**, *14*, 400–409, doi:10.1208/s12248-012-9352-7.

58. Xu, Z.; Mansour, H.M.; Hickey, A.J. Particle Interactions in Dry Powder Inhaler Unit Processes: A Review. *J. Adhes. Sci. Technol.* **2011**, *25*, 451–482, doi:10.1163/016942410X525669.

59. Islam, N.; Gladki, E. Dry Powder Inhalers (DPIs)—A Review of Device Reliability and Innovation. *Int. J. Pharm.* **2008**, *360*, 1–11, doi:10.1016/j.ijpharm.2008.04.044.

60. Canonica, G.W.; Arp, J.; Keegstra, J.R.; Chrystyn, H. Spiromax, a New Dry Powder Inhaler: Dose Consistency under Simulated Real-World Conditions. *J. Aerosol Med. Pulm. Drug Deliv.* **2015**, *28*, 309–319, doi:10.1089/jamp.2015.1216.

61. Azouz, W.; Chetcuti, P.; Hosker, H.S.R.; Saralaya, D.; Stephenson, J.; Chrystyn, H. The Inhalation Characteristics of Patients When They Use Different Dry Powder Inhalers. *J. Aerosol Med. Pulm. Drug Deliv.* **2015**, *28*, 35–42, doi:10.1089/jamp.2013.1119.

62. Al-Showair, R.A.M.; Tarsin, W.Y.; Assi, K.H.; Pearson, S.B.; Chrystyn, H. Can All Patients with COPD Use the Correct Inhalation Flow with All Inhalers and Does Training Help? *Respir. Med.* **2007**, *101*, 2395–2401, doi:10.1016/j.rmed.2007.06.008.

63. Martinelli, F.; Balducci, A.G.; Rossi, A.; Sonvico, F.; Colombo, P.; Buttini, F. “Pierce and Inhale” Design in Capsule Based Dry Powder Inhalers: Effect of Capsule Piercing and Motion on Aerodynamic Performance of Drugs. *Int. J. Pharm.* **2015**, *487*, 197–204, doi:10.1016/j.ijpharm.2015.04.003.

64. Shur, J.; Lee, S.; Adams, W.; Lionberger, R.; Tibbatts, J.; Price, R. Effect of Device Design on the In Vitro Performance and Comparability for Capsule-Based Dry Powder Inhalers. *AAPS J.* **2012**, *14*, 667–676, doi:10.1208/s12248-012-9379-9.

65. Dal Negro, R.W. Dry Powder Inhalers and the Right Things to Remember: A Concept Review. *Multidiscip. Respir. Med.* **2015**, *10*, 13, doi:10.1186/s40248-015-0012-5.

66. Deboer, A.; Hagedoorn, P.; Gjaltema, D.; Goede, J.; Frijlink, H. Air Classifier Technology (ACT) in Dry Powder InhalationPart 1. Introduction of a Novel Force Distribution Concept (FDC) Explaining the Performance of a Basic Air Classifier on Adhesive Mixtures. *Int. J. Pharm.* **2003**, *260*, 187–200, doi:10.1016/S0378-5173(03)00250-3.

67. de Boer, A.H.; Hagedoorn, P.; Gjaltema, D.; Goede, J.; Frijlink, H.W. Air Classifier Technology (ACT) in Dry Powder Inhalation Part 4. Performance of Air Classifier Technology in the Novolizer® Multi-Dose Dry Powder Inhaler. *Int. J. Pharm.* **2006**, 9.

68. Jeswani, H.K.; Azapagic, A. Life Cycle Environmental Impacts of Inhalers. *J. Clean. Prod.* **2019**, *237*, 117733, doi:10.1016/j.jclepro.2019.117733.

69. Newman, S.P.; Pitcairn, G.R.; Hirst, P.H.; Bacon, R.E.; O'Keefe, E.; Reiners, M.; Hermann, R. Scintigraphic Comparison of Budesonide Deposition from Two Dry Powder Inhalers. *Eur. Respir. J.* **2000**, *16*, 178–183, doi:10.1034/j.1399-3003.2000.16a29.x.

70. Westerman, E.M. Studies on Antibiotic Aerosols for Inhalation in Cystic Fibrosis.

71. de Boer, A.H.; Hagedoorn, P.; Woolhouse, R.; Wynn, E. Computational Fluid Dynamics (CFD) Assisted Performance Evaluation of the Twincer™ Disposable High-Dose Dry Powder Inhaler. *J. Pharm. Pharmacol.* **2012**, *64*, 1316–1325, doi:10.1111/j.2042-7158.2012.01511.x.

72. Zhou, Q.T.; Tong, Z.; Tang, P.; Citterio, M.; Yang, R.; Chan, H.-K. Effect of Device Design on the Aerosolization of a Carrier-Based Dry Powder Inhaler—a Case Study on Aerolizer® Foradile®. *AAPS J.* **2013**, *15*, 511–522, doi:10.1208/s12248-013-9458-6.

73. Jetzer, M.W.; Morrical, B.D. Investigation of Electrostatic Behavior of Dry Powder-Inhaled Model Formulations. *J. Pharm. Sci.* **2019**, *108*, 2949–2963, doi:10.1016/j.xphs.2019.04.013.

74. Kurt, M.; Saban Kamber, O.; Kaynak, Y.; Atakok, G.; Girit, O. Experimental Investigation of Plastic Injection Molding: Assessment of the Effects of Cavity Pressure and Mold Temperature on the Quality of the Final Products. *Mater. Des.* **2009**, *30*, 3217–3224, doi:10.1016/j.matdes.2009.01.004.

75. Dang, X.-P. General Frameworks for Optimization of Plastic Injection Molding Process Parameters. *Simul. Model. Pract. Theory* **2014**, *41*, 15–27, doi:10.1016/j.simpat.2013.11.003.

76. Kashyap, S.; Datta, D. Process Parameter Optimization of Plastic Injection Molding: A Review. *Int. J. Plast. Technol.* **2015**, *19*, 1–18, doi:10.1007/s12588-015-9115-2.

77. Suwanpitak, K.; Lim, L.-Y.; Singh, I.; Sriamornsak, P.; Thepsonthi, T.; Huanbutta, K.; Sangnim, T. Development of an Add-On Device Using 3D Printing for the Enhancement of Drug Administration Efficiency of Dry Powder Inhalers (Accuhaler). *Pharmaceutics* **2022**, *14*, 1922, doi:10.3390/pharmaceutics14091922.

78. Suwandecha, T.; Wongpoowarak, W.; Srichana, T. Computer-Aided Design of Dry Powder Inhalers Using Computational Fluid Dynamics to Assess Performance. *Pharm. Dev. Technol.* **2016**, *21*, 54–60, doi:10.3109/10837450.2014.965325.

79. ElKasabgy, N.A.; Adel, I.M.; Elmeligy, M.F. Respiratory Tract: Structure and Attractions for Drug Delivery Using Dry Powder Inhalers. *AAPS PharmSciTech* **2020**, *21*, 238, doi:10.1208/s12249-020-01757-2.

80. Drug Delivery to the Lungs 20. **2021**, *32*.

81. *〈601〉 Inhalation and Nasal Drug Products: Aerosols, Sprays, and Powders—Performance Quality Tests*;

82. Finlay, W.H.; Stapleton, K.W.; Zuberbuhler, P. Fine Particle Fraction as a Measure of Mass Depositing in the Lung during Inhalation of Nearly Isotonic

Nebulized Aerosols. *J. Aerosol Sci.* **1997**, *28*, 1301–1309, doi:10.1016/S0021-8502(97)00017-7.

83. Chew, N.Y.K.; Tang, P.; Chan, H.-K.; Raper, J.A. How Much Particle Surface Corrugation Is Sufficient to Improve Aerosol Performance of Powders? *Pharm. Res.* **2005**, *22*, 148–152, doi:10.1007/s11095-004-9020-4.

84. Zellnitz, S.; Zellnitz, L.; Müller, M.T.; Meindl, C.; Schröttner, H.; Fröhlich, E. Impact of Drug Particle Shape on Permeability and Cellular Uptake in the Lung. *Eur. J. Pharm. Sci.* **2019**, *139*, 105065, doi:10.1016/j.ejps.2019.105065.

85. Lavorini, F.; Magnan, A.; Christophe Dubus, J.; Voshaar, T.; Corbetta, L.; Broeders, M.; Dekhuijzen, R.; Sanchis, J.; Viejo, J.L.; Barnes, P.; et al. Effect of Incorrect Use of Dry Powder Inhalers on Management of Patients with Asthma and COPD. *Respir. Med.* **2008**, *102*, 593–604, doi:10.1016/j.rmed.2007.11.003.

86. van Beerendonk, I.; Mesters, I.; Mudde, A.N.; Tan, T.D. Assessment of the Inhalation Technique in Outpatients with Asthma or Chronic Obstructive Pulmonary Disease Using a Metered-Dose Inhaler or Dry Powder Device. *J. Asthma* **1998**, *35*, 273–279, doi:10.3109/02770909809068218.

87. Rau, J.L. Practical Problems With Aerosol Therapy in COPD. *Respir. CARE* **2006**, *51*, 15.

88. Lavorini, F.; Pistolesi, M.; Usmani, O.S. Recent Advances in Capsule-Based Dry Powder Inhaler Technology. *Multidiscip. Respir. Med.* **2017**, *12*, 11, doi:10.1186/s40248-017-0092-5.

89. Azouza, W.; Chrystyn, H. Clarifying the Dilemmas about Inhalation Techniques for Dry Powder Inhalers: Integrating Science with Clinical Practice. *Prim. Care Respir. J.* **2012**, *21*, 208–213, doi:10.4104/pcrj.2012.00010.

90. Gustafsson, P.; Taylor, A.; Zanen, P.; Chrystyn, H. Can Patients Use All Dry Powder Inhalers Equally Well?: CAN PATIENTS USE ALL DRY POWDER INHALERS EQUALLY WELL? *Int. J. Clin. Pract.* **2005**, *59*, 13–18, doi:10.1111/j.1368-504X.2005.00722.x.

91. Ashurst, I.; Malton, A.; Prime, D.; Sumby, B. Latest Advances in the Development of Dry Powder Inhalers. *Pharm. Sci. Technol. Today* **2000**, *3*, 246–256, doi:10.1016/S1461-5347(00)00275-3.

92. D'Arcy, S.; MacHale, E.; Seheult, J.; Holmes, M.S.; Hughes, C.; Sulaiman, I.; Hyland, D.; O'Reilly, C.; Glynn, S.; Al-Zaabi, T.; et al. A Method to Assess Adherence in Inhaler Use through Analysis of Acoustic Recordings of Inhaler Events. *PLoS ONE* **2014**, *9*, e98701, doi:10.1371/journal.pone.0098701.

93. Li, Y.; Bohr, A.; Jensen, H.; Rantanen, J.; Cornett, C.; Beck-Broichsitter, M.; Bøtker, J.P. Medication Tracking: Design and Fabrication of a Dry Powder Inhaler with Integrated Acoustic Element by 3D Printing. *Pharm. Res.* **2020**, *37*, 38, doi:10.1007/s11095-020-2755-8.

94. Xiroudaki, S.; Schoubben, A.; Giovagnoli, S.; Rekkas, D.M. Dry Powder Inhalers in the Digitalization Era: Current Status and Future Perspectives. *Pharmaceutics* **2021**, *13*, 1455, doi:10.3390/pharmaceutics13091455.

95. Kushwah, V.; Arora, S.; Tamás Katona, M.; Modhave, D.; Fröhlich, E.; Paudel, A. On Absorption Modeling and Food Effect Prediction of Rivaroxaban, a BCS II Drug Orally Administered as an Immediate-Release Tablet. *Pharmaceutics* **2021**, *13*, 283, doi:10.3390/pharmaceutics13020283.

96. The EINSTEIN–PE Investigators Oral Rivaroxaban for the Treatment of Symptomatic Pulmonary Embolism. *N. Engl. J. Med.* **2012**, *366*, 1287–1297, doi:10.1056/NEJMoa1113572.

97. Kvasnicka, T.; Malikova, I.; Zenahlikova, Z.; Kettnerova, K.; Brzezkova, R.; Zima, T.; Ulrych, J.; Briza, J.; Netuka, I.; Kvasnicka, J. Rivaroxaban - Metabolism, Pharmacologic Properties and Drug Interactions. *Curr. Drug Metab.* **2017**, *18*, doi:10.2174/1389200218666170518165443.

98. Samama, M.; Contant, G.; Spiro, T.E.; Perzborn, E.; Le Flem, L.; Guinet, C.; Gourmelin, Y.; Rohde, G.; Martinoli, J.-L. Laboratory Assessment of Rivaroxaban: A Review. *Thromb. J.* **2013**, *11*, 11, doi:10.1186/1477-9560-11-11.

99. Marcelino, G.; Hemett, O.M.; Descombes, E. Acute Renal Failure in a Patient with Rivaroxaban-Induced Hypersensitivity Syndrome: A Case Report with a Review of the Literature and of Pharmacovigilance Registries. *Case Rep. Nephrol.* **2020**, *2020*, 1–6, doi:10.1155/2020/6940183.

100. Kubitza, D.; Becka, M.; Voith, B.; Zuehlsdorf, M.; Wensing, G. Safety, Pharmacodynamics, and Pharmacokinetics of Single Doses of BAY 59-7939, an Oral, Direct Factor Xa Inhibitor. *Clin. Pharmacol. Ther.* **2005**, *78*, 412–421, doi:10.1016/j.clpt.2005.06.011.

101. Lehmann, T.; Hofer, K.; Baumann, M.; Hasler, K.; Ceschi, A.; Kupferschmidt, H.; Rohde, G.; Korte, W. Massive Human Rivaroxaban Overdose. *Thromb. Haemost.* **2014**, *112*, 834–836, doi:10.1160/TH14-02-0138.

102. Wu, L.; Miao, X.; Shan, Z.; Huang, Y.; Li, L.; Pan, X.; Yao, Q.; Li, G.; Wu, C. Studies on the Spray Dried Lactose as Carrier for Dry Powder Inhalation. *Asian J. Pharm. Sci.* **2014**, *9*, 336–341, doi:10.1016/j.ajps.2014.07.006.

103. AboulFotouh, K.; Zhang, Y.; Maniruzzaman, M.; Williams, R.O.; Cui, Z. Amorphous Solid Dispersion Dry Powder for Pulmonary Drug Delivery: Advantages and Challenges. *Int. J. Pharm.* **2020**, *587*, 119711, doi:10.1016/j.ijpharm.2020.119711.

104. Corrigan, D.O.; Corrigan, O.I.; Healy, A.M. Physicochemical and in Vitro Deposition Properties of Salbutamol Sulphate/Ipratropium Bromide and Salbutamol Sulphate/Excipient Spray Dried Mixtures for Use in Dry Powder Inhalers. *Int. J. Pharm.* **2006**, *322*, 22–30, doi:10.1016/j.ijpharm.2006.05.022.

105. Adi, H.; Young, P.M.; Chan, H.-K.; Agus, H.; Traini, D. Co-Spray-Dried Mannitol–Ciprofloxacin Dry Powder Inhaler Formulation for Cystic Fibrosis and Chronic Obstructive Pulmonary Disease. *Eur. J. Pharm. Sci.* **2010**, *40*, 239–247, doi:10.1016/j.ejps.2010.03.020.

106. Kou, X.; Chan, L.W.; Steckel, H.; Heng, P.W.S. Physico-Chemical Aspects of Lactose for Inhalation. *Adv. Drug Deliv. Rev.* **2012**, *64*, 220–232, doi:10.1016/j.addr.2011.11.004.

107. Rodrigues, C.I.; Marta, L.; Maia, R.; Miranda, M.; Ribeirinho, M.; Máguas, C. Application of Solid-Phase Extraction to Brewed Coffee Caffeine and Organic Acid Determination by UV/HPLC. *J. Food Compos. Anal.* **2007**, *20*, 440–448, doi:10.1016/j.jfca.2006.08.005.

108. Groß, R.; Berkenfeld, K.; Schulte, C.; Ebert, A.; Sule, S.; Sule, A.; Lamprecht, A. State of the Art in Capsule-Based Dry Powder Inhalers: Deagglomeration Techniques and the Consequences for Formulation Aerosolization. *Pharmaceutics* **2022**, *14*, 1185, doi:10.3390/pharmaceutics14061185.

109. Groß, R.; Berkenfeld, K.; Schulte, C.; Ebert, A.; Sule, S.; Sule, A.; Lamprecht, A. Effect of Texture and Surface Chemistry on Deagglomeration and Powder Retention in Capsule-Based Dry Powder Inhaler. *AAPS PharmSciTech* **2022**, *23*, 281, doi:10.1208/s12249-022-02436-0.

110. Kožák, J., Chrétien, C., Pellequer, Y., & Lamprecht, A. 2022. Rivaroxaban lyospheres prepared by a dimethyl sulfoxide-based spray-freeze-drying process. International Journal of Pharmaceutics, 627, 122235.

111. Perzborn, E.; Strassburger, J.; Wilmen, A.; Pohlmann, J.; Roehrig, S.; Schlemmer, K.-H.; Straub, A. In Vitro and in Vivo Studies of the Novel Antithrombotic Agent BAY 59-7939-an Oral, Direct Factor Xa Inhibitor. *J. Thromb. Haemost.* **2005**, *3*, 514–521, doi:10.1111/j.1538-7836.2005.01166.x.

112. Wang, L.; Gai, S.; Zhang, X.; Xu, X.; Gou, N.; Wang, X.; Zhou, N.; Feng, T. Simultaneous Determination of Rivaroxaban and TAK-438 in Rat Plasma by LC–MS/MS: Application to Pharmacokinetic Interaction Study. *Bioanalysis* **2020**, *12*, 11–22, doi:10.4155/bio-2019-0130.

113. Laux, V.; Perzborn, E.; Kubitza, D.; Misselwitz, F. Preclinical and Clinical Characteristics of Rivaroxaban: A Novel, Oral, Direct Factor Xa Inhibitor. *Semin. Thromb. Hemost.* **2007**, *33*, 515–523, doi:10.1055/s-2007-982083.

114. Mueck, W.; Stampfuss, J.; Kubitza, D.; Becka, M. Clinical Pharmacokinetic and Pharmacodynamic Profile of Rivaroxaban. *Clin. Pharmacokinet.* **2014**, *53*, 1–16, doi:10.1007/s40262-013-0100-7.

115. Graff, J.; von Hentig, N.; Misselwitz, F.; Kubitza, D.; Becka, M.; Breddin, H.-K.; Harder, S. Effects of the Oral, Direct Factor Xa Inhibitor Rivaroxaban on Platelet-Induced Thrombin Generation and Prothrombinase Activity [1]. *J. Clin. Pharmacol.* **2007**, *47*, 1398–1407, doi:10.1177/0091270007302952.

116. Sakr, Y.; Giovini, M.; Leone, M.; Pizzilli, G.; Kortgen, A.; Bauer, M.; Tonetti, T.; Duclos, G.; Zieleskiewicz, L.; Buschbeck, S.; et al. Pulmonary Embolism in Patients with Coronavirus Disease-2019 (COVID-19) Pneumonia: A Narrative Review. *Ann. Intensive Care* **2020**, *10*, 124, doi:10.1186/s13613-020-00741-0.

117. Akel, T.; Qaqa, F.; Abuarqoub, A.; Shamoon, F. Pulmonary Embolism: A Complication of COVID 19 Infection. *Thromb. Res.* **2020**, *193*, 79–82, doi:10.1016/j.thromres.2020.05.033.

118. Harrison, T.W. Plasma Concentrations of Fluticasone Propionate and Budesonide Following Inhalation from Dry Powder Inhalers by Healthy and Asthmatic Subjects. *Thorax* **2003**, *58*, 258–260, doi:10.1136/thorax.58.3.258.

119. Thorsson, L.; Edsbäcker, S.; Källén, A.; Löfdahl, C.-G. Pharmacokinetics and Systemic Activity of Fluticasone via Diskus ® and PMDI, and of Budesonide via Turbuhaler ®: *PK and PD of Fluticasone and Budesonide*. *Br. J. Clin. Pharmacol.* **2001**, *52*, 529–538, doi:10.1046/j.0306-5251.2001.01493.x.

120. Mäkelä, M.J.; Backer, V.; Hedegaard, M.; Larsson, K. Adherence to Inhaled Therapies, Health Outcomes and Costs in Patients with Asthma and COPD. *Respir. Med.* **2013**, *107*, 1481–1490, doi:10.1016/j.rmed.2013.04.005.

121. Lipworth, B.J. Systemic Adverse Effects of Inhaled Corticosteroid Therapy: A Systematic Review and Meta-Analysis. *Arch. Intern. Med.* **1999**, *159*, 941, doi:10.1001/archinte.159.9.941.

122. Soriano, J.B.; Rabe, K.F.; Vermeire, P.A. Predictors of Poor Asthma Control in European Adults. *J. Asthma* **2003**, *40*, 803–813, doi:10.1081/JAS-120023572.

123. Partridge, M.R.; Busse, W.W. Attitudes and Actions of Asthma Patients on Regular Maintenance Therapy: The INSPIRE Study. *BMC Pulm. Med.* **2006**, 9.

124. Price, D.; Bosnic-Anticevich, S.; Briggs, A.; Chrystyn, H.; Rand, C.; Scheuch, G.; Bousquet, J. Inhaler Competence in Asthma: Common Errors, Barriers to Use and Recommended Solutions. *Respir. Med.* **2013**, *107*, 37–46, doi:10.1016/j.rmed.2012.09.017.

125. Murphy, A.C.; Proeschal, A.; Brightling, C.E.; Wardlaw, A.J.; Pavord, I.; Bradding, P.; Green, R.H. The Relationship between Clinical Outcomes and Medication Adherence in Difficult-to-Control Asthma: Table 1. *Thorax* **2012**, *67*, 751–753, doi:10.1136/thoraxjnl-2011-201096.

126. Williams, L.K.; Pladevall, M.; Xi, H.; Peterson, E.L.; Joseph, C.; Lafata, J.E.; Ownby, D.R.; Johnson, C.C. Relationship between Adherence to Inhaled Corticosteroids and Poor Outcomes among Adults with Asthma. *J. Allergy Clin. Immunol.* **2004**, *114*, 1288–1293, doi:10.1016/j.jaci.2004.09.028.

127. Pedersen, S.; Hansen, O.R.; Fuglsang, G. Influence of Inspiratory Flow Rate upon the Effect of a Turbuhaler. *Arch. Dis. Child.* **1990**, *65*, 308–310, doi:10.1136/adc.65.3.308.

128. Sheth, K.; Wasserman, R.L.; Lincourt, W.R.; Locantore, N.W.; Carranza-Rosenzweig, J.; Crim, C. Fluticasone Propionate/Salmeterol Hydrofluoroalkane via Metered-Dose Inhaler with Integrated Dose Counter: Performance and Patient Satisfaction: METERED-DOSE INHALER WITH INTEGRATED DOSE COUNTER. *Int. J. Clin. Pract.* **2006**, *60*, 1218–1224, doi:10.1111/j.1742-1241.2006.01138.x.

129. Pekka Malmberg, L.; Sovijärvi, A.R.A.; Paajanen, E.; Piirilä, P.; Haahtela, T.; Katila, T. Changes in Frequency Spectra of Breath Sounds During Histamine Challenge Test in Adult Asthmatics and Healthy Control Subjects. *Chest* **1994**, *105*, 122–131, doi:10.1378/chest.105.1.122.

130. Sánchez Morillo, D.; Astorga Moreno, S.; Fernández Granero, M.Á.; León Jiménez, A. Computerized Analysis of Respiratory Sounds during COPD Exacerbations. *Comput. Biol. Med.* **2013**, *43*, 914–921, doi:10.1016/j.compbiomed.2013.03.011.

131. McCartan, T.A.; Taylor, T.E.; Sulaiman, I.; Costello, R.W.; Reilly, R.B. Changes in Inhaler Inhalation Acoustic Features during Induced Bronchoconstriction: A Pilot Study. In Proceedings of the 2016 38th Annual International Conference of the IEEE Engineering in Medicine and Biology Society (EMBC); IEEE: Orlando, FL, August 2016; pp. 3749–3752.

132. Berkenfeld, K.; McConville, J.T.; Lamprecht, A. (Solvato-) Polymorphism of Formulations of Rifampicin for Pulmonary Drug Delivery Prepared Using a Crystallization/Spray Drying Process. *Int. J. Pharm.* **2020**, *590*, 119932, doi:10.1016/j.ijpharm.2020.119932.

133. Berkenfeld, K.; McConville, J.T.; Lamprecht, A. Inhalable Dry Powders of Rifampicin Highlighting Potential and Drawbacks in Formulation Development for Experimental Tuberculosis Aerosol Therapy. *Expert Opin. Drug Deliv.* **2020**, *17*, 305–322, doi:10.1080/17425247.2020.1720644.

134. Sulaiman, I.; Greene, G.; MacHale, E.; Seheult, J.; Mokoka, M.; D'Arcy, S.; Taylor, T.; Murphy, D.M.; Hunt, E.; Lane, S.J.; et al. A Randomised Clinical Trial of Feedback on Inhaler Adherence and Technique in Patients with Severe Uncontrolled Asthma. *Eur. Respir. J.* **2018**, *51*, 1701126, doi:10.1183/13993003.01126-2017.

135. Toumas-Shehata, M.; Price, D.; Amin Basheti, I.; Bosnic-Anticevich, S. Exploring the Role of Quantitative Feedback in Inhaler Technique Education: A Cluster-Randomised, Two-Arm, Parallel-Group, Repeated-Measures Study. *Npj Prim. Care Respir. Med.* **2014**, *24*, 14071, doi:10.1038/npjpcrm.2014.71.

136. Benque, B.; Khinast, J.G. Understanding the Motion of Hard-Shell Capsules in Dry Powder Inhalers. *Int. J. Pharm.* **2019**, *567*, 118481, doi:10.1016/j.ijpharm.2019.118481.

137. Coates, M.S.; Chan, H.-K.; Fletcher, D.F.; Raper, J.A. Influence of Air Flow on the Performance of a Dry Powder Inhaler Using Computational and Experimental Analyses. *Pharm. Res.* **2005**, *22*, 1445–1453, doi:10.1007/s11095-005-6155-x.

138. Mohammed, H.; Roberts, D.L.; Copley, M.; Hammond, M.; Nichols, S.C.; Mitchell, J.P. Effect of Sampling Volume on Dry Powder Inhaler (DPI)-Emitted

Aerosol Aerodynamic Particle Size Distributions (APSDs) Measured by the Next-Generation Pharmaceutical Impactor (NGI) and the Andersen Eight-Stage Cascade Impactor (ACI). *AAPS PharmSciTech* **2012**, *13*, 875–882, doi:10.1208/s12249-012-9797-0.

139. Lin, Y.-W.; Wong, J.; Qu, L.; Chan, H.-K.; Zhou, Q. Powder Production and Particle Engineering for Dry Powder Inhaler Formulations. *Curr. Pharm. Des.* **2015**, *21*, 3902–3916, doi:10.2174/1381612821666150820111134.

140. Islam, N.; Cleary, M.J. Developing an Efficient and Reliable Dry Powder Inhaler for Pulmonary Drug Delivery – A Review for Multidisciplinary Researchers. *Med. Eng. Phys.* **2012**, *34*, 409–427, doi:10.1016/j.medengphy.2011.12.025.

141. Coates, M.S.; Fletcher, D.F.; Chan, H.-K.; Raper, J.A. The Role of Capsule on the Performance of a Dry Powder Inhaler Using Computational and Experimental Analyses. *Pharm. Res.* **2005**, *22*, 923–932, doi:10.1007/s11095-005-4587-y.

142. Demoly, P.; Hagedoorn, P.; de Boer, A.H.; Frijlink, H.W. The Clinical Relevance of Dry Powder Inhaler Performance for Drug Delivery. *Respir. Med.* **2014**, *108*, 1195–1203, doi:10.1016/j.rmed.2014.05.009.

143. Hassan, M.S.; Lau, R.W.M. Effect of Particle Shape on Dry Particle Inhalation: Study of Flowability, Aerosolization, and Deposition Properties. *AAPS PharmSciTech* **2009**, *10*, 1252, doi:10.1208/s12249-009-9313-3.

144. Yadav, N.; Lohani, A. Dry Powder Inhalers: A Review. 12.

145. Schoubben, A.; Blasi, P.; Giontella, A.; Giovagnoli, S.; Ricci, M. Powder, Capsule and Device: An Imperative Ménage à Trois for Respirable Dry Powders. *Int. J. Pharm.* **2015**, *494*, 40–48, doi:10.1016/j.ijpharm.2015.08.012.

146. Coates, M.S.; Fletcher, D.F.; Chan, H.-K.; Raper, J.A. Effect of Design on the Performance of a Dry Powder Inhaler Using Computational Fluid Dynamics. Part 1: Grid Structure and Mouthpiece Length. *J. Pharm. Sci.* **2004**, *93*, 2863–2876, doi:10.1002/jps.20201.

147. Coates, M.S.; Chan, H.-K.; Fletcher, D.F.; Chiou, H. Influence of Mouthpiece Geometry on the Aerosol Delivery Performance of a Dry Powder Inhaler. *Pharm. Res.* **2007**, *24*, 1450–1456, doi:10.1007/s11095-007-9262-z.

148. Pinto, J.T.; Wutscher, T.; Stankovic-Brandl, M.; Zellnitz, S.; Biserni, S.; Mercandelli, A.; Kobler, M.; Buttini, F.; Andrade, L.; Daza, V.; et al. Evaluation of the Physico-Mechanical Properties and Electrostatic Charging Behavior of Different Capsule Types for Inhalation Under Distinct Environmental Conditions. *AAPS PharmSciTech* **2020**, *21*, 128, doi:10.1208/s12249-020-01676-2.

149. Mehta, P.P.; Pawar, A.P.; Mahadik, K.R.; Kadam, S.S.; Dhapte-Pawar, V. Dry Powder Coating Techniques and Role of Force Controlling Agents in Aerosol. In *Polymer Coatings*; Inamuddin, Boddula, R., Ahamed, M.I., Asiri, A.M., Eds.; Wiley, 2020; pp. 41–74 ISBN 978-1-119-65499-5.

150. Zhou, Q. (Tony); Tang, P.; Leung, S.S.Y.; Chan, J.G.Y.; Chan, H.-K. Emerging Inhalation Aerosol Devices and Strategies: Where Are We Headed? *Adv. Drug Deliv. Rev.* **2014**, *75*, 3–17, doi:10.1016/j.addr.2014.03.006.

151. Heng, D.; Lee, S.H.; Ng, W.K.; Chan, H.-K.; Kwek, J.W.; Tan, R.B.H. Novel Alternatives to Reduce Powder Retention in the Dry Powder Inhaler during Aerosolization. *Int. J. Pharm.* **2013**, *452*, 194–200, doi:10.1016/j.ijpharm.2013.05.006.

152. Behara, S.R.B.; Farkas, D.R.; Hindle, M.; Longest, P.W. Development of a High Efficiency Dry Powder Inhaler: Effects of Capsule Chamber Design and Inhaler Surface Modifications. *Pharm. Res.* **2014**, *31*, 360–372, doi:10.1007/s11095-013-1165-6.

153. Behara, S.R.B.; Longest, P.W.; Farkas, D.R.; Hindle, M. Development of High Efficiency Ventilation Bag Actuated Dry Powder Inhalers. *Int. J. Pharm.* **2014**, *465*, 52–62, doi:10.1016/j.ijpharm.2014.01.043.

154. Behara, S.R.B.; Worth Longest, P.; Farkas, D.R.; Hindle, M. Development and Comparison of New High-Efficiency Dry Powder Inhalers for Carrier-Free Formulations. *J. Pharm. Sci.* **2014**, *103*, 465–477, doi:10.1002/jps.23775.

155. Chu, P.K.; Chen, J.Y.; Wang, L.P.; Huang, N. Plasma-Surface Modification of Biomaterials. **2002**, 64.

156. Jelil, R.A. A Review of Low-Temperature Plasma Treatment of Textile Materials. *J. Mater. Sci.* **2015**, *50*, 5913–5943, doi:10.1007/s10853-015-9152-4.

157. von Keudell, A.; Schulz-von der Gathen, V. Foundations of Low-Temperature Plasma Physics—an Introduction. *Plasma Sources Sci. Technol.* **2017**, *26*, 113001, doi:10.1088/1361-6595/aa8d4c.

158. Adamovich, I.; Baalrud, S.D.; Bogaerts, A.; Bruggeman, P.J.; Cappelli, M.; Colombo, V.; Czarnetzki, U.; Ebert, U.; Eden, J.G.; Favia, P.; et al. The 2017 Plasma Roadmap: Low Temperature Plasma Science and Technology. *J. Phys. Appl. Phys.* **2017**, *50*, 323001, doi:10.1088/1361-6463/aa76f5.

159. Vesel, A.; Mozetic, M.; Zalar, A. XPS Study of Oxygen Plasma Activated PET. *Vacuum* **2007**, *82*, 248–251, doi:10.1016/j.vacuum.2007.07.021.

160. Grace, J.M.; Gerenser, L.J. Plasma Treatment of Polymers. *J. Dispers. Sci. Technol.* **2003**, *24*, 305–341, doi:10.1081/DIS-120021793.

161. Cvelbar, U.; Pejovnik, S.; Mozetiè, M.; Zalar, A. Increased Surface Roughness by Oxygen Plasma Treatment of Graphite/Polymer Composite. *Appl. Surf. Sci.* **2003**, *210*, 255–261, doi:10.1016/S0169-4332(02)01286-2.

162. Junkar, I.; Vesel, A.; Cvelbar, U.; Mozetič, M.; Strnad, S. Influence of Oxygen and Nitrogen Plasma Treatment on Polyethylene Terephthalate (PET) Polymers. *Vacuum* **2009**, *84*, 83–85, doi:10.1016/j.vacuum.2009.04.011.

163. Phan, L.; Yoon, S.; Moon, M.-W. Plasma-Based Nanostructuring of Polymers: A Review. *Polymers* **2017**, *9*, 417, doi:10.3390/polym9090417.

164. Tsougeni, K.; Vourdas, N.; Tserepi, A.; Gogolides, E.; Cardinaud, C. Mechanisms of Oxygen Plasma Nanotexturing of Organic Polymer Surfaces: From Stable Super Hydrophilic to Super Hydrophobic Surfaces. *Langmuir* **2009**, *25*, 11748–11759, doi:10.1021/la901072z.

165. Manoharan, K.; Bhattacharya, S. Superhydrophobic Surfaces Review: Functional Application, Fabrication Techniques and Limitations. *J. Micromanufacturing* **2019**, *2*, 59–78, doi:10.1177/2516598419836345.

166. Zanini, S.; Riccardi, C.; Orlandi, M.; Esena, P.; Tontini, M.; Milani, M.; Cassio, V. Surface Properties of HMDSO Plasma Treated Polyethylene Terephthalate. *Surf. Coat. Technol.* **2005**, *200*, 953–957, doi:10.1016/j.surfcoat.2005.01.093.

167. Kang, S.K.; Kim, P.Y.; Koo, I.G.; Kim, H.Y.; Jung, J.-C.; Choi, M.Y.; Lee, J.K.; Collins, G.J. Non-Stick Polymer Coatings for Energy-Based Surgical Devices Employed in Vessel Sealing. *Plasma Process. Polym.* **2012**, *9*, 446–452, doi:10.1002/ppap.201100155.

168. Ji, Y.Y.; Chang, H.K.; Hong, Y.C.; Lee, S.H. Water-Repellent Improvement of Polyester Fiber via Radio Frequency Plasma Treatment with Argon/Hexamethyldisiloxane (HMDSO) at Atmospheric Pressure. *Curr. Appl. Phys.* **2009**, *9*, 253–256, doi:10.1016/j.cap.2008.02.003.

169. Berkenfeld, K.; McConville, J.T.; Lamprecht, A. Inhalable Formulations of Rifampicin by Spray Drying of Supersaturated Aqueous Solutions. *Eur. J. Pharm. Biopharm.* **2020**, *153*, 14–22, doi:10.1016/j.ejpb.2020.05.007.

170. Son, Y.-J.; McConville, J.T. Preparation of Sustained Release Rifampicin Microparticles for Inhalation: Sustained-Release Inhaled Rifampicin. *J. Pharm. Pharmacol.* **2012**, *64*, 1291–1302, doi:10.1111/j.2042-7158.2012.01531.x.

171. Buttini, F.; Brambilla, G.; Copelli, D.; Sisti, V.; Balducci, A.G.; Bettini, R.; Pasquali, I. Effect of Flow Rate on *In Vitro* Aerodynamic Performance of NEXThaler ® in Comparison with Diskus ® and Turbohaler ® Dry Powder Inhalers. *J. Aerosol Med. Pulm. Drug Deliv.* **2016**, *29*, 167–178, doi:10.1089/jamp.2015.1220.

172. Kim, Y.G.; Lim, N.; Kim, J.; Kim, C.; Lee, J.; Kwon, K.-H. Study on the Surface Energy Characteristics of Polydimethylsiloxane (PDMS) Films Modified by C4F8/O2/Ar Plasma Treatment. *Appl. Surf. Sci.* **2019**, *477*, 198–203, doi:10.1016/j.apsusc.2017.11.009.

173. Maradia, U.; Filisetti, E.; Boccadoro, M.; Roten, M.; Dutoit, J.-M.; Hengsberger, S. Increasing the Injection Moulding Productivity through EDM Surface Modulation. *Procedia CIRP* **2018**, *68*, 58–63, doi:10.1016/j.procir.2017.12.022.

174. Matschuk, M.; Larsen, N.B. Injection Molding of High Aspect Ratio Sub-100 Nm Nanostructures. *J. Micromechanics Microengineering* **2013**, *23*, 025003, doi:10.1088/0960-1317/23/2/025003.

175. Maghsoudi, K.; Jafari, R.; Momen, G.; Farzaneh, M. Micro-Nanostructured Polymer Surfaces Using Injection Molding: A Review. *Mater. Today Commun.* **2017**, *13*, 126–143, doi:10.1016/j.mtcomm.2017.09.013.

176. Friebel, C.; Steckel, H.; Müller, B.W. Rational Design of a Dry Powder Inhaler: Device Design and Optimisation. *J. Pharm. Pharmacol.* **2012**, *64*, 1303–1315, doi:10.1111/j.2042-7158.2012.01525.x.

12. Appendix

13. State of the Art in Capsule-Based Dry Powder Inhalers: Deagglomeration Techniques and the Consequences for Formulation Aerosolization

This work was published as:

Groß, R.; Berkenfeld, K.; Schulte, C.; Ebert, A.; Sule, S.; Sule, A.; Lamprecht, A. State of the Art in Capsule-Based Dry Powder Inhalers: Deagglomeration Techniques and the Consequences for Formulation Aerosolization. Pharmaceutics 2022, 14, 1185, doi:10.3390/pharmaceutics14061185.

13.1 Graphical abstract

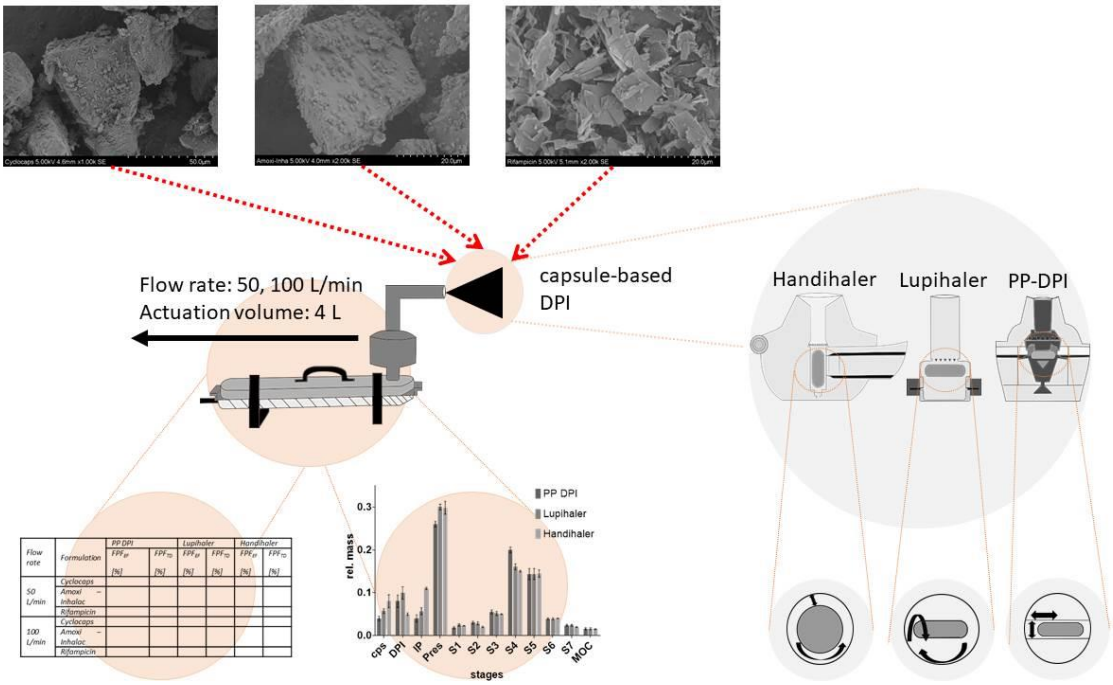

13.2 Abstract

Commercially available dry powder inhalers (DPIs) are usually devices in a fixed combination with the intended formulation, and a change in medication by the physician often forces the patient to use a different device, requiring the patient to relearn how to use it, resulting in lower adherence and inadequate therapy. To investigate whether DPIs can achieve successful outcomes regardless of the formulation and flow rate used, a novel DPI and two commercially available devices were compared in vitro for their deagglomeration behavior for different binary blends and a spray-dried particle formulation. The results demonstrate that the novel device achieved the highest fine particle fraction (FPF) regardless of the formulations tested. In the binary mixtures tested, the highest emitted fraction was obtained by shaking out the powder due to the oscillating motion of the capsule in the novel device during actuation. For DPIs with high intrinsic resistance to airflow, similar FPFs were obtained with the respective DPI and formulation, regardless of the applied flow rate. Additionally, the development and use of binary blends of spray-dried APIs and carrier

particles may result in high FPF and overcome disadvantages of spray-dried particles, such as high powder retention in the capsule.

13.3 Introduction

Dry powder inhalers (DPIs) are widely used for the therapy of lung diseases such as asthma, chronic obstructive pulmonary disease (COPD), or bacterial infections [88,133]. To achieve a sufficient therapeutic effect by deposition of the powder in the lower respiratory tract, the powder particles should have an aerodynamic diameter of <5 µm [29]. For this purpose, special manufacturing processes such as jet-milling of the active pharmaceutical ingredient (API) are used in the pharmaceutical industry to produce micronized particles in the inhalable size range [30,31,139]. However, increasing the total particle surface area by this technology often results in very cohesive particles that have poor aerosolization efficiency and flowability [33]. To overcome this problem and produce flowable and deagglomerable powder formulations, various formulation techniques are used, such as mixing the jet-milled particles with large carrier particles (e.g., lactose) to form interactive blends [34,106]. This method of formulation is preferred in the pharmaceutical industry due to the resulting high storage stability of the crystalline APIs [32]. In the case of particle engineered approaches, such as spray-dried particle formulations, the device should overcome the cohesive particle interactions during inhalation [103]. Apart from the formulation's characteristics, it is known that the success of therapy with passive breath-actuated DPIs depends mainly on the physiological conditions of the patient and the inhalation profiles generated [60]. Inhalation performed with insufficient respiratory force and duration results in an unintentionally low emitted dose with insufficient powder deagglomeration and thus insufficient therapeutic success [61,62]. Since a COPD patient cannot achieve the same inspirational flow profile as a healthy person, this leads to decreased deposition of the powder in the lungs. To counteract this problem, high intrinsic resistance devices are being developed that should deliver the same amount of aerosol regardless of airway resistance and applied inhalation flow rate [65,88,89]. In addition to the aforementioned inhalation properties of the patient, the delivered powder fraction and the resulting aerodynamic properties of the

aerosol are also related to the device properties, which include the opening mechanism of the capsule being used, the movement of the capsule (vibration, rotation, shaking), and the interaction between the powder, the capsule, and the inhaler wall [140]. The size and position of the holes pierced in the capsule also influence the aerosol properties [141].

Since the success of inhalation depends on many factors, as described, marketed delivery systems are designed as combination products consisting of the formulation and the DPI to minimize the number of potential sources of error. The formulation and the device are designed to work together to achieve a satisfactory therapeutic effect [56,57]. This results in a marketed formulation being prescribed by the physician only with the inhaler intended for it and patients having to relearn how to use a different inhaler when they change medications, which could affect treatment adherence [124]. Since different inhalers result in different deagglomeration of the same powder, developing and marketing a generic device is challenging.

To investigate what the current market looks like, the study compared three capsule-based DPIs. Due to geometry and airflow, each unit has a different capsule motion and consequently a different mechanism for deagglomerating the powder. The study was designed to show which deagglomeration unit provides the highest fine particle fraction ($FPF_{TD/EF}$ = fraction of particles with an aerodynamic diameter < 5 µm of the total dose/emitted fraction) regardless of the formulation tested and actuation conditions used. To determine the influence of capsule movement on powder ejection and the number of particles that can potentially reach the lungs, devices with axial capsule vibration (Handihaler® (Boehringer Ingelheim, Ingelheim am Rhein, Germany)), capsule rotation (Lupihaler® (Lupin Limited, Mumbai, India) = RS01 equivalent device), and oscillating capsule movement (Presspart prototype DPI = PP-DPI) were compared (Fig. 18) [63,64]. While the Handihaler® and Lupihaler® DPI are marketed devices that are well-known and extensively described, the Presspart prototype DPI is a novel capsule-based device. In order to analyze the “applicability of the devices for different formulations”, a series of drug formulations developed with different formulation techniques were tested. While the marketed formulation Cyclocaps® (PB Pharma

GmbH, Meerbusch, Germany) is an interactive blend of micronized albuterol sulfate and alpha lactose monohydrate, a spray-dried rifampicin formulation was also tested [132,133]. To demonstrate the potential use of carrier particles for spray-dried API particles, a spray-dried batch of amoxicillin was mixed with Inhalac 251® (MEGGLE GmbH & Co. KG, Wasserburg am Inn, Germany) (ratio 1:24) in a further step to form a binary mixture, which was aerosolized using the above inhalers. To demonstrate the potentially flow-profile-independent deagglomeration behavior of the selected DPIs for the tested formulations, 50 L/min was selected as the low flow rate and 100 L/min as the high flow rate. These settings were also chosen because they closely approximate the actual flow rates of the low (Lupihaler) or high intrinsic resistance (PP-DPI, Handihaler) devices used in this study at a pressure drop of 4. To analyze the deagglomeration behavior of the devices for each formulation, in addition to the relative powder deposition in each stage, the $FPF_{TD/EF}$ was compared.

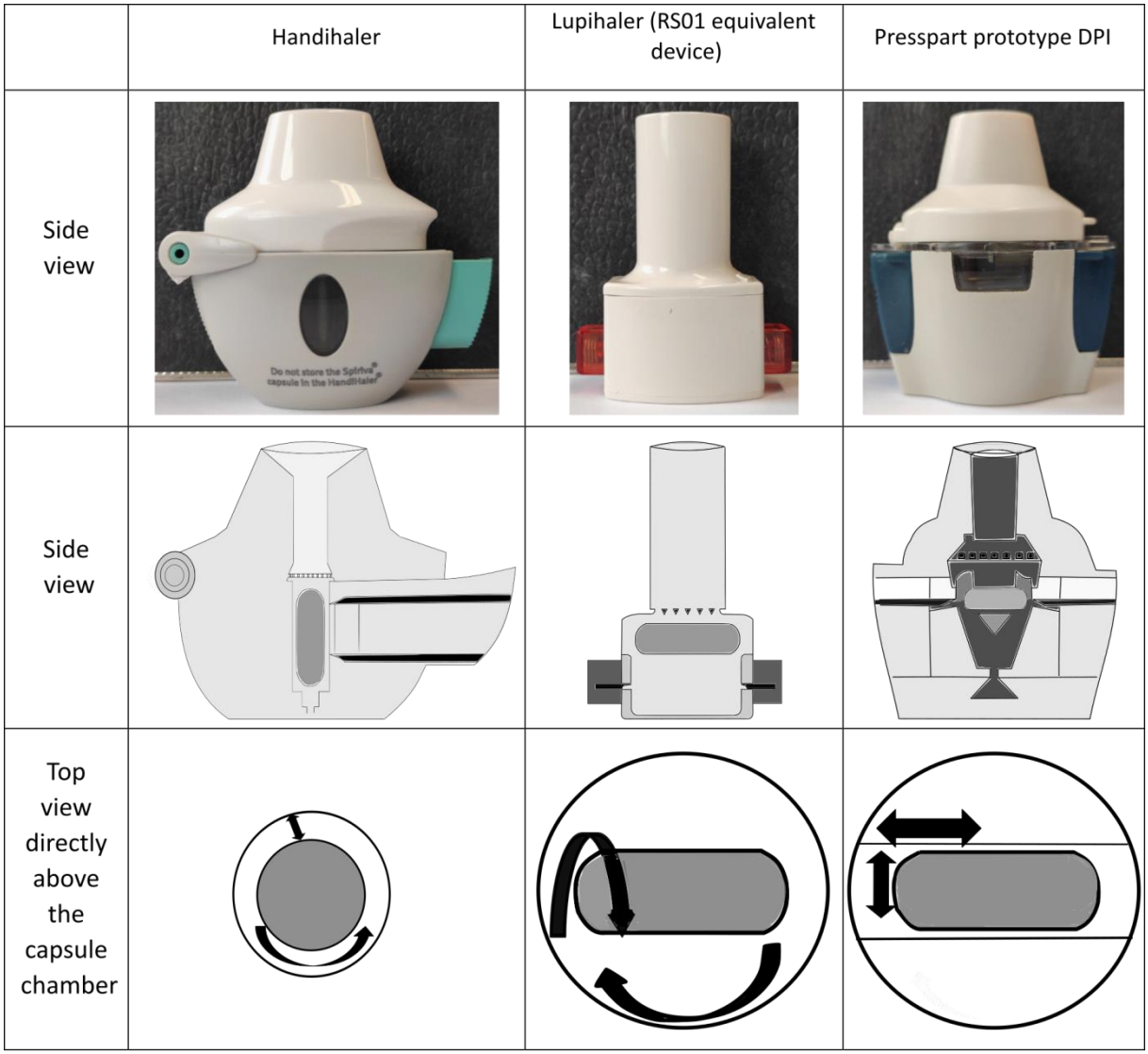

Figure 18: Schematic representation of the tested dry powder inhalers (DPIs) and the possible capsule movements that can be achieved in the various DPIs during inhalation. Modified from [22, 23].

13.4 Materials and Methods

13.4.1 Materials

The albuterol sulfate–alpha lactose monohydrate formulation (Cyclocaps®) (PB Pharma GmbH, Meerbusch, Germany) was purchased from a pharmacy. For spray-drying, rifampicin and amoxicillin were ordered from TCI (Tokyo, Japan). Except for

water, which was purified in-house (Merck-Millipore Biocel A10, Burlington, MA, USA), all other solvents were HPLC grade. Inhalac 251® was a kind gift from MEGGLE GmbH & Co. KG (Wasserburg am Inn, Germany). The Lupihaler® devices (Lupin Limited, Mumbai, India) were purchased from a pharmacy in India. The Handihaler® and Presspart prototype DPI inhalers were gifts from Boehringer Ingelheim (Ingelheim am Rhein, Germany) and H&T Presspart (Blackburn, United Kingdom), respectively.

13.4.2 Spray-Drying of the Rifampicin and Amoxicillin APIs

Rifampicin was spray-dried as described in [132]. Briefly summarized, the drug was suspended in ethanol (38 mg/mL) and sonicated in an ultrasonic bath (Typ DT 106, Bandelin electronic, Berlin, Germany) under controlled temperature conditions (25 °C) for 10 min. To keep the temperature constant during the water change, a thermostat (DC 10, Haake Technik GmbH, Vreden, Germany) was used. A B-290 spray-dryer equipped with a high-performance cyclone, a B-296 dehumidification unit, a B-295 (all Buchi, Flawil, Switzerland) inert loop, and an anemometer (AF89-AD1AA13C0AA, Fluid components Intl. San Marcos, CA, USA) was used for spray-drying under inert atmosphere (N_2). A modified three-fluid nozzle (Buchi, inner channel blocked) was used to atomize the suspension. During the entire manufacturing process, the suspension was constantly stirred.

For spray-drying of amoxicillin, the same spray-drying equipment was used. Prior to the spray process, 2 g of the API was dissolved in 185 mL MeOH, and the solution obtained was spray-dried (Tab. S3).

13.4.3 Mixing the Amoxicillin—Lactose Binary Blend

To generate the binary mixture, the spray-dried active ingredient was mixed with the carrier lactose monohydrate (Inhalac 251) in a ratio of 1:24. For this purpose, both materials were mixed in a sequential mixing process using a Turbula Mixer (Willy A. Bachofen, Muttenz, Schweiz) at 46 rpm for 5 min per mixing step until the mentioned mixing ratio was achieved.

13.4.4 Airflow Resistance of the Various DPIs

In order to measure the pressure drop across the devices and calculate the intrinsic resistance to airflow, each DPI was connected with a suitable adapter to a Dosage Unit Sampling Apparatus (DUSA), and that was connected with a flow meter (DFM 2000), a critical flow controller (CFC) (TPK 2100-R) and two vacuum pumps (HCP 5, all Copley Scientific Limited, Nottingham, United Kingdom). The pressure port of the DUSA was connected to the pressure port of the CFC. Measurements were made with a pressure drop from 1 to 8 kPa, and the specific resistance to airflow was calculated from the linear relationship between the square root of the pressure drop and the resulting flow rate (Fig. S10).

13.4.5 Test Procedure for the Aerosol Classification with the Next-Generation Impactor

While the Cyclocaps® capsules (albuterol sulfate–lactose) were purchased ready dosed, 5 mg of the rifampicin formulation and 30 mg of the amoxicillin–lactose blend formulation was filled into size 3 gelatine capsules. A Next-Generation Impactor (NGI) (Copley Scientific Limited, Nottingham, United Kingdom) was used to characterize the aerosol properties of the different formulations actuated with the different devices. Prior to the experiments, each cup was coated with a 1% glycerol-methanol (m/v) solution, and 15 mL of the diluent was placed in the preseparator unit. For analyzing the powder de-agglomeration behavior of the DPIs, the particles were dissolved from each stage (capsule–MOC). While a water–methanol mixture (1:1% v/v) was used for albuterol sulfate and amoxicillin, rifampicin was dissolved in a solution of ascorbic acid in methanol (0.5% m/v). Flow rates of 50 and 100 L/min and an actuation volume of 4 L were used to compare the different devices in terms of aerosolization properties for the respective formulation. Unless otherwise reported, all experiments were performed in triplicate.

13.4.6 Scanning Electron Microscopy (SEM)

The samples were sputter-coated with gold for two cycles of two minutes each after being fixed with carbonaceous conductive paste on an aluminum sample holder. Subsequent imaging of the different formulations was performed in a high vacuum using a Hitachi SU-3500 SEM (Hitachi Ltd., Tokyo, Japan). While the magnification and working distance for each sample were set as needed and are reported in the SEM images, the accelerating voltage was set to 5 kV for all samples.

13.4.7 High-Performance Liquid Chromatography Analysis

Quantification of the active compounds deposited in the different NGI stages was performed by high-performance liquid chromatography (HPLC) analysis (Shimadzu, LC-2030C 3D Plus, Kyoto, Japan) using an RP18 column (Lichrospher 100 RP 18-5µ EC, 250 × 4.6 mm). To detect the APIs, the photodiode array detector was set to 337 nm for rifampicin, 275 nm for albuterol sulfate, and amoxicillin was detected at a wavelength of 230 nm. The mobile phase for both binary mixtures consisted of phosphate buffer/methanol (80:20 v/v (%)), and the buffer was adjusted to pH 3.0 in the case of albuterol sulfate and pH 4.0 for the amoxicillin. An isocratic flow of 1.4 mL/min (albuterol sulfate) or 1.0 mL/min (amoxicillin) was applied. For rifampicin, a flow rate of 1 mL/min of a mixture of a phosphate buffer pH 5.2/methanol/acetonitrile (33/50/17% v/v/v) was set. With the exception of rifampicin, which had a column temperature of 25 °C during quantification, the other active ingredients were analyzed at 40 °C. The limit of detection (LOD) and limit of quantification (LOQ) were calculated using the values of the intercepts and the slope of the calibration curve. For albuterol sulfate, the LOD and LOQ were determined to be 0.36 µg/mL and 1.08 µg/mL, whereas, for amoxicillin, the LOD and LOQ were calculated to be 0.97 µg/mL and 2.94 µg/mL. For rifampicin, the LOD was 0.30 µg/mL, and the LOQ was 0.90 µg/mL [132].

13.4.8 Statistics and Data Processing

To determine statistically significant differences in relative powder deposition in the different stages of the NGI (capsule–MOC) after actuation with different DPIs, results

were compared using rank-sum ANOVA followed by Dunn`s test ($p < 0.05$) (Prism 8.0.2, GraphPad software). The choice of a non-parametric test was mainly based on the rather limited sample size of n = 3 in order to increase the robustness of the statistical decision, although all data were normally distributed. The NGI plots show the relative powder deposition in the different stages. The error bars indicate one standard deviation. Cumulative undersize plots from S1 to MOC were created and linearized by log transformation of the stage boundaries and probit transformation of the relative abundances. For calculating the fine particle fraction, a linear regression model was used ($FPF_{TD/EF}$ (fraction of particles with an aerodynamic diameter < 5 µm of the total dose/emitted fraction)), as described in USP <601> [81].

13.5 Results

The Presspart prototype DPI can be classified into a top and a bottom unit. While the upper unit consists of a mouthpiece, a mesh, and a classifier, the lower unit is composed of the capsule chamber, the air inlet, and two buttons, each with a needle for piercing the capsule and the housing. Similar to the RS01 equivalent device, the capsule is placed horizontally in the capsule chamber and pierced from both sides, creating centered holes at the top and bottom of the capsule body. The air inlet is located below the capsule chamber, and a separator in the center of the inlet divides the airflow into two separate flow paths that flow past the top of the capsule or the side of the body. This results in an oscillating movement of the capsule with an axial rotation and vibration during actuation, which causes the powder to exit the capsule. After passing the classifier inlet, which sets the powder and the air stream into a cyclonic, dynamic airflow, a straight flow behavior is achieved by a subsequent mesh in combination with a vortex breaker in the mouthpiece until it exits the device (Fig. S11).

To classify the new device as having low or high intrinsic resistance, the specific resistance to airflow was calculated from the linear relationship between Δp and the resulting flow rate (L/min). The inspiratory resistance of the novel DPI was determined as 0.044 $kPa^{0.5}$ L/min; the inspiratory flow rate at a pressure drop of 4 kPa was 45 L/min. The device can be categorized as a DPI with medium–high intrinsic resistance

to airflow. The intrinsic resistance of 0.018 $kPa^{0.5}$ L/min and the flow rate of 111 L/min at a pressure drop of 4 kPa, which was determined for the RS01 equivalent DPI, are in agreement with values found in the literature. This DPI is a low intrinsic resistance device. Due to the intrinsic resistance of 0.046 $kPa^{0.5}$ L/min, the Handihaler can be classified as DPI with high intrinsic resistance to airflow (Fig. 19) [65].

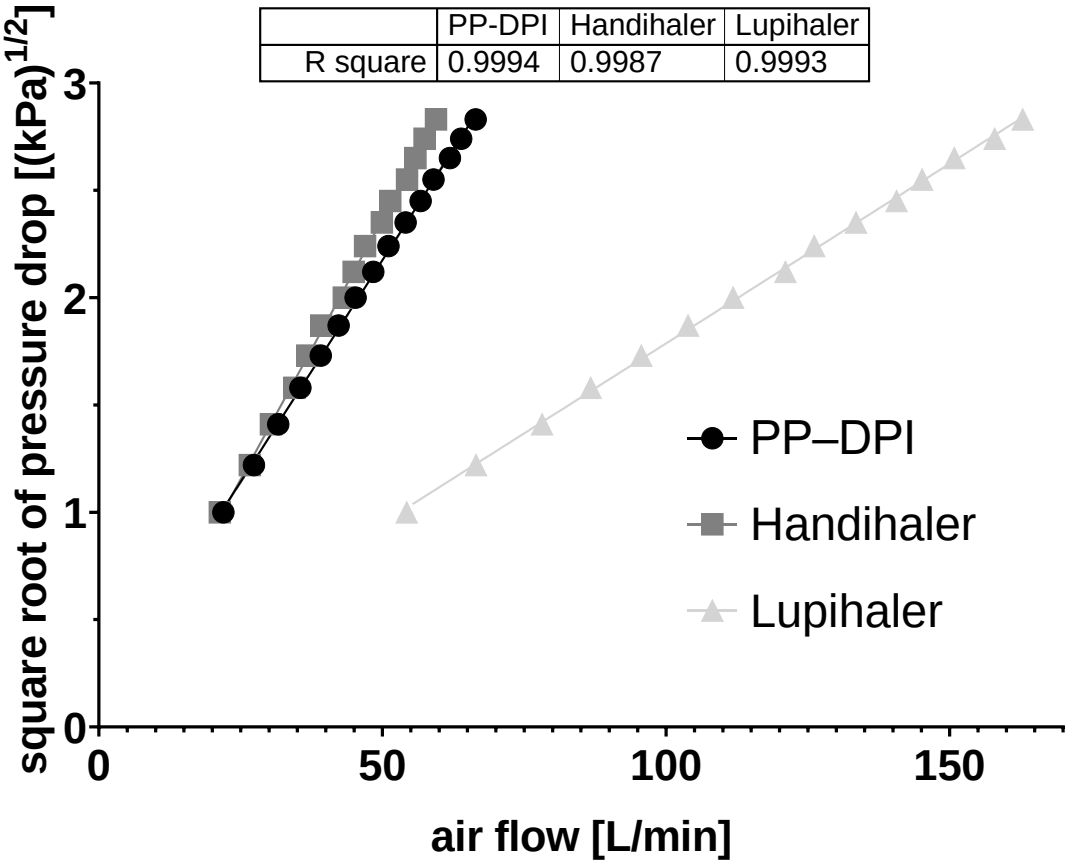

Figure 19: Relationship between the square root of pressure drop and the flow rate (L/min) across the novel (Presspart prototype dry powder inhaler (PP-DPI)) and both marketed DPIs (n = 3, mean ± SD).

SEM pictures in figure 20 show the size and shape of the particles of the formulations used. In the case of rifampicin, flocculent, platelet-shaped microparticles were seen. In the amoxicillin–lactose mixture, the spray-dried active ingredient, which had a spherical shape with a particle size in the lower micrometer range, was adsorbed onto the larger lactose carriers.

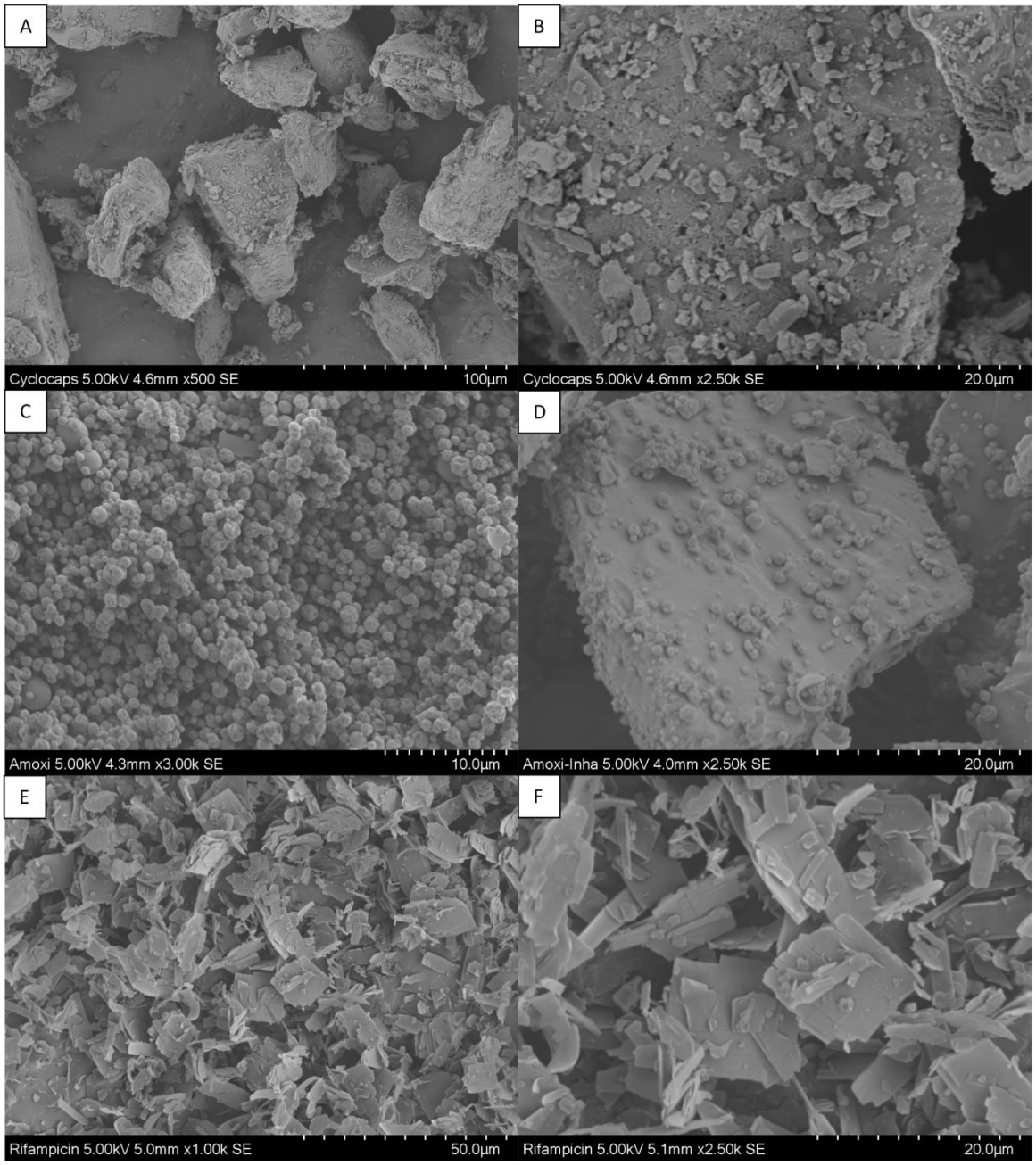

Figure 20: Scanning electron microscopy (SEM) images of the different formulations in different magnifications. (A, B) Cyclocaps [albuterol sulfate—lactose blend]; (C) amoxicillin; (D) amoxicillin–lactose blend; (E, F): rifampicin.

Testing the albuterol sulfate formulation with the different devices at 50 L/min re-sulted in a high powder deposition in the preseparator in every case (Fig. 21a). While powder retention in the capsule was not affected by the different flow rates, there was less

deposition in the device at the higher flow rate, regardless of the DPI used. The lower powder retention in the Handihaler, as well as the lower powder deposition in the induction port (IP) after using the Presspart prototype DPI, resulted in a higher FPF than with the Lupihaler (Tab. 8). While powder deposition in the preseparator was similar for each DPI used when operated at 50 L/min, operation at 100 L/min for the Presspart prototype DPI resulted in a lower deposition in the preseparator compared to the other two DPIs (Fig. 21b).

*Table 8: Fine particle fraction of the emitted (FPF_{EF}) or total dose (FPF_{TD}) for the different formulations (AS * = albuterol sulfate –lactose binary blend; amoxi – lactose blend * = amoxicillin – lactose blend; rifampicin) tested with various devices.*

Flow rate	**Formu-lation**	**PP-DPI**		**Lupihaler**		**Handihaler**	
[L/min]		**FPF_{EF}[%]**	**FPF_{TD}[%]**	**FPF_{EF}[%]**	**FPF_{TD}[%]**	**FPF_{EF}[%]**	**FPF_{TD}[%]**
50	AS*	34.7 ± 2.1	30.5 ± 1.8	25.1 ± 1.6	20.6 ± 1.3	27.2 ± 1.3	25.2 ± 1.2
	Amoxi-lactose *	66.4 ± 2.1	57.2 ± 1.8	50.3 ± 2.0	42.4 ± 1.7	45.2 ± 1.8	39.3 ± 1.6
	Rifampicin	73.0 ± 3.2	56.9 ± 2.5	66.3 ± 5.5	58.4 ± 4.8	47.8 ± 4.2	44.1 ± 3.8
100	AS*	41.3 ± 2.4	37.4 ± 2.2	27.3 ± 1.6	23.9 ± 1.4	29.6 ± 2.0	27.6 ± 1.9
	Amoxi-lactose*	68.8 ± 1.2	60.3 ± 1.1	55.2 ± 1.1	48.1 ± 1.0	52.5 ± 1.0	46.1 ± 0.9
	Rifampicin	63.5 ± 4.2	55.2 ± 3.6	53.7 ± 4.2	49.2 ± 3.8	46.6 ± 4.1	44.4 ± 3.9

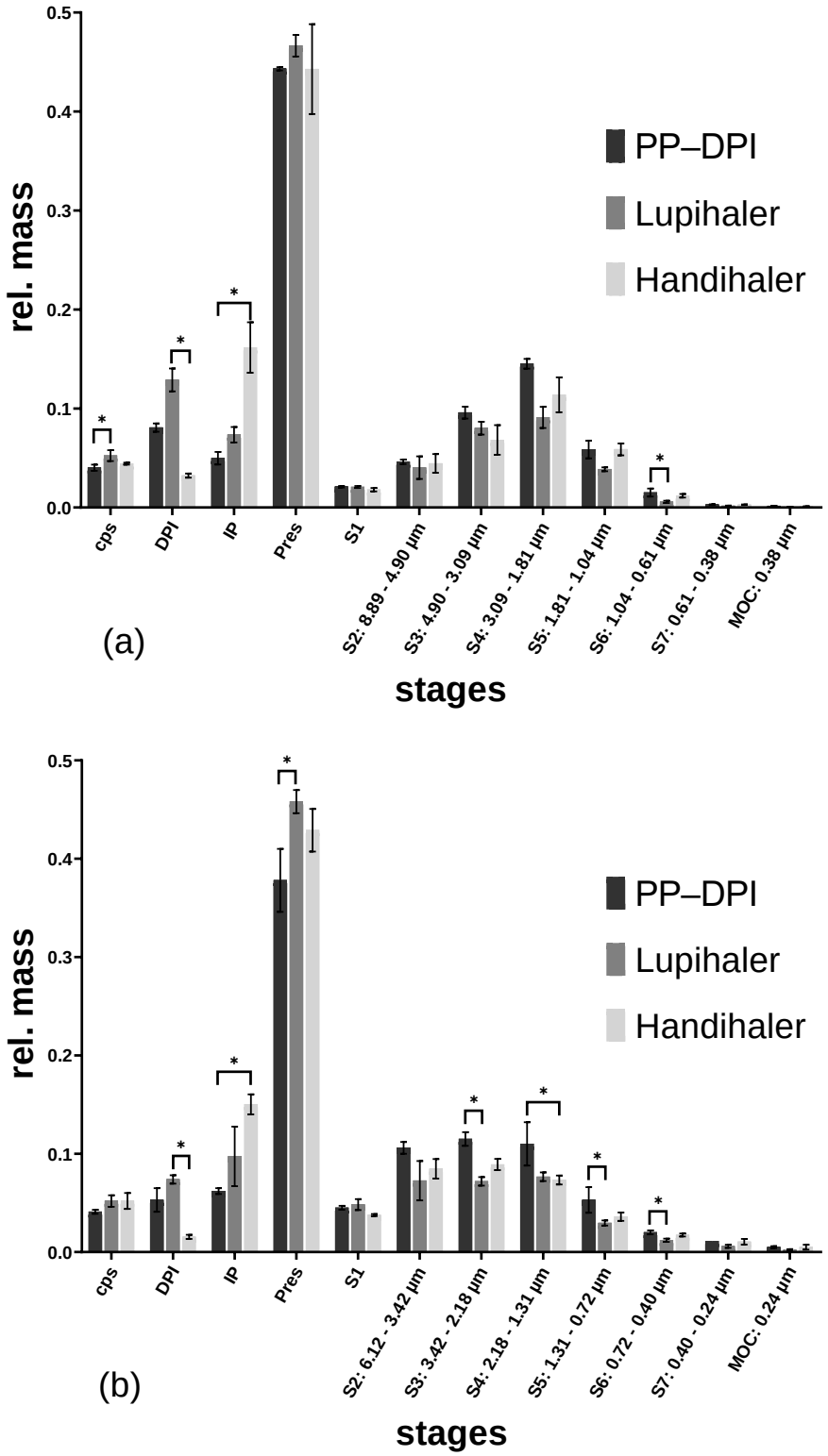

Figure 21: NGI results of the albuterol sulfate formulation actuated with different devices at different flow rates. (a) 50 L/min; (b) 100 L/min, (capsule = cps; dry powder inhaler = DPI; induction port = IP; preseparator = Pres), ($p < 0.05$).*

For the binary amoxicillin blend, the lowest powder retention in the capsule combined with the lowest powder deposition in the IP was observed after actuation with the Presspart prototype DPI, regardless of the flow rate applied (Fig. 22). Comparing the influence of the inhalation airflow (50, 100 L/min) on the aerosolization of the powder actuated with the same device, no differences could be observed in the stages (capsule to preseparator). These resulted in similar FPFs of the emitted- or the total dose for both flow rates. While the Handihaler and the Lupihaler showed similar deagglomeration behavior for this formulation, with the exception of powder deposition within the capsule, the device, and the IP, the Presspart prototype DPI achieved the highest fine particle fraction (Tab. 8).

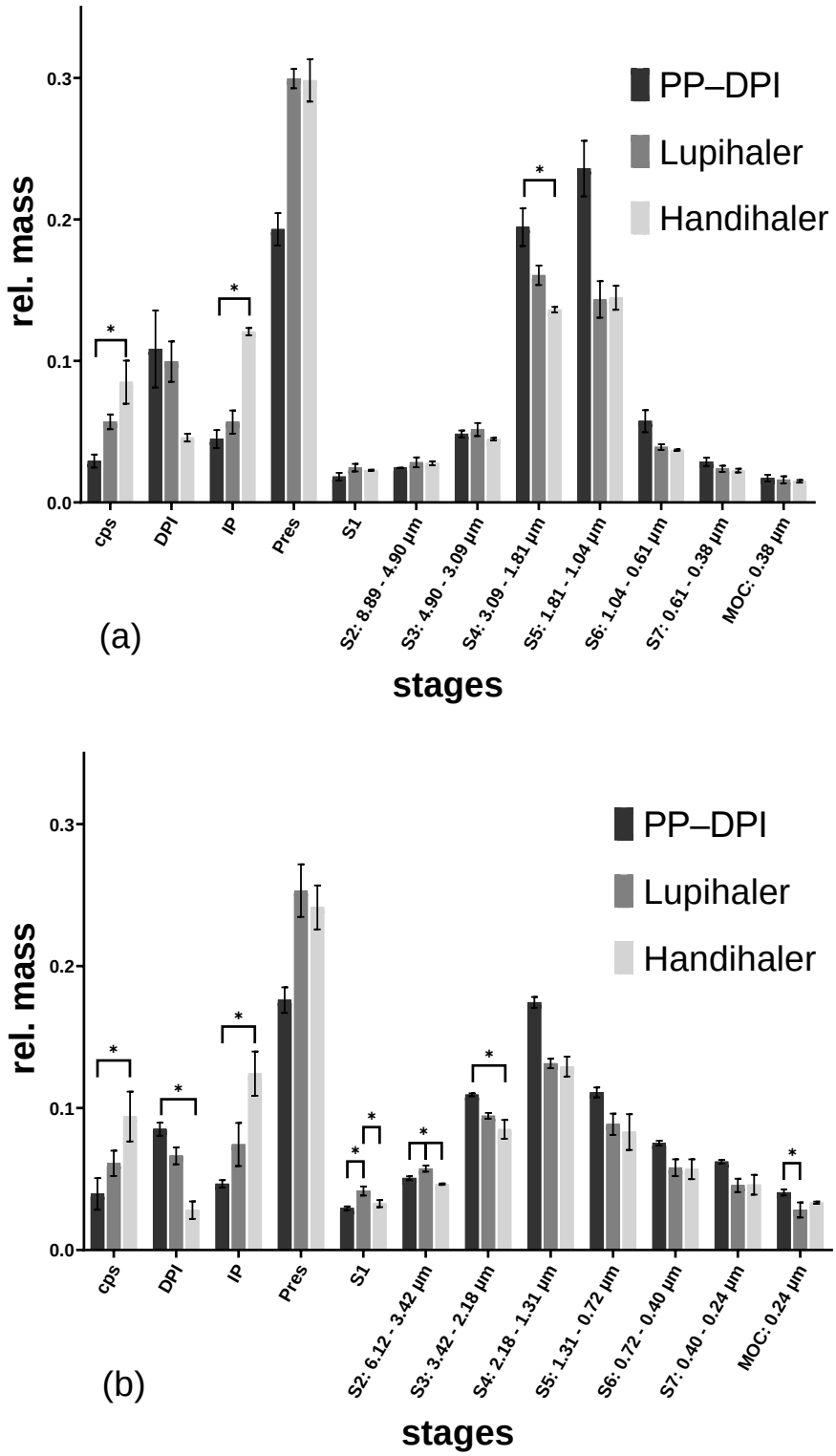

Figure 22: NGI results of the amoxicillin – lactose formulation actuated with different devices at different flow rates. (a) 50 L/min; (b) 100 L/min, (capsule = cps; dry powder inhaler = DPI; induction port = IP; preseparator = Pres), ($p < 0.05$).*

The results in figure 23 show that rifampicin powder retention in the capsule was the highest when using the Presspart prototype DPI. This powder retention was independent of the flow rate applied. Of all the devices tested, the Handihaler had the lowest powder deposition in the DPI but also the highest powder deposition in the IP. Compared to the other units tested, this DPI exhibited similar powder deposition in the various stages of the NGI at both flow rates. This is underpinned by the consistent $FPF_{EF/TD}$ (Tab. 8). Due to the high powder deposition in the IP, a lower FPF was achieved compared to that of the Lupihaler or Presspart prototype DPI.

While the Handihaler and Lupihaler showed similar deagglomeration behavior for the binary mixtures tested, resulting in similar powder deposition on S1 – MOC, differences were evident for rifampicin between all devices tested. When comparing the powder deposition on the mentioned stages for the tested flow rate of 50 L/min, it is noticeable that with the Handihaler, the highest powder deposition was observed in stages S2 – S3. While a high amount of API was deposited on S2 – S4 when using the Lupihaler device, the Presspart Prototype DPI achieved a high powder deposition on the stages S4 and S5 (Fig. 23a). At 100 L/min, a high amount of powder was deposited on S2 – S4 for each DPI used (Fig. 23b). Instead of the high powder deposition in the preseparator observed for both binary mixtures, regardless of the device used and the flow rate applied, a higher powder deposition in the IP was observed when actuating the rifampicin formulation.

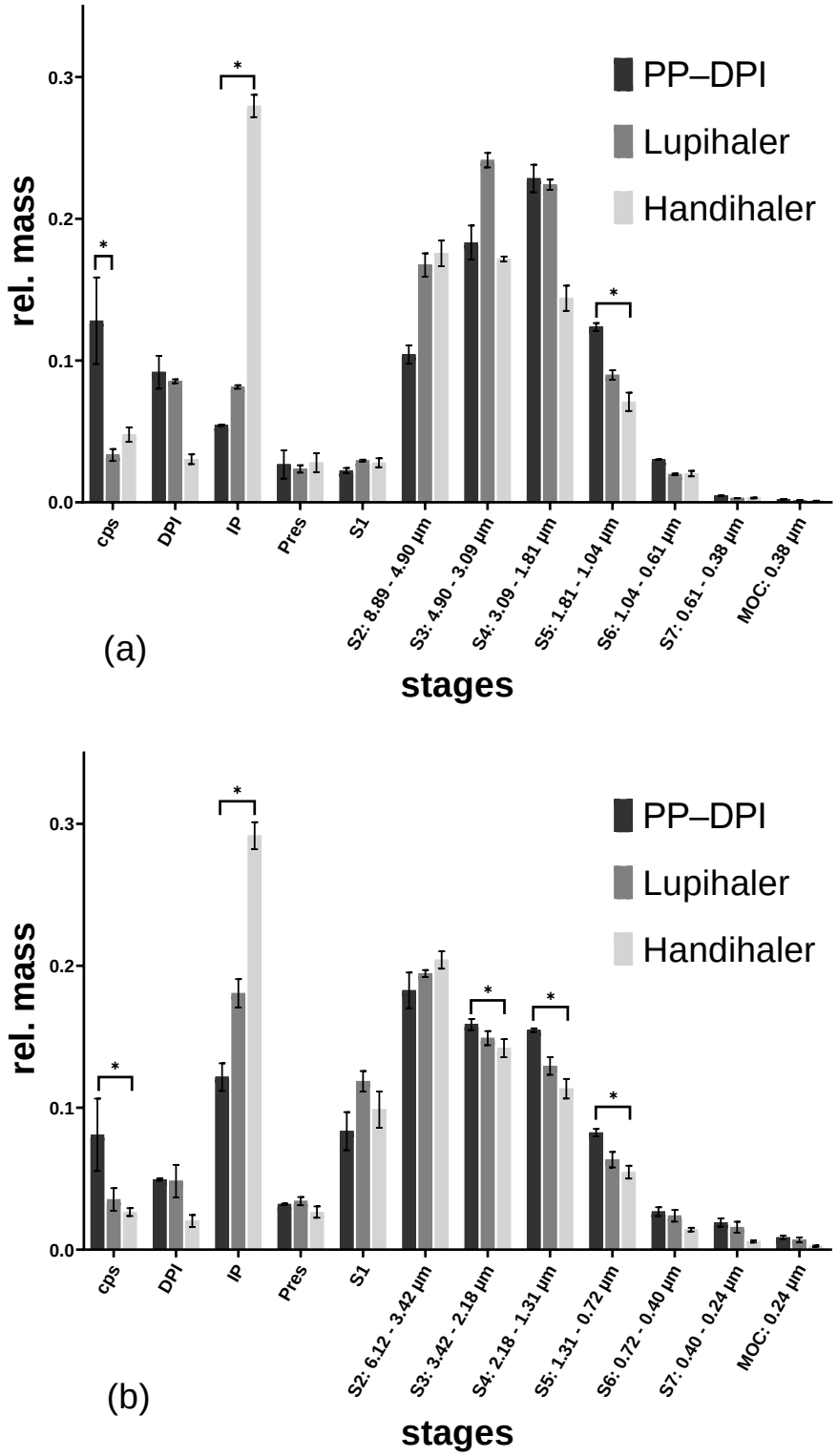

Figure 23: NGI results of the spray-dried rifampicin formulation actuated with different devices at different flow rates. (a) 50 L/min; (b) 100 L/min, (capsule = cps; dry powder inhaler = DPI; induction port = IP; preseparator = Pres), ($p < 0.05$).*

At the tested flow rate of 50 L/min, the highest $FPF_{EF/TD}$ was achieved with the rifampicin formulation, regardless of the DPI used. Due to the high powder retention in the capsule when using the Presspart prototype DPI, the FPF_{TD} was similar to that of the Lupihaler. The results of the 100 L/min data set showed a decrease in FPF for this formulation, which is due to the higher powder deposition in the IP, so the amoxicillin – lactose mixture had the best deagglomeration properties (Tab. 8).

13.6 Discussion

Since there are currently insufficient data on different DPIs and their ability to aerosolize different formulations not developed for the particular DPI, the idea arose to conduct a comparative study showing the advantages and disadvantages of selected DPIs in terms of deagglomeration and aerosolization of different drug formulations developed using different manufacturing techniques. These results could be used to derive state of the art in DPI development and indicate which deagglomeration mechanism offers potential for future development. This knowledge could be used for future commercialization of generic DPIs. To compare the different deagglomeration mechanisms, which are also influenced by the different movements of the capsule, a new capsule-based DPI with oscillating capsule movement was tested in addition to the two known commercially available DPIs (Handihaler, Lupihaler).

Classifying the novel device as a DPI with low or high intrinsic resistance to airflow and determining the pressure drop as a function of flow rate is an important parameter for verifying test conditions for conducting future studies. Due to the designed geometry resulting in intrinsic resistance of 0.044 $kPa^{0.5}$ L/min and a flow rate of 45 L/min at a pressure drop of 4 kPa, the new capsule-based DPI can be classified as a device with medium – high intrinsic resistance to airflow. Based on the studies described in the introduction and the published results for this class of DPIs, the novel device should deliver the loaded powder uniformly to the patient regardless of the inhalation conditions, which could lead to higher treatment adherence in vivo [142]. With regard to the design of the novel DPI, a new approach was developed to eject the powder

from the capsule by an oscillating movement. Considering that the capsule was pierced by two needles in each device tested, the influence of the number of needles and the resulting holes on powder output and deagglomeration was not part of this study. Nevertheless, previous studies have shown that the number and diameter of the needles, as well as the opening mechanism of the capsule, could have an influence on the aerosolization of the powder [63,141]. However, the current study focused on the influence of the device geometry, the resulting airflow through the DPI, and the resulting capsule movement.

For both binary mixtures, oscillatory capsule motion was shown to result in a higher emitted fraction than axial capsule vibration (Handihaler) or capsule rotation (Lupihaler), regardless of the flow rate applied. It can be concluded that for well-flowing binary blend formulations, the powder can be easily shaken out [30,31]. In the case of the rifampicin formulation, the inhalation force does not seem to be sufficient to eject the powder from the capsule, which could be due to the small particle size and the resulting increase in total surface area after spray-drying, leading to greater adhesion and cohesion forces of the powder and consequently greater adherence to the inside of the capsule wall or formation of aggregates [31]. In a previous study, it was also found that a platelet shape of particles reduces the flowability of the powder due to the resulting strong interactions between the individual particles [143]. Therefore, the oscillating motion of the capsule is not sufficient to overcome these interactions. Comparing the results of the albuterol sulfate or amoxicillin formulation obtained with the Lupihaler and the Handihaler device, it could be seen that similar powder deposition in the preseparator was observed in both cases. In addition, a higher API deposition in the IP was observed with the Handihaler compared to that of the Lupihaler. Both tendencies indicate that the deagglomeration of the powder and the detachment of the active ingredient from the carrier particles are insufficient, leading to the deposition of the mixture in the mentioned fractions. While for the albuterol sulfate formulation, the amount of drug deposited was independent of the flow rate applied, for the amoxicillin mixture, higher airflow resulted in less powder deposition in the preseparator, suggesting that this formulation was easier to deagglomerate. Comparing these observations with the results of these two formulations obtained with

the Presspart prototype DPI, it was found that the amount of active ingredient decreased more in the two fractions mentioned, indicating a better deagglomeration behavior and possibly due to the high circulation speed in the classifier, which leads to a better detachment of the active ingredient from the carrier particles [67]. While no differences in powder deposition in the preseparator were observed for the albuterol sulfate formulation when the Lupihaler or Handihaler were used at different flow rates, a lower amount of drug was found using the Presspart prototype device when the flow rate was increased, which also reflects the better deagglomeration behavior of the new DPI for binary blends.

Despite the higher powder retention of the rifampicin formulation in the capsule, better deagglomeration of the emitted powder was observed with the Presspart prototype DPI than with the other two DPIs. The capsule movement described above, in combination with the device design, geometry, and airflow within the DPI, promotes powder deagglomeration so that the weak powder output from the capsule can be compensated.

Comparing the FPF_{TD}, the Presspart prototype DPI achieved the highest FPF regardless of the formulation tested, and the flow rate applied, highlighting the functionality of the deagglomeration behavior for binary blends and spray-dried particle formulations. Since there were differences in powder deposition in the capsule–preseparator compartments, this resulted in differences in FPF_{EF} when comparing the two flow rates for a device and the respective formulation. While whether the powder remains in the capsule or DPI after inhalation is not important for therapeutic success, FPF_{TD} appears to be better suited to assess the independence of powder deagglomeration from inhalation conditions, as it describes the amount of powder of the loaded dose that can be adequately deagglomerated by the device and delivered to the lung in vitro, regardless of the inhalation conditions applied. Comparing the FPF_{TD} obtained for a formulation with the DPIs, it is noticeable that the two DPIs with high intrinsic resistance to the airflow achieved identical values at both flow rates, indicating that powder deagglomeration was not affected by the airflow.

From the device side, it can be summarized that the deagglomeration mechanism of the new DPI appears to offer an advantage over the known devices tested here in terms of powder deagglomeration, regardless of whether the formulation is a binary mixture or a particle engineered formulation. Although a high FPF was always achieved under the tested conditions, further development of the oscillating capsule movement mechanism could lead to increased powder ejection, especially for spray-dried particles.

13.7 Conclusions

From this study, firstly, it can be concluded that progress is being made in the development of DPIs with respect to the aerosolization behavior of various formulations not designed for the specific device and that, for this reason, the DPI could be marketed in the future regardless of the formulation. The development of DPIs with device geometry that provides high intrinsic resistance to airflow could lead to powder aerosolization that is much more independent of inhalation conditions than is currently the case. Second, the development of binary mixtures consisting of spray-dried active ingredients and carrier particles could be an interesting approach for future formulations, as the advantages of both formulation techniques can be combined to increase the number of particles that have suitable aerodynamic particle properties to reach the lungs.

14. Effect of texture and surface chemistry on deagglomeration and powder retention in capsule-based dry powder inhaler

This work was published as:

Groß, R.; Berkenfeld, K.; Schulte, C.; Ebert, A.; Sule, S.; Sule, A.; Lamprecht, A. Effect of Texture and Surface Chemistry on Deagglomeration and Powder Retention in Capsule-Based Dry Powder Inhaler. AAPS PharmSciTech 2022, 23, 281, doi:10.1208/s12249-022-02436-0.

14.1 Graphical abstract

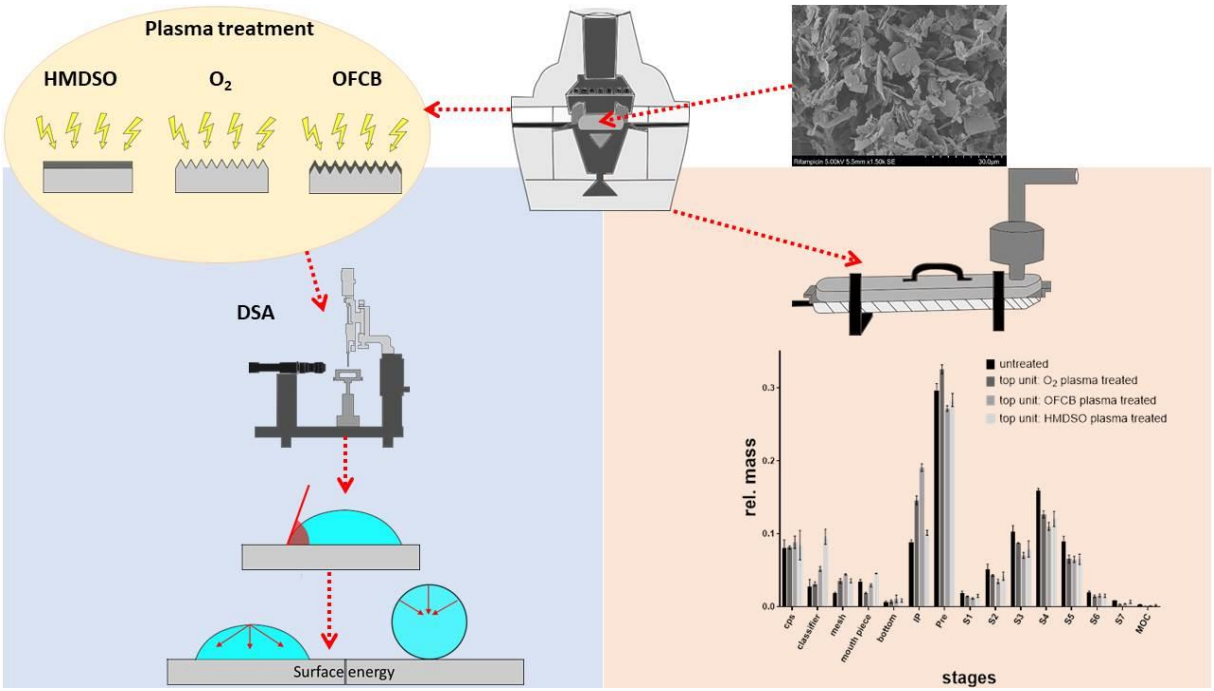

14.2 Abstract

Pulmonary delivery systems should administer a high dose of the required formulation with the designated dry powder inhaler (DPI) to achieve therapeutic success. While the effects of device geometry and individual components used on powder dispersion are described in literature, potential effects of DPI surface properties on powder retention within the device and deagglomeration have not been adequately studied, but could impact inhalation therapy by modifying the available dose. For this, inner parts of a model DPI were modified by plasma treatment using various processes. Since both, the hydrophilic-hydrophobic and structural properties of the surface were altered, conclusions can be drawn for future optimization of devices. The results show that surface topography has a greater influence on powder deposition and deagglomeration than hydrophilic or hydrophobic surface modification. The most important modification was observed with an increased rough surface texture in the mouth piece, resulting in lower powder deposition in this part (from 5 % to 1 % quantified amount of powder), without any change in powder deagglomeration compared to an untreated device. In summary, increasing the surface roughness of

DPI components in the size range of a few nanometers could be an approach for future optimization of DPIs to increase the delivered dose.

14.3 Introduction

Capsule-based dry powder inhalers (DPIs) are devices commonly used to treat respiratory diseases [144]. In general, the therapeutic success is linked to adequate deposition of the powder in the lower respiratory tract. Therefore, the device should be able to deagglomerate the formulation during inhalation so that the powder particles have an aerodynamic diameter of < 5 µm [29]. Despite the progress and optimization achieved, the development and realization of an "ideal DPI" is challenging, as many mechanisms are not yet fully understood and require further investigation [29,91]. However, to minimize potential sources of error (e.g., insufficient inspiratory air flow, duration) and to ensure sufficient powder deposition in the lungs, delivery systems are marketed in a fixed combination of the DPI and formulation [56,57].

In order to identify the impact of device layout or components on powder retention in the DPI and also for the subsequent deagglomeration, numerous studies have been carried out. For capsule-based DPIs, the opening mechanism (e.g., size, number and position of holes in pin-based systems) prior to actuation, as well as the capsule material, size and movement during actuation (rotation, vibration, shaking) can affect the deagglomeration and ejection of the powder [63,136,141,145]. The grid, which primarily separates the capsule chamber from the mouth piece, is intended to prevent fragments of the opened capsule from entering the patient's oropharynx during the inhalation flow and causing local irritation or aborting inhalation. In addition, the grid can straighten the passing air flow, which reduces the tangential flow behavior in the mouth piece and results in reduced powder deposition in this area and thus increasing the fine particle fraction (FPF) [146]. While modifying the mouth piece by reducing its length from the original geometry had no effect on powder retention within the DPI or powder deagglomeration, increasing the diameter of the circular mouth piece exit resulted in lesser powder deposition in the induction port (IP) due to a lower air flow and particle exit velocity [72,147].

In addition to the general device geometry and the specifically dedicated components (e.g. classifier, vortex breaker) for improving powder aerosolization, minimizing powder retention in the device is an issue that has become increasingly important in recent years. Powder retention in inhalation devices can significantly affect therapeutic outcomes due to mechanical anchoring of the powder to the device surface and/or electrostatic charge generated during powder dispersion. Triboelectrification is an unavoidable consequence of contact or friction between particles and devices during actuation [148]. One focus for overcoming this problem is the "dry powder coating" method through the use of force control agents such as amino acids or metal stearates. As the safety profile is well known, magnesium stearate and leucine are widely used and numerous studies have been conducted to improve device retention and aerosolization performance by coating drugs and/or carrier particles with these pharmaceutical lubricants [149,150]. In the last decade, an alternative strategy has been pursued, aimed at lower powder retention, by coating the inner surface of the DPI and also of the capsule with lubricants. It has been shown that, depending on the concentration of the magnesium stearate suspension used for surface modification, significant differences in powder retention can be achieved in both compartments [151]. In addition to the use of classic lubricants, the coating of DPI plastic with a polytetrafluoroethylene (PTFE) film has also been tested in recent years to create a hydrophobic surface characterized by a high water contact angle and low surface energy. In previous studies, the capsule and device were coated with a commercial PTFE suspension (LUTM 708; SprayonTM Products, Ohio) [152–154]. It was shown that this surface modification resulted in a higher emitted fraction without affecting the FPF.

Despite these findings, the critical factor of reducing powder adhesion to the inhaler wall is still not fully understood, so there is no commercially approved surface modification for DPIs to reduce powder adhesion. The present study aimed to investigate the influence of a modified inner DPI surface firstly on the powder deposition within the device and secondly on the deagglomeration behavior for the tested formulation. For the surface modifications described above, it is not clear whether the low surface energy or the surface texture achieved by the deposited

magnesium stearate particles or the PTFE suspension is the important parameter for reducing powder retention within the DPI, so this study aimed to investigate the influence of both surface modifications on powder ejection and also powder aerosolization.

In order to modify the chemical surface properties as well as the nanotexture of the DPI surface, various cold-plasma processes were developed and applied to the DPI surface using a low-pressure plasma unit. In general, the species generated during the process, such as ions, radicals, neutrals or metastables, which have a temperature close to room temperature, can interact with the surface of the starting material. For this reason, this modification method is generally preferred for thermolabile materials in industry [155]. Since the modified materials are only changed at a depth of a few nanometers, only the outer layer is affected, while the bulk properties are not changed. This allows in the ability to produce desired surface properties depending on factors such as gas type, pressure in the chamber, gas ignition power, treatment time and the type of starting material used. In general, four basic processes can be distinguished. *Surface activation* is intended to create new functional groups on the material surface, leading to a different surface energy and usually preparing the surface for a subsequent *plasma polymerization* step by coating the surface through polymerization of a monomer. While *surface cleaning* by plasma aims to remove contaminants from the substrate surface, *surface etching* aims to remove and degrade material from the treated surface by physical and chemical reactions, producing volatile products [156–158].

For oxygen, numerous effects are described in the literature, including the mentioned surface activation, -cleaning and –etching [159,160]. On this basis, oxygen plasma was used to create hydrophilic surfaces, while an octafluorocyclobutane (OFCB) process was intended to create hydrophobic surfaces. Both processes also cause the surface topography to become irregular and the roughness to increase [161–165]. In order to estimate not only the effects of a plasma-induced rough surface, but also the extent of a smooth and non-sticking surface produced by the plasma coating, the monomer hexamethyldisiloxane (HMDSO) was used for in situ polymerization [166–168]. The

results obtained were compared with those of untreated DPIs, which also have a smooth surface due to the injection molding process used during manufacturing. The study here was run with a DPI type composed of individual components which allows for a clearer identification of which surface modifications may have an impact on powder deposition, as DPI components can be plasma treated separately. To demonstrate differences in powder retention within the DPI or in deagglomeration behavior, an unmodified device was used as control and an in-house developed spray-dried particle formulation of the active pharmaceutical ingredient rifampicin was actuated. Since therapy with classical asthma and chronic obstructive pulmonary disease (COPD) drugs is well known and there is a growing interest in the pulmonary use of antibiotics, this formulation was focused on [133,169,170]. While it was initially assumed that the hydrophilic or hydrophobic surface properties produced by plasma treated could reduce powder deposition within the DPI, the surface topography of the inhaler revealed its impact on the aerosolization of the drug powder.

14.4 Materials & Methods

14.4.1 Materials

Rifampicin (> 98.0%, lot number: 6K4AF-RO) was ordered from TCI (Tokyo, Japan). With the exception of water, which was purified in-house (Merck-Millipore Biocel A10, Burlington, MA, USA), all solvents were HPLC grade. Oxygen- (99.99%), the octafluorocyclobutane- (OFCB) (99.99%) and nitrogen (N2) (99.99%) gases were purchased from Air Liquide (Paris, France), hexamethlydisiloxane (HMDSO) was order from Sigma-Aldrich (St. Louis, Missouri, USA). Polyamide (PA) plastic material used to develop the plasma processes was kindly provided by Hadi-Plast (Hadi-Plast GmbH & Co. KG, Hövelhof, Germany). The Presspart prototype DPI (PP DPI) tested was provided by Heitkamp & Thumann ltd (Blackburn, United Kingdom). The set-up of this novel DPI was described and explained in a previous study [108].

14.4.2 Spray-drying process for the rifampicin formulation

Rifampicin was spray-dried as described in [108,132]. The powder was dispersed in a predefined amount of ethanol (38 mg/ml) and the suspension was sonicated with an ultrasonic bath (type DT 106, Bandelin electronic, Berlin, Germany) under controlled temperature conditions (25°C) to homogeneously disperse the particles. A thermostat (DC 10, Haake Technik GmbH, Vreden, Germany) was used to keep the temperature constant during the water exchange. For spray-drying under inert atmosphere (N2) a B-290 spray-dryer equipped with a high-performance cyclone, a B-295 inert loop, a B-296 dehumidification unit (all Buchi, Flawil, Switzerland), and an anemometer (AF89-AD1AA13C0AA, Fluid components Intl. San Marcos, CA, USA) were used. Throughout the manufacturing process, the suspension was continuously stirred until atomization using a modified three-fluid nozzle with a blocked inner channel (Buchi).

14.4.3 Test procedure for the aerosol classification with the Next Generation Impactor

5 mg of the rifampicin formulation was filled into size 3 gelatine capsules. A Next Generation Impactor (NGI) connected with two vacuum pumps (HCP 5) (all Copley Scientific Limited, Nottingham, United Kingdom) was used to characterize the aerosol properties obtained with the untreated and the plasma treated devices. Prior to the experiments, 15 mL of the diluent was added to the preseparator, and each cup was coated with 1% glycerol-methanol solution (m/v). To analyze the powder deagglomeration behavior of unmodified and different modified DPIs by quantifying the active ingredient at the different stages (capsule – MOC), the rifampicin particles were dissolved in a solution of ascorbic acid in methanol (0.5 % m/v). For each experiment, an actuation volume of 4 liters was used in combination with a flow rate of 50 L/min, corresponding to USP conditions at a pressure drop of 4 kPa [81,171].

14.4.4 Developing the plasma processes

To modify the surface of the plastic samples, a low-pressure system unit (Diener Plasma GmbH & Co. KG, Ebhausen, Germany) with a radiofrequency generator (13.56

MHz, 0 – 200 W) was used. For treating the surface, the samples were placed inside a heatable vacuum chamber (rectangular, aluminum, H: 240mm x D: 600mm x W: 240 mm) at a specified position to obtain uniform and reproducible process conditions. The development of the various plasma processes was carried out on PA material. In the case of oxygen, a flow rate of 44 sccm, resulting in a pressure of 0.3 mbar, was ignited with a generator power of 90% and a duration of 60 min. For OFCB, to obtain hydrophobic surfaces, the C_4F_8 gas was used as a Teflon film precursor after an oxygen treatment step to polymerize the fluorocarbon units on the surface at a flow in the chamber of 9 sccm, a pressure of 0.1 mbar and a generator power of 20%.

For the HMDSO process, the monomer was heated to 110°C to convert the liquid to the gas state. For the plasma process, the monomer was mixed with oxygen in a ratio of 1:4, resulting in an oxygen gas flow in the chamber of 21 - 25 sccm at a pressure of 0.3 mbar. To ignite the plasma, 80% of the generator power was used for a duration of 5 minutes.

14.4.5 Contact angle measurements and surface energy calculation

In order to verify the applied surface modifications by the plasma treatment and to analyze potential ageing effects of a generated hydrophobic (OFCB) or hydrophilic (oxygen) surface as an extreme case under the plasma modifications tested here, contact angles were determined at ambient conditions with deionized water using a FM40 Easy Drop – drop shape analyzer (Krüss GmbH, Hamburg, Germany). The sessile drop measurement principle was applied, and drops of 10 µL were analyzed. The method of Owens, Wendt, Rabel and Kaelble (OWRK method) was used to calculate the surface energy directly after plasma treatment and after storage times of 3 and 6 weeks [172]. Deionized water as the polar component and diiodomethane as the lipophilic component were used as test fluids. Using the linearized equation of Owens and Wendt, the surface energy was calculated as follows:

$$\sigma_s = \frac{(1+\cos\theta) * \sigma_l}{\sqrt[2]{\sigma_l^D}} * \sqrt{\sigma_s^P} * \sqrt{\frac{\sigma_l^P}{\sigma_l^D}} + \sqrt{\sigma_s^D}$$

σ_s: Surface free energy of the solid surface [mJ/m^2].

σ_l: Surface tension of the wetting medium [mN/m].

Θ: contact angle [°].

σ^D_l: Dispersed fraction of the wetting medium [mN/m].

σ^P_l: Polar fraction of the wetting agent [mN/m].

σ^P_s: Polar fraction of the wetting surface [mJ/m^2].

σ^D_s: Disperse fraction of the wetting surface [mJ/m^2].

Equation 3: Calculation of the surface energy.

14.4.6 Measurement of the frequency of the capsule oscillation during actuation

To determine the oscillation frequency of the capsule during actuation within an untreated and a plasma treated DPI, the capsule motion was recorded for one second using the camera of a cell phone (Samsung Galaxy s20, 960 fps). For this purpose, the DPI was connected to the NGI and a flow rate of 50 L/min was applied. A frame-by-frame analysis was performed to count the oscillations of the capsule.

14.4.7 Scanning electron microscopy (SEM)

The samples were fixed with carbonaceous conductive paste on an aluminum sample holder and then coated with gold for two cycles of two minutes each. Subsequent imaging was performed in high vacuum using a Hitachi SU-3500 SEM (Hitachi Ltd., Tokyo, Japan). The accelerating voltage was 5 kV, the magnification and working distance were adjusted as needed and are indicated on the SEM images.

14.4.8 Laser diffractometry (LD)

The particle size distribution of the formulation was determined with a LA-940 laser scattering particle size distribution analyzer (Horiba ltd., Kyoto, Japan) using following procedure: Rifampicin was suspended in a solution of 0.1 w/w (%) Span 80 in n-hexane in an amount that resulted in suitable attenuation of the laser beams. The suspension was stirred in a quartz cuvette during analysis (n = 5) [132].

14.4.9 High performance liquid chromatography analysis

Quantification of the drug deposited in the different NGI stages was performed by high-performance liquid chromatography (HPLC) analysis (Shimadzu, LC-2030C 3D Plus, Kyoto, Japan) using an RP18 column (Lichrospher 100 RP 18-5µ EC, 250 x 4.6 mm). To detect the rifampicin, the photodiode array detector was set to 337 nm. The mobile phase consisted of a mixture of a phosphate buffer pH 5.2/methanol/acetonitrile (33/50/17 % v/v/v), and an isocratic flow rate of 1.0 mL/min was set in combination with a column temperature of 25 °C [108]. The values of the intercepts and the slope of the calibration curve were used to calculate the limit of detection (LOD) and limit of quantification (LOQ). The LOD and LOQ for rifampicin were determined to be 0.30 µg/mL and 0.90 µg/mL.

14.4.10 Data processing and statistics

The NGI plots show the relative powder deposition of the drug on the different stages (capsule – MOC). Error bars indicate one standard deviation. All experiments were performed in triplicate, unless otherwise reported. To determine statistically significant differences in the contact angle measurements, surface energy calculation and in relative powder deposition in the different stages of the NGI (capsule - MOC) after actuation with untreated and plasma treated DPIs, results were compared using Kruskal-Wallis test followed by Dunn`s test ($p < 0.05$) (Prism 8.0.2, GraphPad software).

14.5 Results

14.5.1 Characterization of the surface structures and chemical changes of the surface obtained by plasma treatment

Comparison of the surfaces of the mesh in the initial state and after modification by the various plasma treatments revealed differences in their nanostructures. The surface texture of the untreated and HMDSO plasma treated surface is smoother compared to the other two treated surfaces. For the untreated material, residues probably originating from injection molding are characteristic [173–175]. In the case of HMDSO, a thin layer covered these residues and also the interstices, resulting in a flatter surface structure. Increased roughness in the nanometer range is observed on the plastic surfaces treated with oxygen and OFCB compared to the structure of the untreated surface. This nanotexturing is more dominant in the case of the oxygen process than for the OFCB treated surface (Fig. 24).

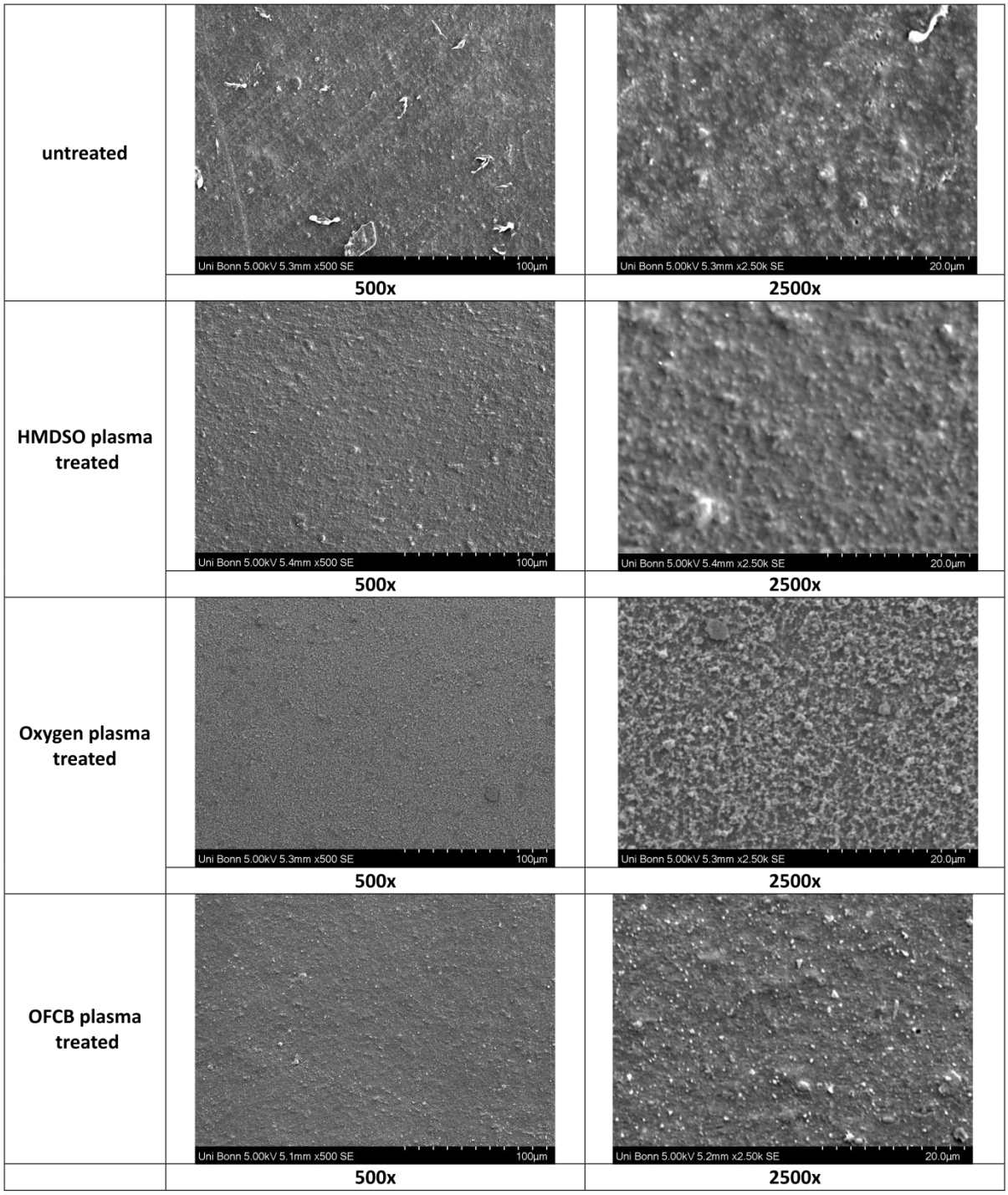

Figure 24: Scanning electron microscopy (SEM) images of the untreated and the plasma treated surfaces of the mesh after application of the above plasma modifications (hexamethyldisiloxane = HMDSO; octafluorocyclobutane = OFCB).

To characterize the change of the chemical surface properties due to plasma modification, the contact angle was measured and the surface energy was calculated over a storage period of 6 weeks after plasma treatment with measurement steps of 3 weeks (initial, 3 weeks, 6 weeks) (Fig. 25). In the case of the oxygen plasma treatment, it was observed that the wettability of the surface increased, resulting in a lower contact angle with water directly after surface modification. After 3 and 6 weeks, the wettability decreased until the initial condition of the untreated material was regained after 6 weeks to a contact angle of about 60°, so that this effect was reversible. The OFCB treated surfaces were found to be hydrophobic, characterized by a contact angle with water of 120°, which remained constant over time, unlike the hydrophilic surface modification (Fig. 25a).

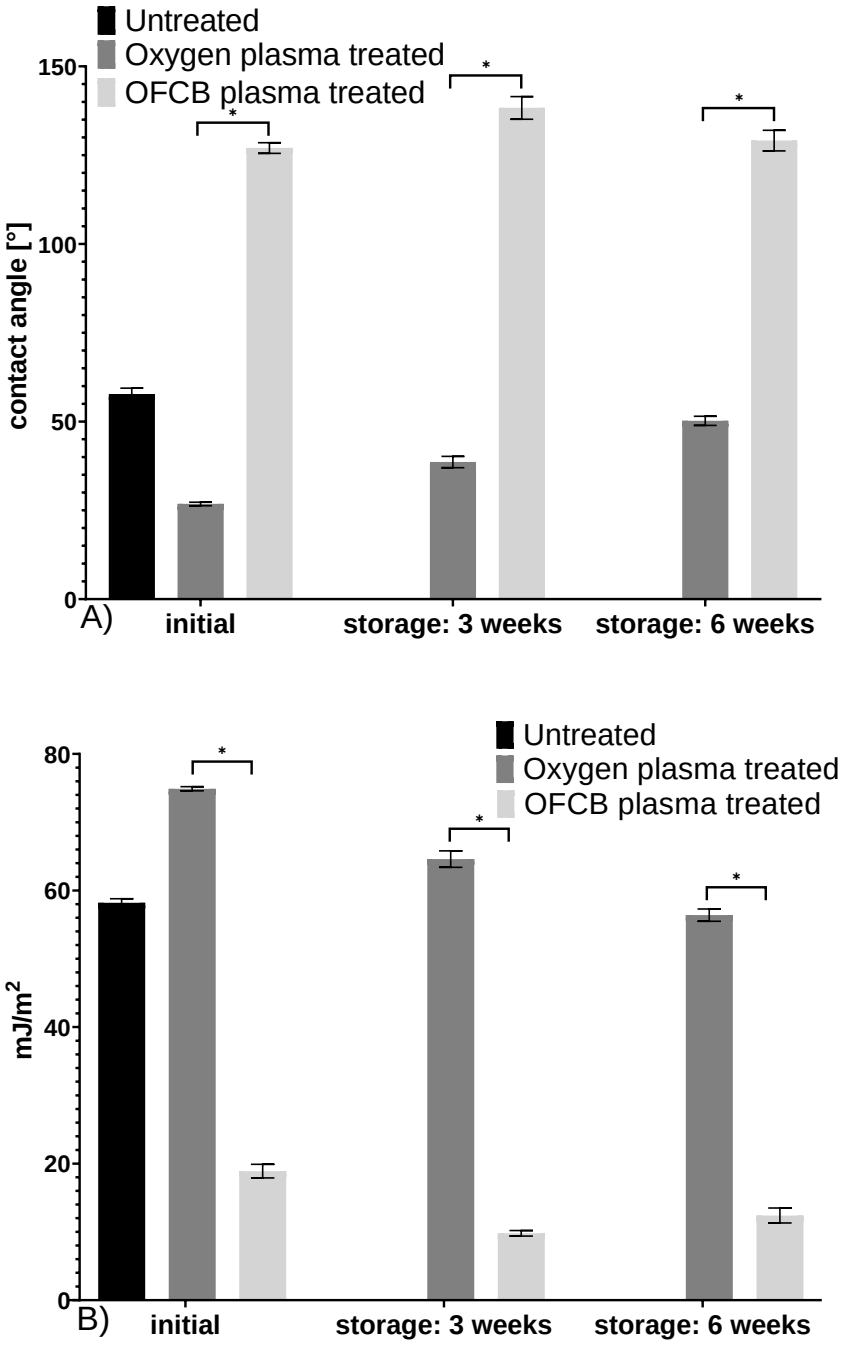

Figure 25: (A): Contact angle measurement with deionized water for untreated and plasma treated polyamide (PA) samples; (B): calculation of the surface energy for the defined time points, (octafluorocyclobutane = OFCB), ($p < 0.05$).*

To estimate the effect of a hydrophilic or hydrophobic surface created by plasma treatment, as well as the effect of a nanotextured surface on the deagglomeration

behavior of the device characterized with the NGI, a storage time of the plasma treated inhaler of 3 weeks after treatment was complied before the devices was tested. To verify the condition that after plasma treatment of the device with the different developed processes, there are no changes in the movement of the capsule during actuation due to the changed surface energy, the oscillation frequency was measured for modified and untreated devices. The results show that the oscillation frequency of the capsule was about 45 Hz for the untreated and the plasma treated devices, so no differences were found (Fig. S12).

14.5.2 Visual characterization and particle size distribution of the spray-dried rifampicin formulation

The spray-dried rifampicin particles have a flake-like and flocculated shape in the lower micrometer range with a d50 < 10 µm (Fig. 26).

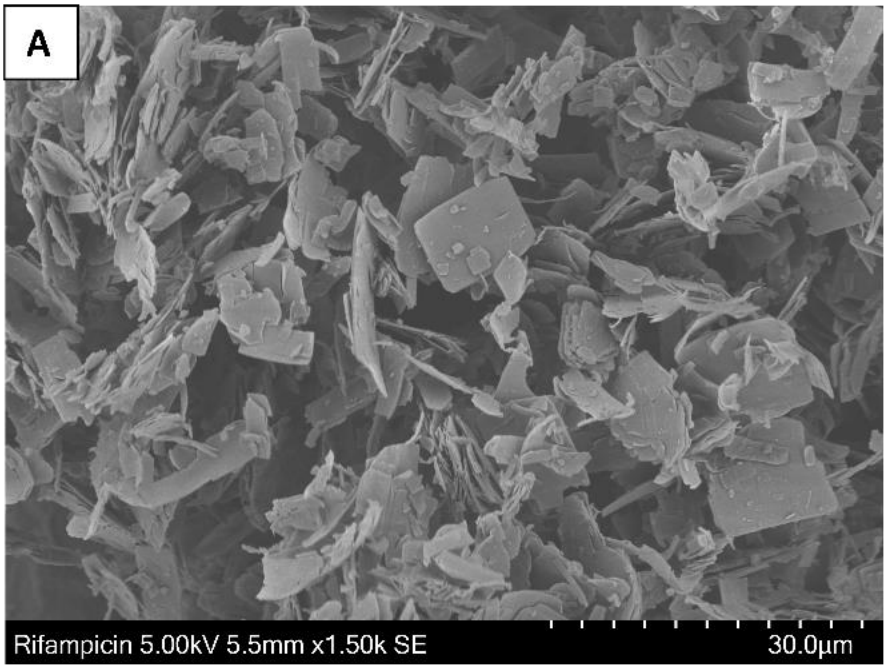

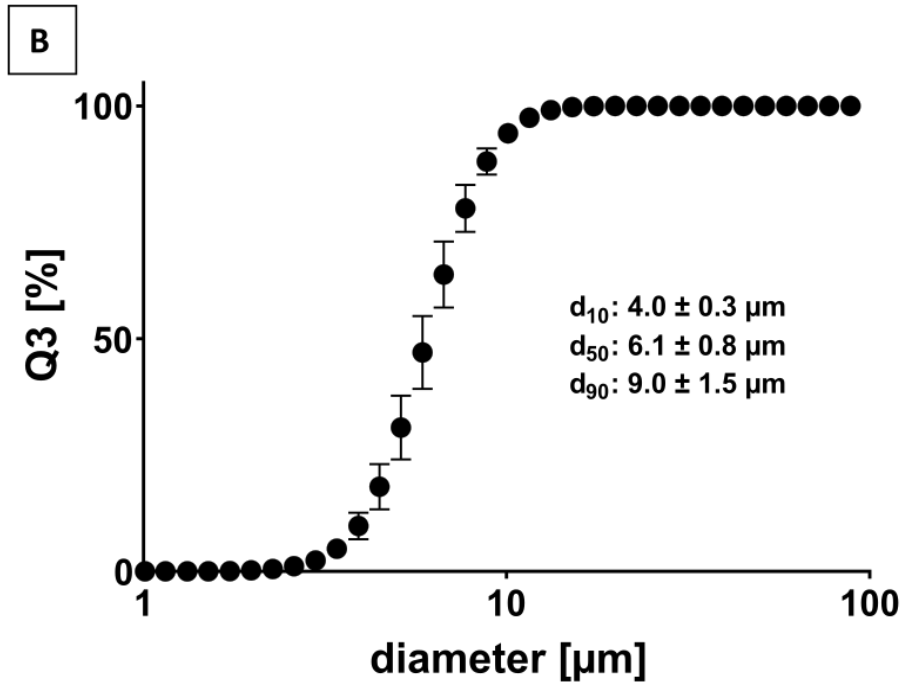

Figure 26: Scanning electron microscopy (SEM) images (A) and particle size distribution (B) of the rifampicin formulation.

14.5.3 Determination of the influence of a plasma modified upper or lower unit of the DPI on powder aerosolization and retention within the device

Figure 27 shows the NGI results obtained after treating the upper unit (comprising classifier, mesh, mouth piece) of the device with different plasma processes. Actuating the spray-dried rifampicin formulation showed increased powder deposition in the IP and also in the preseparator after surface modification with oxygen or OFCB plasma, with OFCB modification resulting in the highest deposition. For both plasma treatments, less powder deposition was observed in the modified mouth piece, with a rougher surface texture resulting in less powder deposition. A similar deagglomeration of the powder was achieved with the DPI treated with HMDSO and the untreated device. Despite a smooth surface, which was observed for both cases, the treatment with HMDSO resulted in a slightly increased powder deposition on the corresponding plastic parts (Fig. 27).

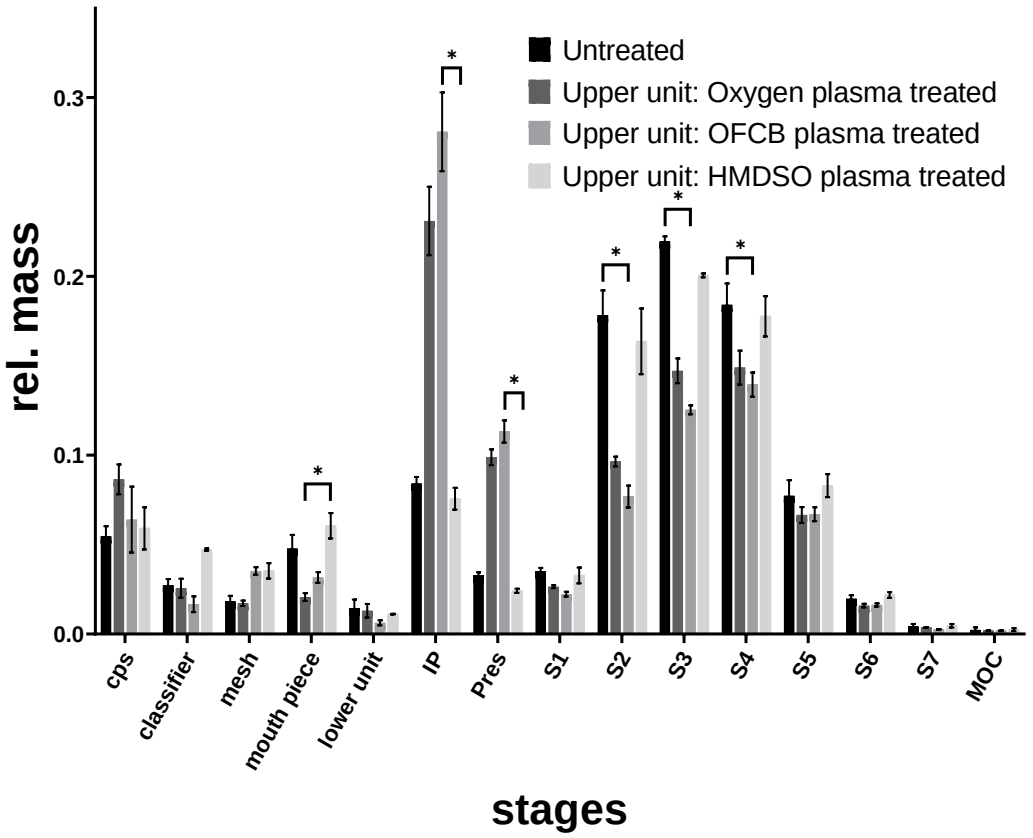

Figure 27: Next Generation Impactor (NGI) results obtained with the rifampicin formulation actuated with a dry powder inhaler (DPI) with untreated and plasma treated upper unit, (capsule = cps; induction port = IP; preseparator = Pres), ($p < 0.05$).*

Plasma treatment of the capsule chamber showed no differences in aerosolization properties when characterizing the deagglomeration behavior of these devices for the rifampicin formulation compared to the untreated one, regardless of the surface modification applied. For the two processes that produced a rough surface texture, a decreased amount of powder was deposited in the capsule chamber shown as "lower unit" in the NGI diagram. For the part treated with HMDSO plasma, the powder deposition was similar to the original part (Fig. 28).

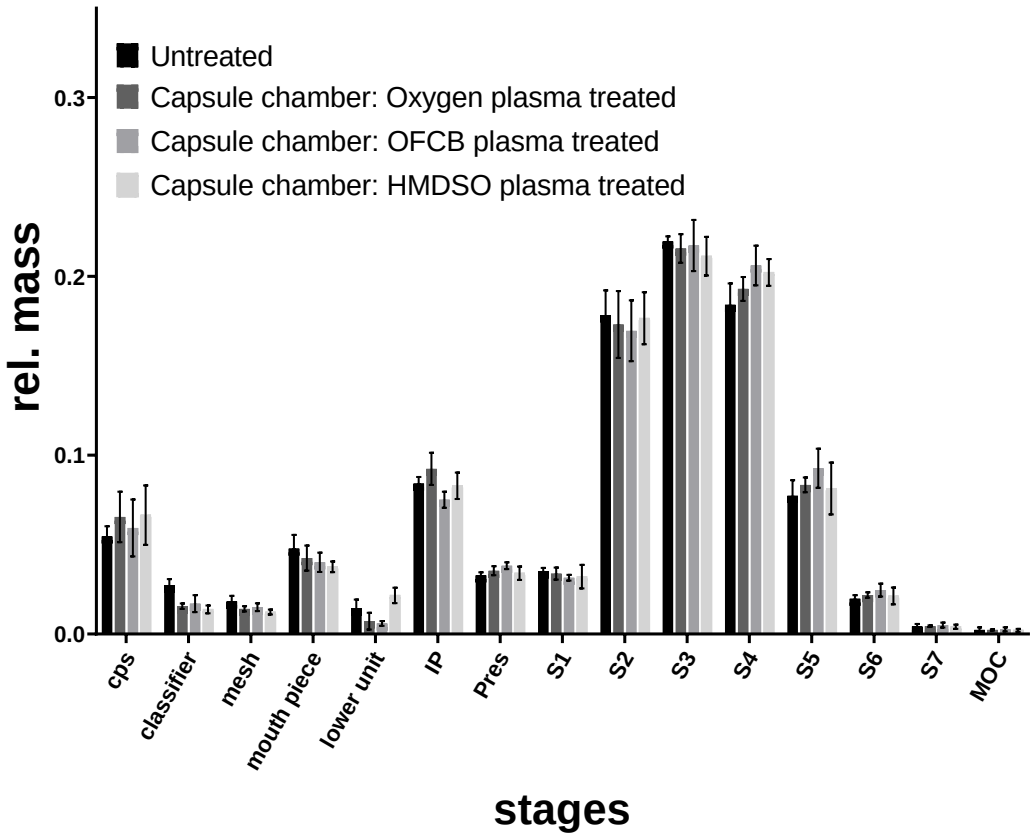

Figure 28: Next Generation Impactor (NGI) results obtained with the rifampicin formulation actuated with an untreated dry powder inhaler (DPI) and after plasma treatment of the capsule chamber (shown as lower unit), (capsule = cps; induction port = IP; preseparator = Pres).

14.5.4 Identification of the influence of the surface structure of the mouth piece on powder retention

Since differences in powder retention in the mouth piece were evident after treatment of the upper unit compared to the untreated unit, the DPIs were tested in a further experiment in which only the mouth piece was treated with plasma. The results in figure 29 show that for both processes, where a nanotextured surface was created in the mouth piece, less powder deposition was observed than for the untreated mouth piece. Of all the modifications the lowest powder retention in this part was observed after treating with oxygen plasma. While no changes were observed in the deagglomeration

of the powder between the oxygen-, HMDSO treated and untreated DPI, an increased power fraction was observed in the IP when using the OFCB coated device, but not as high as shown in figure 27.

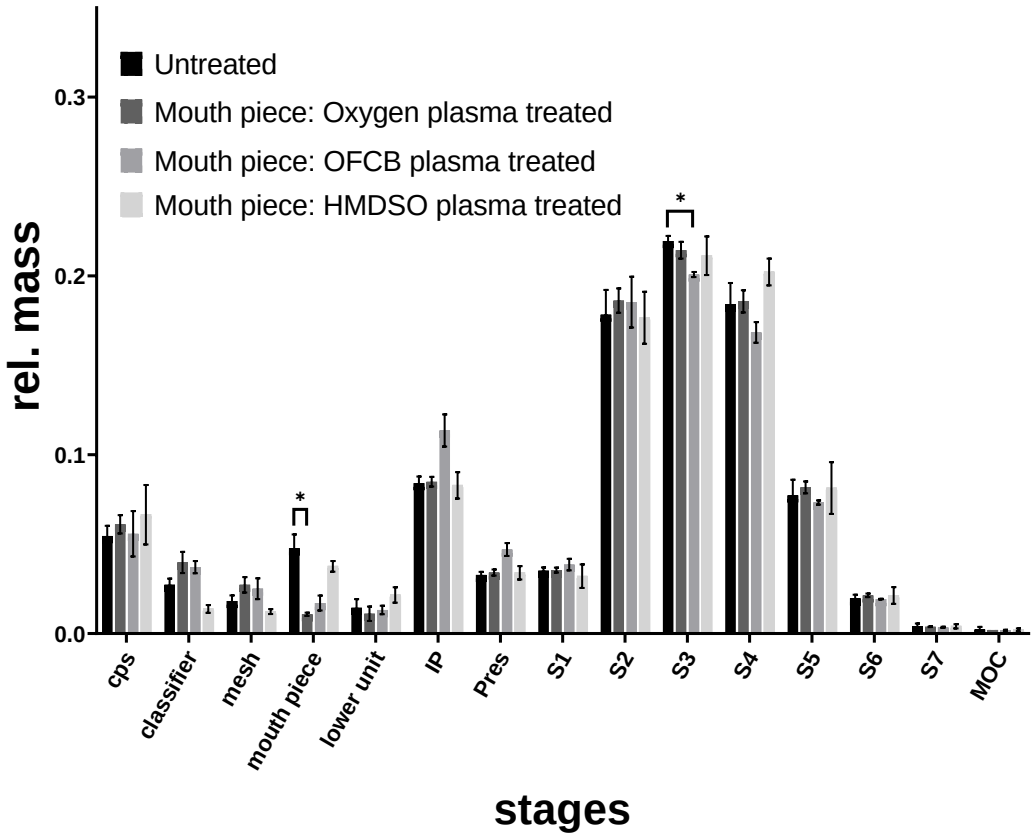

Figure 29: Next Generation Impactor (NGI) results obtained with the rifampicin formulation actuated with a dry powder inhaler (DPI) with untreated and plasma treated mouth piece, (capsule = cps; induction port = IP; preseparator = Pres), ($p < 0.05$).*

14.5.5 Determination of the individual effect of each component after increasing the surface roughness by plasma treatment on powder deagglomeration

Since higher powder deposition occurred after oxygen or OFCB plasma treatment of the entire upper unit in the IP and preseparator, and oxygen gas was used in both processes, which increased the surface roughness of the treated parts, the following experiment was conducted to determine the components that could have a decisive influence on powder deagglomeration after surface treatment. Therefore, the focus

was on the oxygen process, and for each experiment only one treated part was installed and tested, leaving the rest of the DPI untreated (Fig. 30). The results show that an oxygen plasma treated mesh or classifier resulted in higher powder deposition in the IP and also the preseparator, although in both cases the observed amount was not as high as when the entire upper unit of the DPI was treated (Fig. 27). In addition, with the exception of the mouth piece, no reduced powder deposition was observed on the treated parts.

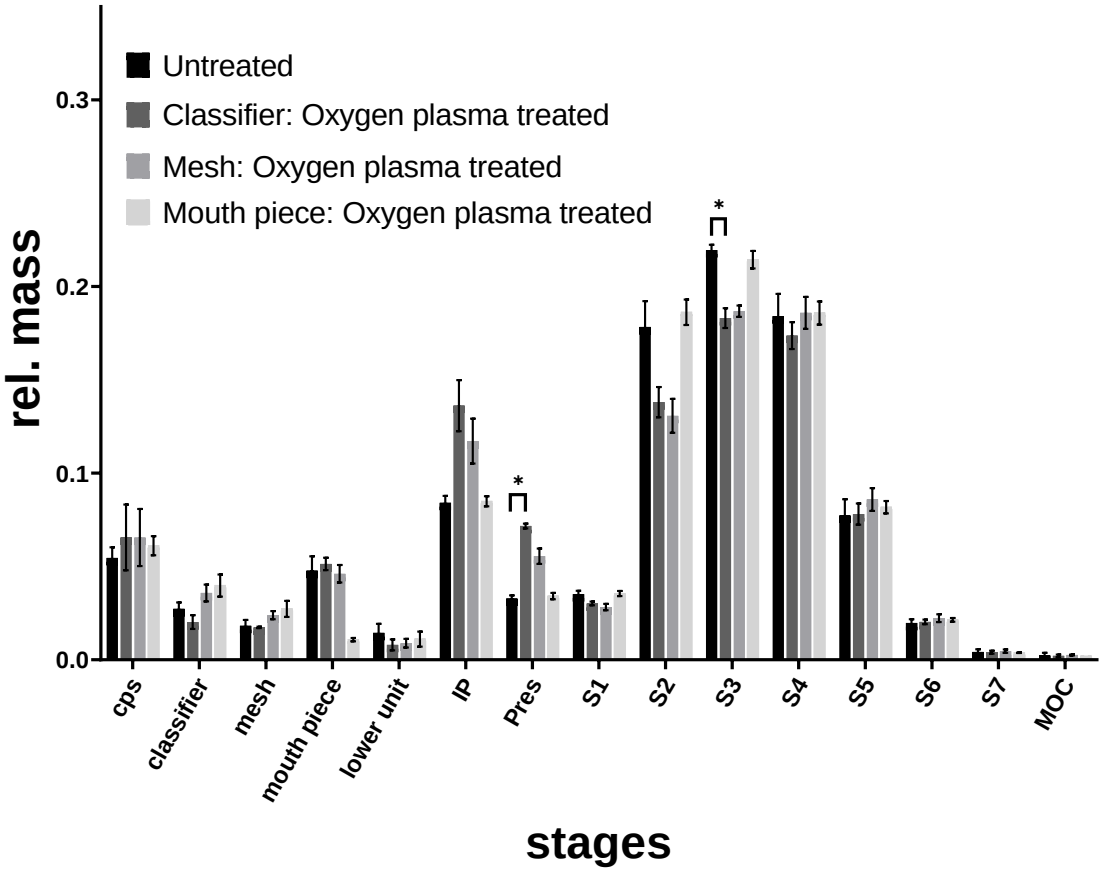

Figure 30: Next Generation Impactor (NGI) results obtained with the rifampicin formulation actuated with an untreated dry powder inhaler (DPI) and after plasma treatment of the individual parts of the upper unit (classifier, mesh, mouth piece) with oxygen plasma, (capsule = cps; induction port = IP; preseparator = Pres), ($p < 0.05$).*

14.6 Discussion

This study clearly demonstrated the effect of various DPI surface modifications by plasma treatment on powder deposition and deagglomeration. It was originally hypothesized that the different surface chemical properties obtained by the various plasma processes could minimize the hydrophilic-hydrophobic interactions between the DPI surface and the drug, resulting in less powder retention.

For this purpose, an oxygen process was developed and used to produce hydrophilic and activated surfaces, while the OFCB plasma process yielded inert-hydrophobic surfaces. Since no differences in the oscillation frequency of the capsule were observed in the experiment, the storage period of 3 weeks seems to have been sufficient to counteract possible altered interactions between capsule and DPI due to the increased surface energy (oxygen plasma process), since otherwise a decrease in the oscillation frequency would have been found. It can be argued that a reduction in surface energy (OFCB plasma process) does not result in minimized interaction between the capsule and the inhaler wall during actuation, since a similar frequency of oscillation was also observed with this modification.

The unaffected capsule oscillation confirmed the results of the NGI experiments obtained after plasma treatment of the lower part of the DPI. Since no differences in powder aerosolization were obtained after applying the different plasma modifications to the capsule chamber, hydrophilic-hydrophobic interactions do not seem to affect the deagglomeration of the powder during actuation in this DPI in the experiments performed.

In addition to the chemical surface modifications, it was shown that the plasma processes used in the experiments led to different surface structures with regard to their nanotexture. While the HMDSO process resulted in a smooth surface structure that was similar to the initial surface, the use of oxygen- with or without OFCB plasma resulted in a nanotextured surface texture in two different size ranges of roughness.

The formulation of spray-dried rifampicin as model drug was chosen because a higher amount of active ingredient was deposited in the DPI compared to commercially available interactive blends. This made it easier to detect differences in powder

deposition due to surface modification by the plasma treatment. Moreover, the aerosolization of the powder by the device resulted in low drug deposition in the preseparator but high deposition in the stages S1 - MOC. Thus, a changed deagglomeration behavior of the device after surface modification can also be observed directly.

Comparison of the NGI results obtained using devices with plasma treated parts of the upper unit suggests that the surface properties affect powder deposition within the DPI and also powder deagglomeration, since differences were observed in the experiments. The use of an untreated DPI or a DPI treated with HMDSO plasma resulted in similar deagglomeration of the powder, which was different from the results obtained with the DPIs treated with oxygen or OFCB plasma, raising the possibility that surface texture rather than hydrophilic or hydrophobic surface properties influenced powder deposition within the DPI and deagglomeration behavior. This is also underlined by the fact that similar powder deagglomeration and deposition were obtained for the DPIs modified with oxygen or OFCB plasma, although a hydrophilic or hydrophobic surface was created.

While increasing the surface roughness of the mouth piece or capsule chamber resulted in lower powder deposition on the respective surfaces, modifying the classifier or mesh seems to be critical, as this resulted in higher powder deposition in the IP or preseparator. The observations can be compared with the results of previous studies, where a device coated with a PTFE suspension spray resulted in a higher emitted fraction, but also in a higher powder deposition in the IP or preseparator, since the fine particle fraction was not increased compared to the untreated device [152–154]. Here, it was found that a hydrophobic coating can increase the emitted fraction without changing the aerosolization properties of the device for the powder. Similar trends for a higher emitted fraction after surface modification were also observed after coating the device and capsule with an ethanol-based magnesium stearate suspension [151]. Compared to these studies, the work described above focused only on the generated surface properties of the device and not on the combined effect of a modified capsule and the device. Furthermore, it should be investigated which modified DPI component

could be responsible for lower powder retention and which part seems to be critical for the surface modification. Since the DPI selected for this study can be decomposed into four main parts, it was possible to identify the most important surfaces for plasma modification. Unlike previous studies, this work did not focus exclusively on forcing agents to achieve friction-reducing or antistatic coatings. Therefore, a more neutral perspective was chosen for the study. Thus, in addition to a hydrophobic coating, the influence of the surface texture was also investigated, which represents a significant difference from the studies conducted so far. Since not only a hydrophobic surface in the mouth piece created by plasma treatment resulted in lower powder retention in this part, it seems logical that the chemical modification is not the main factor for the lower powder retention. This underlines the results of the previous studies, so that a PTFE and a magnesium stearate coating reduces powder deposition. Despite the low surface energy or antistatic surface properties obtained with these methods, the fact that in all cases a suspension was used so that the sprayed particles settled on the surface of the inhaler supports the idea that surface texture, rather than chemical properties, influences aerosolization behavior.

Since increasing the surface roughness of the mesh or classifier resulted in high powder deposition in the IP, increased turbulent flow behavior could occur at these generated nanotextured surfaces after plasma modification, which could not be straightened in the mouth piece. This altered air flow could therefore cause the particles to move differently, so that they could no longer follow the air flow. Compared to the mesh and classifier, the modification of the mouth piece had no real influence on the overall aerosolization behavior of the device for the powder, which could be explained by the fact that for this component, the characteristic dimension of the air flow channel is much larger than for the mentioned components. This results in the overall flow profile being less affected by the near-wall turbulence created by the surface roughness generated by the plasma treatment [72,147,176].

In summary, this study pointed out that surface properties affect the deagglomeration and deposition of the powder in the DPI, and surface structure appears to have a greater influence on aerosolization behavior than the created hydrophilic or

hydrophobic surface properties. In the experiments carried out, the mouth piece proved to be an interesting screw for these surface changes with regard to an unchanged deagglomeration behavior of the DPI for the powder with simultaneously reduced powder deposition. Modifying this component by increasing its roughness could be an interesting point for future device optimization and development, as a higher amount of drug could be available for pulmonary therapy. Increasing the amount of therapeutically available drug surely would improve the therapeutic effect. In addition, a decreased amount of drug formulation would need to be loaded into the device if more powder exits the DPI during an inhalation procedure. This could increase efficacy and patients' compliance by reducing the number of inhalations required per day.

The use of a suitable method that only changes the surface topography could be an interesting way to clarify what influence the dimensions of the surface profile and the degree of roughness (height or width of the elevations) have on the powder deposition in the device. Whether there is an optimum surface roughness or whether it depends on formulation aspects like particle size, shape and the formulation technique used (e.g., binary mixture, spray-dried) should be analyzed. In subsequent preliminary experiments with another formulation, a binary blend of albuterol sulfate and lactose monohydrate (Asthalin rotacaps®, Cipla ltd, Mumbai, India), we observed trends similar to the results with rifampicin (data not shown) which indicated that the effects were rather independent from the formulation but mainly depended on the modified DPI surface.

However, the aspect of formulation properties and the interaction of different formulations with rough surfaces of different size ranges surely needs to be clarified in more detail in subsequent studies. Besides, numerous parameters such as the potential influence of the DPI wall material, the dimensions of the airflow channel used in the different DPI components need to be analyzed. This is in view of a potential optimum dimension of the air flow channel for each component used in the respective device, so that an increase in the surface roughness of this component leads to reduced powder deposition without altered deagglomeration behavior.

14.7 Conclusion

This study has shown that surface structure has a high impact on the deagglomeration and retention of the powder in the device, which has not been sufficiently considered so far and could be used for device optimization in the future. It has been shown that a nanotextured surface of the mouth piece can reduce powder deposition inside the inhaler, resulting in a higher emitted fraction. Since the development of pulmonary delivery systems usually focuses on the aspect of formulation development and optimization, this study has shown that the surface structure can have a major impact on the overall deagglomeration behavior and offers another opportunity to improve this form of therapy.

15. Supplements

Table S1: Particle size distribution of the different Inhalac® samples used.

	Inhalac® 70	*Inhalac® 251*	*Inhalac® 400*
	Sieved lactose	*Sieved lactose*	*Milled lactose*
D_{10} [µm]	*110 - 160*	*7 - 22*	*0.8 – 1.6*
D_{50} [µm]	*180 - 250*	*40 - 70*	*4 – 11*
D_{90} [µm]	*270 - 340*	*80 - 120*	*15 – 35*

Table S2: Determination of the residual solvents methanol (MeOH) and dichlomethane (DCM) a) initial after the spray-drying process and b) after post-processing in the vacuum chamber for 48 h and 40°C.

Initial	MeOH	DCM
	ppm	ppm
Riva001	839 ± 13	6529 ± 1479
Riva002	808 ± 22	4081 ± 441
Riva003	0	10649 ± 348
Riva004	0	34586 ± 4348

a)

48 h drying, 40°C	MeOH	DCM
	ppm	ppm
Riva001	0	80 ± 39
Riva002	0	0
Riva003	0	236 ± 6
Riva004	0	2700 ± 98

b)

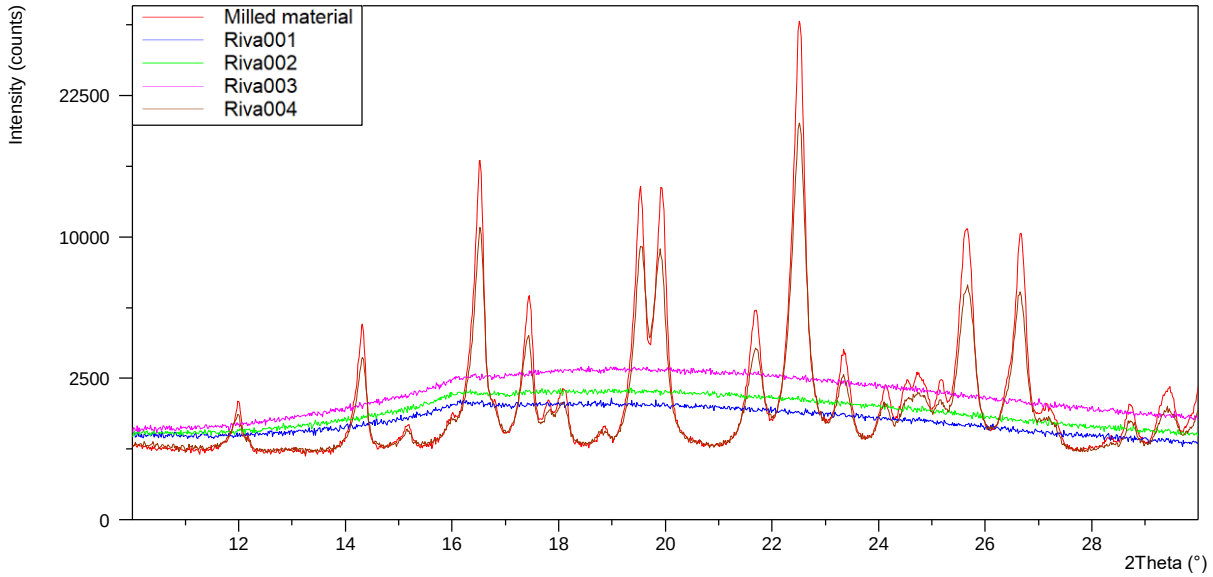

Figure S1: Results of the XRPD analysis of the milled material and the different spray-dried batches of rivaroxaban.

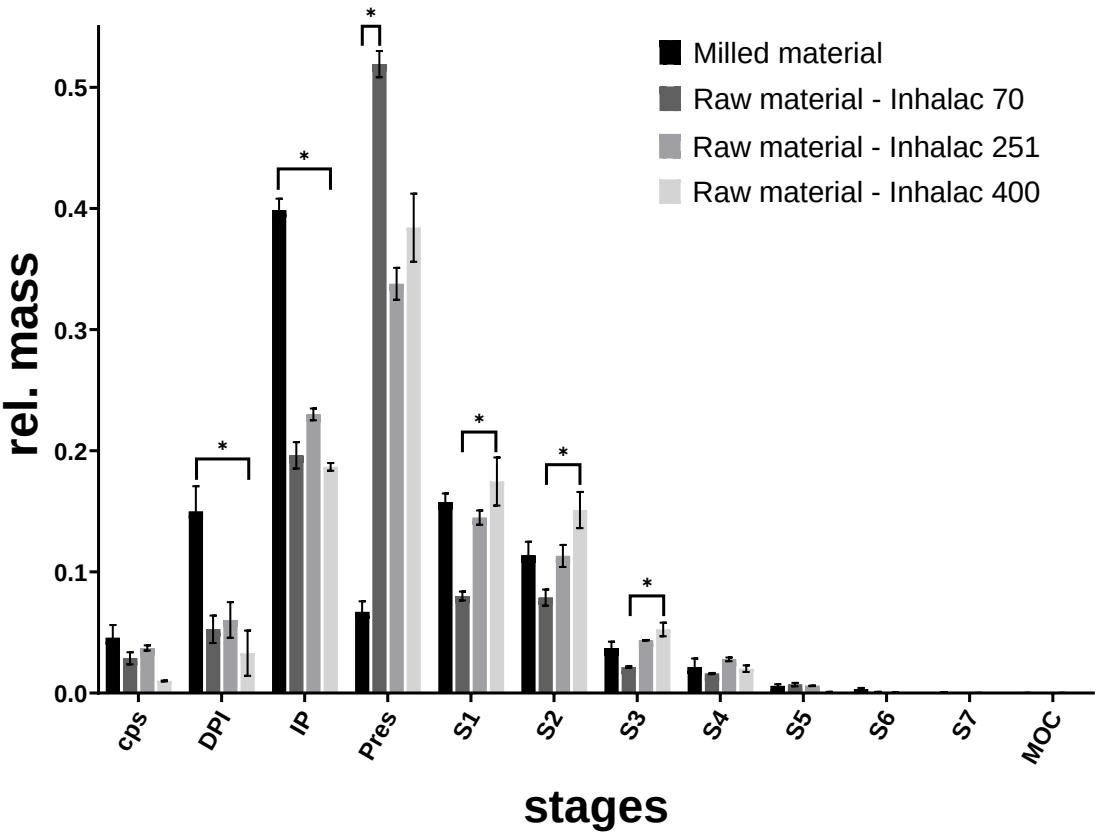

*Figure S2: NGI results obtained with the Breezhaler when actuating the binary blends consisting of the milled rivaroxaban material and Inhalac® 70/251/400, (capsule = cps; dry powder inhaler = DPI; induction port = IP; preseparator = Pres), (*p < 0.05).*

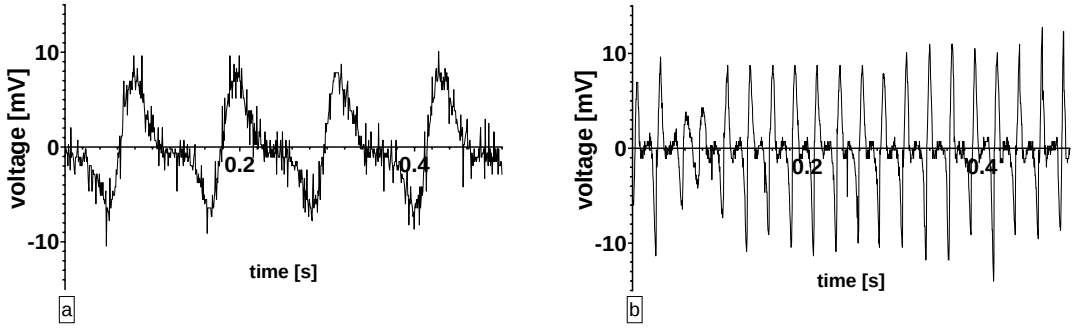

Figure S3: Comparing the voltage signals regarded from the magnet rotation at the stirring rod (a = 8 Hz) and the capsule movement during inhalation (b = 40 Hz).

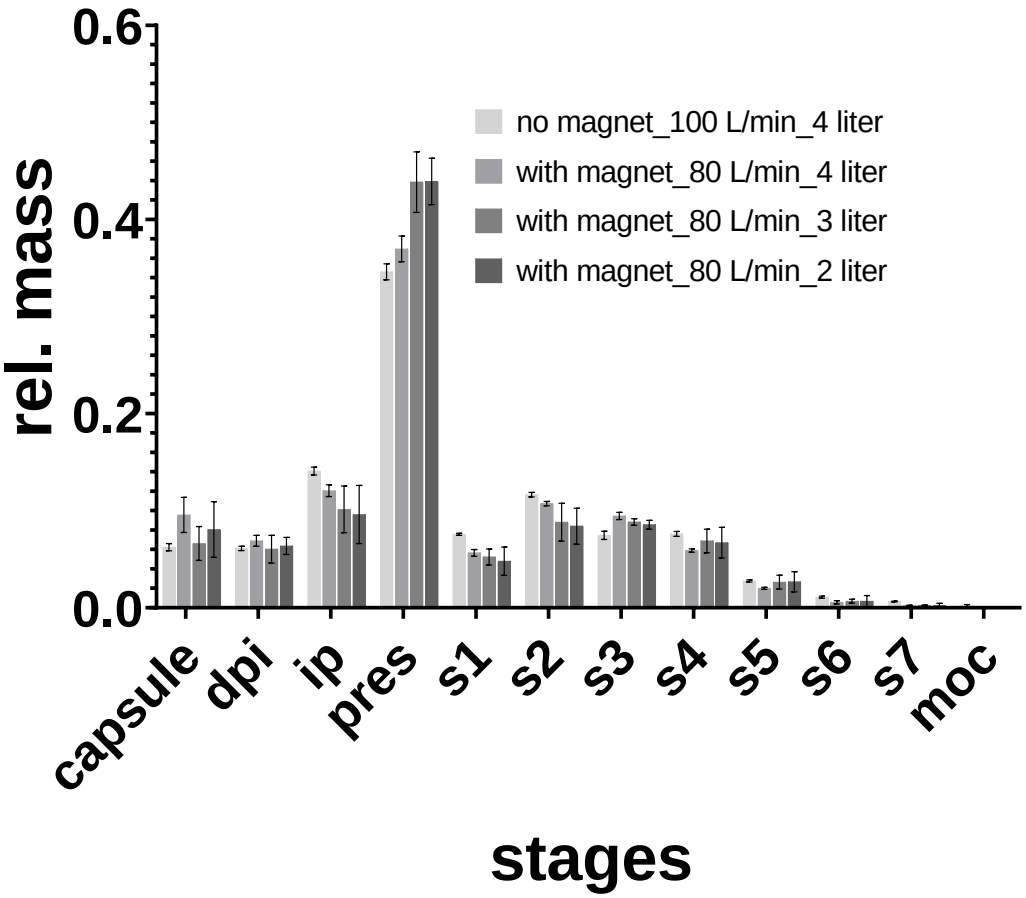

Figure S4: NGI results of the Cyclocaps® formulation by using the Lupihaler device for different actuation volumes (2 - 4 liter) and a tested flow rate of 80 L/min.

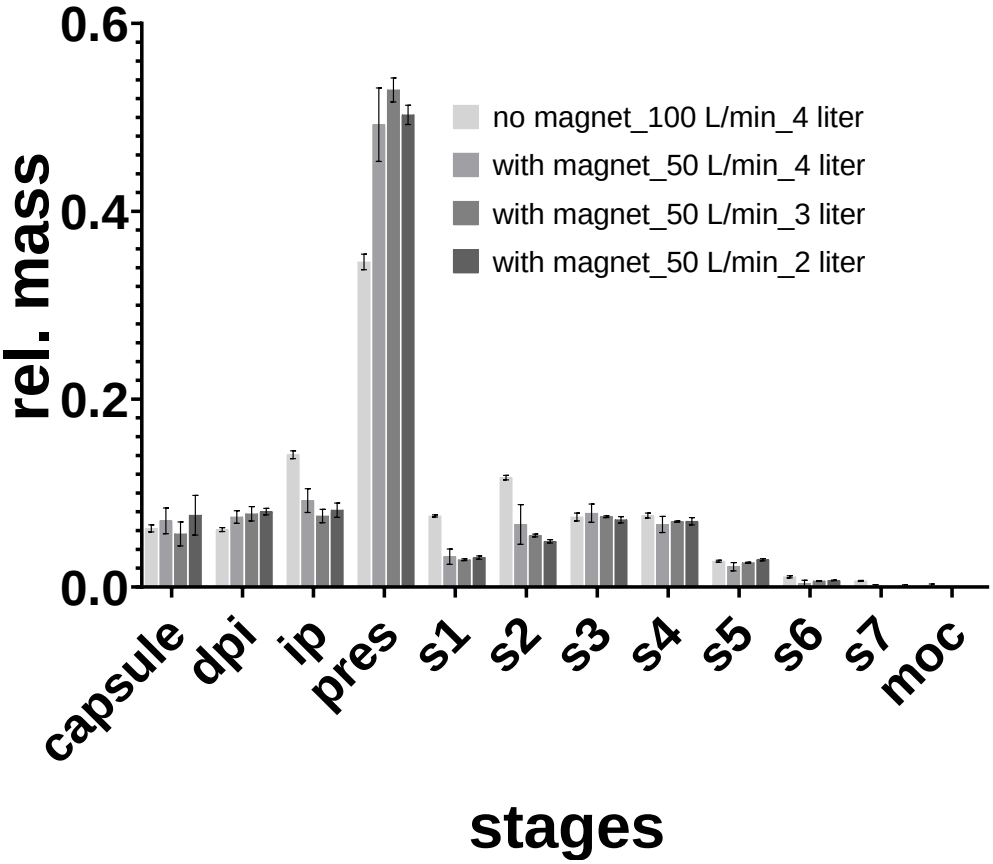

Figure S5: NGI results of the Cyclocaps® formulation by using the Lupihaler device for different actuation volumes (2 - 4 liter) and a tested flow rate of 50 L/min.

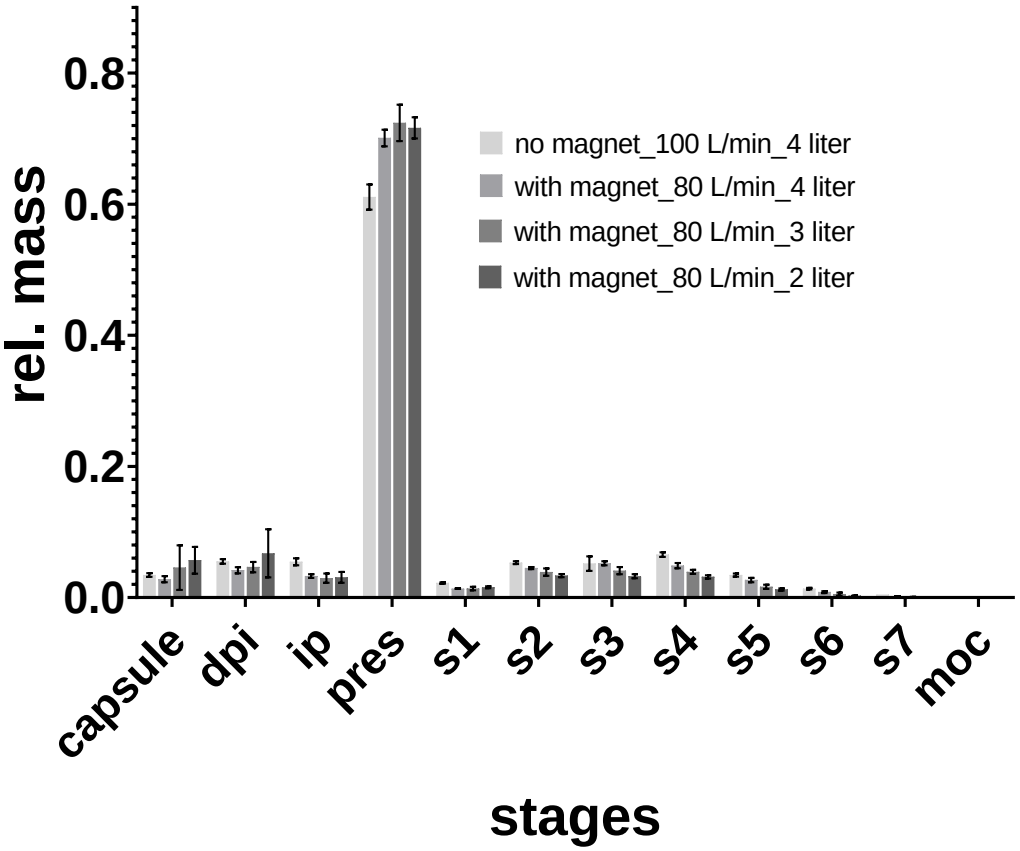

Figure S6: NGI results of the Ventilastin® formulation by using the Lupihaler device for different actuation volumes (2 - 4 liter) and a tested flow rate of 80 L/min.

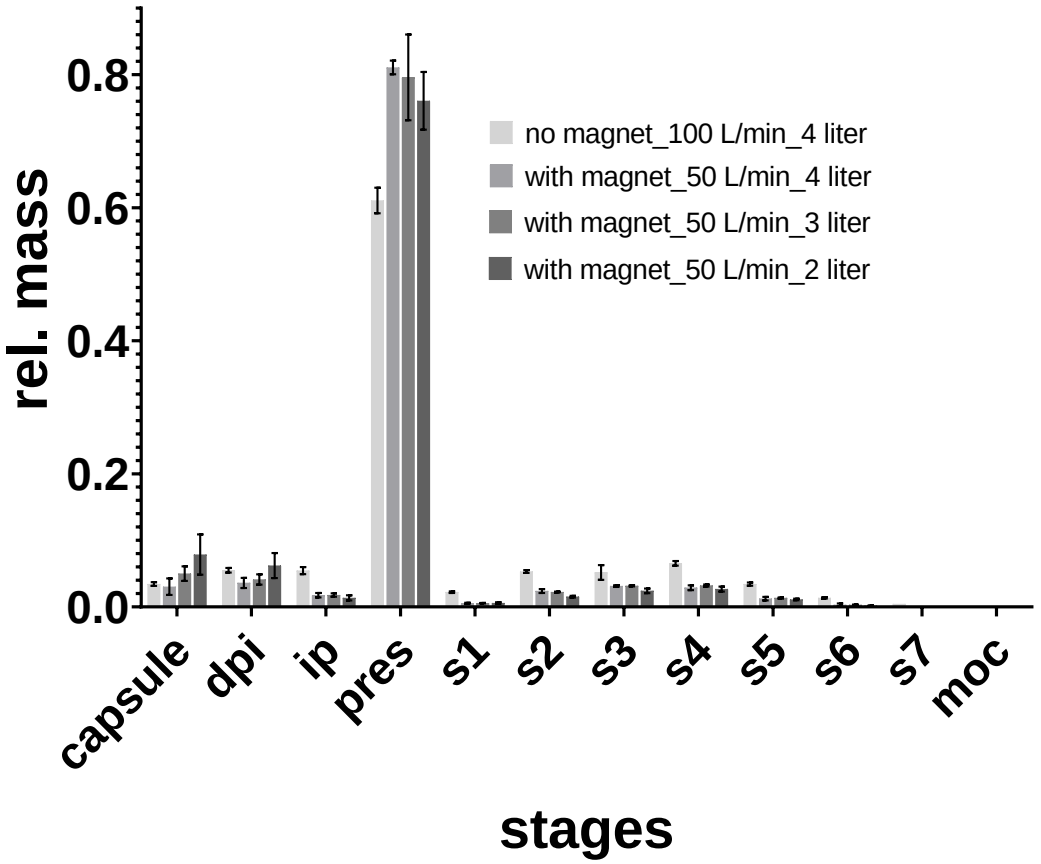

Figure S7: NGI results of the Ventilastin® formulation by using the Lupihaler device for different actuation volumes (2 - 4 liter) and a tested flow rate of 50 L/min.

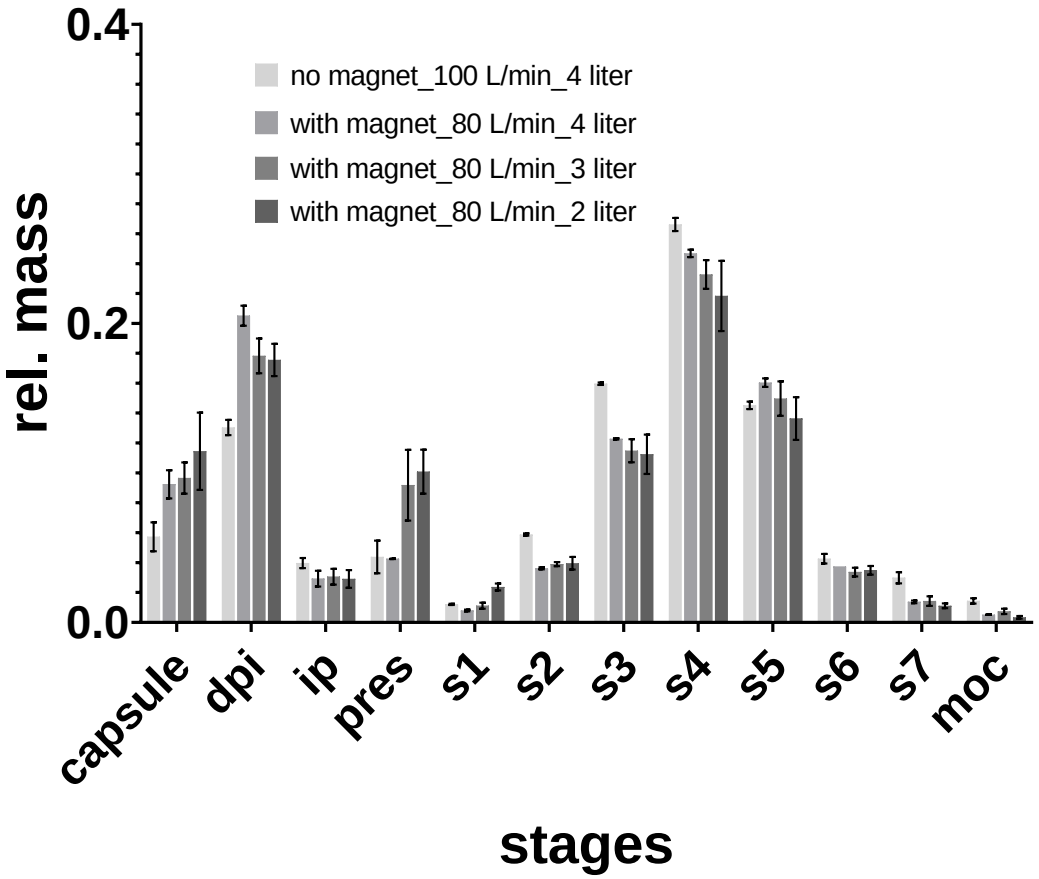

Figure S8: NGI results of the spray-dried rifampicin by using the Lupihaler device for different actuation volumes (2 - 4 liter) and a tested flow rate of 80 L/min.

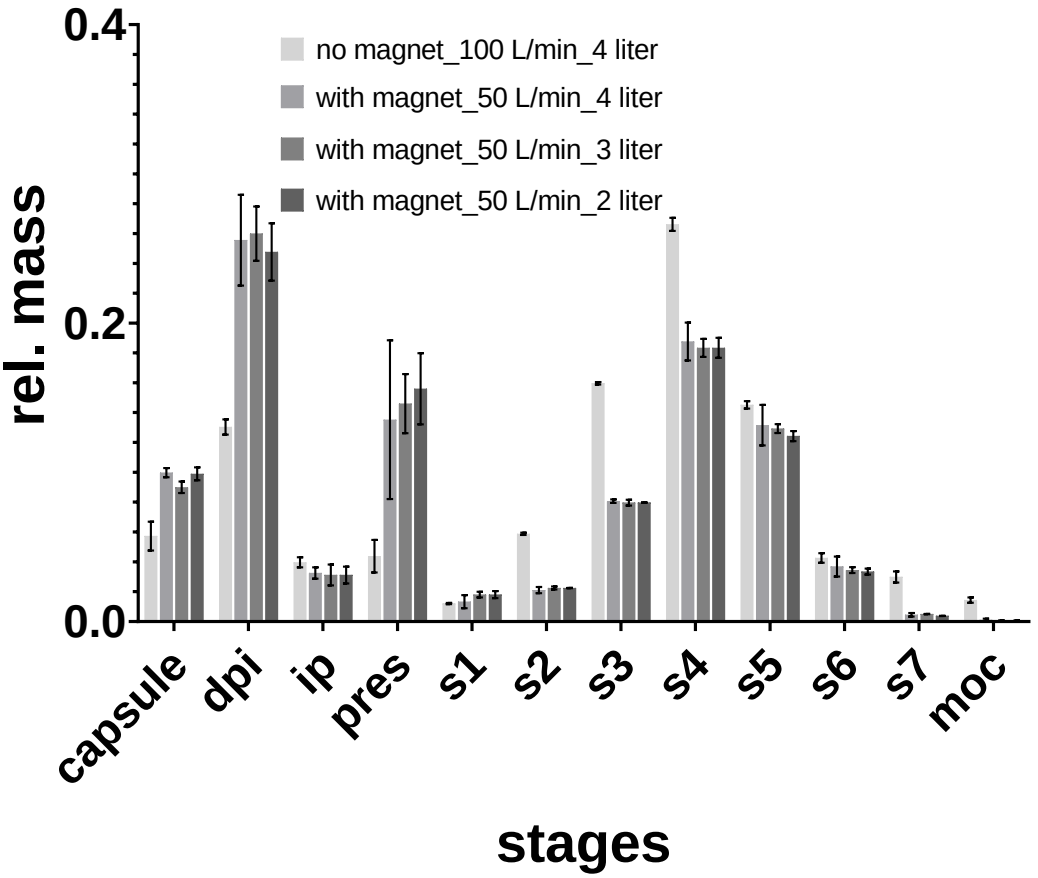

Figure S9: NGI results of the spray-dried rifampicin by using the Lupihaler device for different actuation volumes (2 - 4 liter) and a tested flow rate of 50 L/min.

Table S3. Parameters used for spray-drying the rifampicin or amoxicillin particle formulations.

Formulation	**Rifampicin**	**Amoxicillin**
Feed rate [mL/min]	7.4	7.4
Spray gas flow [L/h]	375	601
Outlet temperature [°C]	60	85

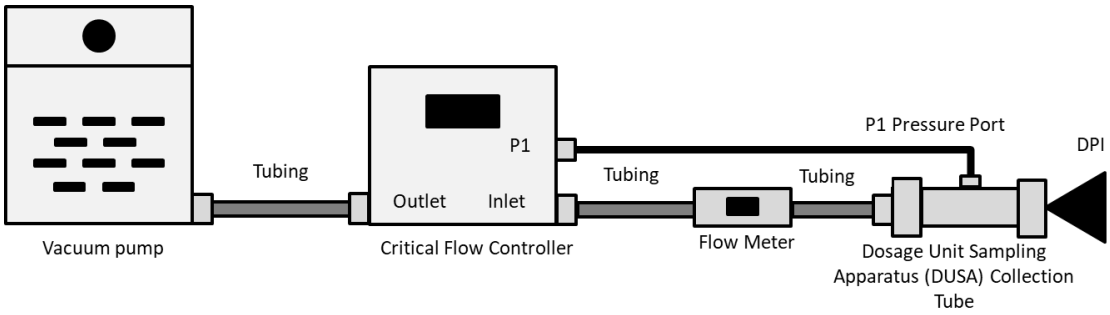

Figure S10. Schematic diagram of the setup for determining the airflow resistance of the various dry powder inhalers (DPIs), (P1 = Pressure Port1).

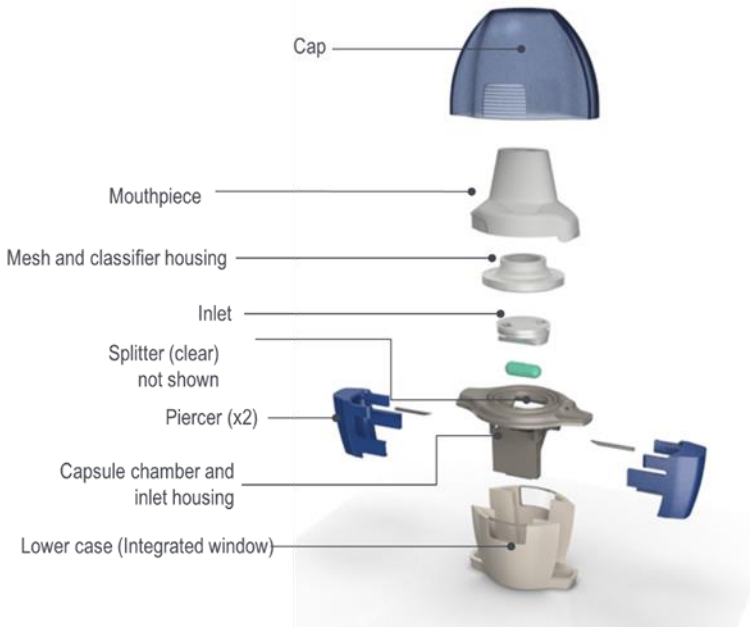

Figure S11. Exploded-view drawing of the Presspart prototype dry powder inhaler (PP-DPI).

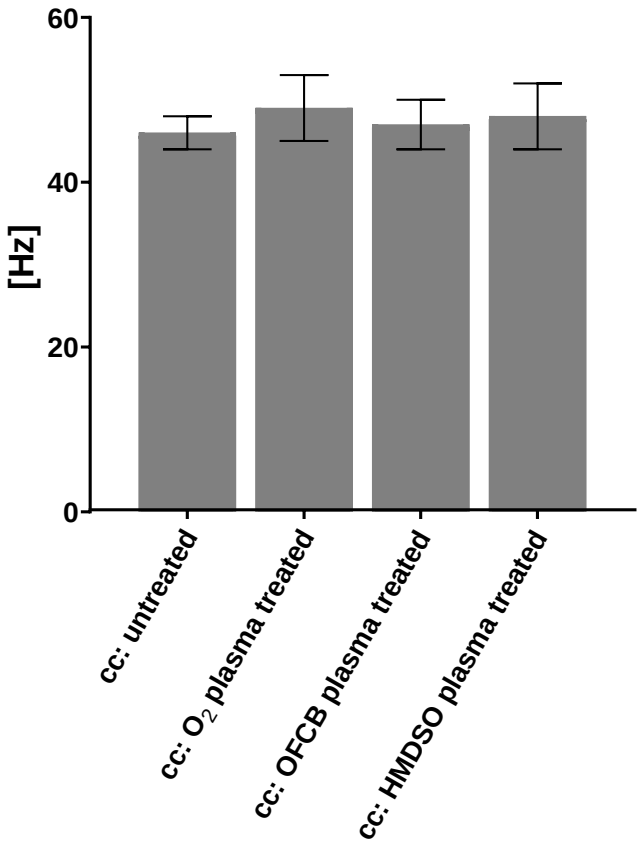

Figure S12: Measured oscillation frequency of the capsule during actuation using a DPI with an untreated and plasma treated capsule chamber.